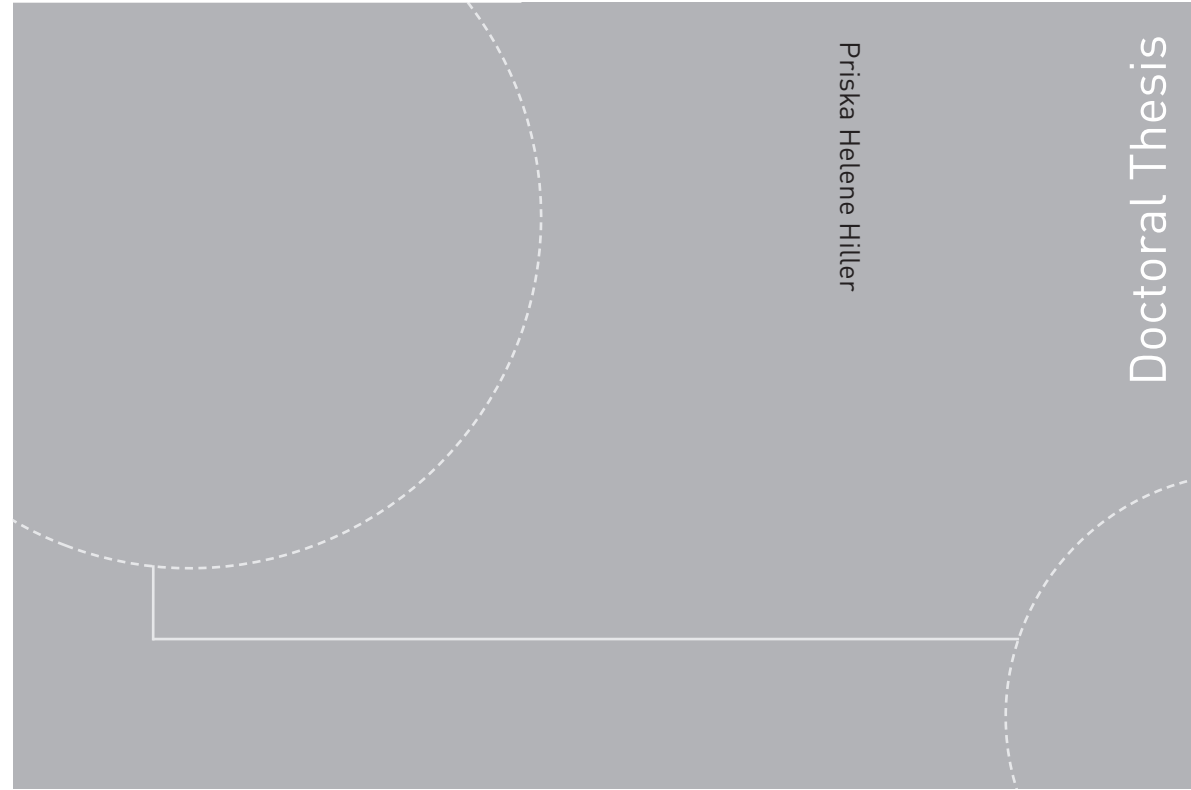


Doctoral theses at NTNU, 2017:140

Priska Helene Hiller

## Riprap design on the downstream slopes of rockfill dams



ISBN 978-82-326-2352-5 (printed version)  
ISBN 978-82-326-2353-2 (electronic version)  
ISSN 1503-8181

Department of Civil and Environmental Engineering

NTNU  
Norwegian University of  
Science and Technology  
Faculty of Engineering

Doctoral theses at NTNU, 2017:140

NTNU

 **NTNU**  
Norwegian University of  
Science and Technology

 **NTNU**  
Norwegian University of  
Science and Technology

Priska Helene Hiller

# Riprap design on the downstream slopes of rockfill dams

Thesis for the degree of Philosophiae Doctor

Trondheim, May 2017

Norwegian University of Science and Technology  
Faculty of Engineering  
Department of Civil and Environmental Engineering



Norwegian University of  
Science and Technology

**NTNU**

Norwegian University of Science and Technology

Thesis for the degree of Philosophiae Doctor

Faculty of Engineering

Department of Civil and Environmental Engineering

© Priska Helene Hiller

ISBN 978-82-326-2352-5 (printed version)

ISBN 978-82-326-2353-2 (electronic version)

ISSN 1503-8181

Doctoral theses at NTNU, 2017:140



Printed by Skipnes Kommunikasjon as

# Abstract

Riprap is widely used as erosion protection. To prevent erosion in case of accidental overtopping or trough flow, the downstream slopes of rockfill dams can be secured with riprap. The present thesis focuses on the stability and design of dumped and placed riprap made of natural stone. Placed riprap for the tests was constructed by setting stones in an interlocking pattern, with their longest axes inclined towards a slope of 1:1.5 (vertical: horizontal). Riprap parameters, failure mechanisms, hydraulic parameters and existing stability approaches were addressed to optimize riprap design on steep slopes. Riprap stability was investigated with physical model tests in different scales and was expressed through the critical stone-related Froude number.

In order to quantify the forces acting on a specific stone, the novel 'Smart-stone' monitoring equipment was tested. A Smartstone probe was mounted in a riprap stone to measure the acceleration in the moment when the stone was eroded from the riprap. However, the current version of the Smartstone equipment needs further development to allow for the desired application.

Physical model tests and field tests with large-scale riprap stones were carried out to investigate riprap stability. For dumped riprap, similarity was found between the field and model tests in terms of riprap stability, packing density and visually observed flow pattern. The model tests and field tests with placed riprap showed good agreement with regard to flow pattern and overtopping height. However, the placed ripraps in the model had a higher packing density and were more stable. Displacements within the riprap layer were monitored during the model tests. The displacements lead to a gap at the transition between the horizontal crest and the downstream slope. The riprap became unstable when the gap exceeded approximately one stone length. Accumulating displacements were hence identified as failure mechanism for placed riprap on steep slopes. Due to the gradual development of the displacements, the dimension of time is recommended to be included in stability analyses in addition to discharge. Placed riprap had on average a seven times higher critical stone-related Froude number than dumped riprap. However, dumped riprap might provide sufficient stability for certain applications, and placed riprap should just be considered if increased stability is required. For an optimized riprap design, the requirements about riprap type, stone size and packing density as well as the corresponding costs have to be balanced with the desired level of stability.



# Sammendrag

Erosjonssikring av stein er mye brukt, blant annet for å sikre nedstrøms skråning på steinfyllingsdammer mot erosjon fra ulykkeslaster som overtopping eller gjennomstrømning. Denne avhandlingen fokuserer på stabiliteten og utformingen av erosjonssikring av stein lagt som rauset steinsikring eller plastring. Plastring ble bygd ved å sette stein i forband med god innbyrdes kontakt og med lengste akse hellende mot skråningen. Forsøkene ble utført på en skråning på 1:1,5 (vertikalt: horisontalt). Plastringsparametere, bruddmekanismer, hydrauliske parametere og eksisterende stabilitetsanalyser ble undersøkt for å optimalisere utforming av rauset steinsikring og plastring på bratte skråninger. Stabiliteten til erosjonssikringen ble undersøkt med fysiske modellforsøk i ulike målestokk og uttrykt gjennom det kritiske steinbaserte Froudetallet.

For å kvantifisere kreftene som virker på en spesifisk stein, ble det nylig utviklete måleutstyret 'Smartstone' testet. En Smartstone sonde ble montert i en plastringsstein for å måle akselerasjonen i øyeblikket når steinen ble erodert fra plastringen. Den aktuelle versjonen av Smartstone må imidlertid bli videre utviklet for å tillate den ønskede anvendelsen.

Fysiske modellforsøk og feltforsøk med storskala plastringsstein ble utført for å undersøke stabiliteten til rauset steinsikring og plastring. Felt- og modellforsøkene med rauset steinsikring viste god overensstemmelse i forhold til stabilitet, pakningstetthet og det visuelt observerte strømningsmønsteret. Forsøkene utført med plastring hadde bra overensstemmelse mellom felt og modell i forhold til strømningsmønster og overtoppingshøyde. Plastringene i modellforsøkene var imidlertid tettere pakket og mer stabile enn i felt. Forskyvinger i plastringslaget ble målt i modellforsøkene. Forskyvingene førte til en glippe i overgangen mellom den horisontale kronen og skråningen. Plastringen ble ustabil når glipen hadde blitt større enn omtrent en steinlengde. Akkumulerende forskyvinger ble dermed identifisert som bruddmekanisme for plastring på bratte skråninger. Siden forskyvingene utviklet seg gradvis, anbefales det å inkludere tidsdimensjonen i stabilitetsanalyser i tillegg til vannføring. Plastring hadde i gjennomsnitt sju ganger større kritisk steinrelatert Froudetall enn rauset steinsikring. Imidlertid kan rauset steinsikring være stabil nok for noen bruksområder, og plastring bør bare bli vurdert hvis økt stabilitet er nødvendig. For å oppnå optimal utforming av erosjonssikring av stein, må kravene til type erosjonssikring, steinstørrelse og plastringstetthet, samt de tilhørende konstruksjonene, avveies mot det ønskete stabilitetsnivået.



# Zusammenfassung

Deckwerke aus Steinen sind eine weitverbreitete Massnahme gegen Erosion. Sie werden unter anderem auf den luftseitigen Hängen von Staudämmen erstellt, um diese in ausserordentlichen Lastfällen wie Über- oder Durchströmen vor Erosion zu schützen. Die vorliegende Dissertation fokussiert auf die Stabilität solcher Deckwerke, die entweder als Blockwurf oder Blocksatz ausgeführt werden. Bei einem Blockwurf werden die Steine willkürlich verteilt. Ein Blocksatz hingegen besteht aus Steinen, die ineinandergreifend gesetzt werden. Die Steine können zusätzlich mit ihrer längsten Achse gegen den Hang geneigt platziert werden. Für die Versuche hatten die Hänge ein Gefälle von 1:1.5 (horizontal: vertikal). Die Parameter von Deckwerken aus Steinen, Fehlermechanismen, hydraulische Parameter und bestehenden Stabilitätsanalysen wurden untersucht, um die Bauweise der Deckwerke zu optimieren. Die Deckwerksstabilität wurde mit Modellversuchen in verschiedenen Massstäben ermittelt und durch die kritische steinbezogene Froude-Zahl ausgedrückt.

Um die Kräfte, die auf einen spezifischen Stein wirken, zu messen, wurde das neulich entwickelt 'Smartstone' Messgerät getestet. Eine Smartstonesonde wurde in einen Stein eingebaut werden, um die Beschleunigung zu messen, wenn der Stein aus dem Deckwerk erodiert wird. Die aktuelle Version der Smartstones muss jedoch weiterentwickelt werden, um die gewünschte Anwendung zuzulassen.

Physische Modellversuche und Feldversuche mit grossmassstäblichen Steinen wurden durchgeführt, um die Deckwerksstabilität zu untersuchen. Die Stabilität, Setzungsdichte und die visuell beobachteten Strömungsverhältnisse stimmten für Blockwurf zwischen den Feld- und Modellversuchen überein. Die Strömungsverhältnisse und die Überströmungswassertiefe waren für Blocksatz in den Feld- und Modellversuchen ähnlich. Die Blocksätze im Modell waren jedoch dichter gesetzt und stabiler. In den Modellversuchen wurden die Verschiebungen von ausgewählten Steinen im Deckwerk gemessen. Die Verschiebungen führten zu einer Lücke im Übergang von der Dammkrone zum luftseitigen Hang. Der Blocksatz wurde unstabil, als die Lücke die Grösse einer Steinlänge überstieg. Folglich wurden Verschiebungen als Fehlermechanismus für Blocksätze auf steilen Hängen identifiziert. Da die Verschiebungen sukzessive anwuchsen, sollte die zeitliche Dimension in Stabilitätsuntersuchungen zusätzlich zum Abfluss berücksichtigt werden. Die kritische steinbezogene



Froude-Zahl war für Blocksatz im Durchschnitt siebenmal höher als die von Blockwurf. Jedoch kann die Stabilität von Blockwurf für gewisse Anwendungen ausreichen und Blocksatz sollte nur in Betracht gezogen werden, falls eine erhöhte Stabilität erforderlich ist. Um die Bauweise von Steindeckwerken zu optimieren, müssen die Anforderungen wie Art des Deckwerks, Steingrösse und Setzungsdichte im Deckwerk sowohl als auch die damit verbundenen Kosten bezüglich dem gewünschten Stabilitätsniveau abgewogen werden.

# Preface

This thesis is submitted to the Norwegian University of Science and Technology (NTNU) in Trondheim for partial fulfilment of the requirements for the degree of Philosophiae Doctor (PhD).

This work is the result of a four-year PhD program, which was conducted at the Department of Civil and Environmental Engineering with Professor Leif Lia as main supervisor and Professor Jochen Aberle as co-supervisor. The PhD position was allocated to 75% research and 25% teaching. The teaching included supervising students in their semester projects and master theses, and assisting in the course TVM4128 Hydropower and Hydraulic Engineering, Advanced Course.

Funding for this research was first guaranteed by Statkraft and finally financed through the project 'Development of a tool for optimal riprap protection of rockfill dams (PlaF)' coordinated by Energy Norway. Financing was provided 50% by the Norwegian hydropower industry (Agder Energi Vannkraft AS, BKK Produksjon AS, E-CO Energi AS, Hydro Energi AS, Otteraaens Brugseierforening, Sira-Kvina Kraftselskap, SKS Produksjon AS, Statkraft Energi AS) and 50% by the Research Council of Norway (project 235730).

In accordance with the guidelines of the Faculty of Engineering this thesis comprises an introduction to the research that has resulted in three scientific journal papers, six conference papers and one report.

## **Contributions:**

I was responsible for the design of the studies, carrying out the experiments with assistance from students and the writing of the papers I, II and IV. The co-authors contributed to the planning of the experiments and were involved in the writing of the corresponding papers. Paper III was written in collaboration with Trier University. Dr. Oliver Gronz analysed the Smartstone data of the preliminary experiment including the comparison of the stone position derived by video tracking. I contributed the description of the Smartstone equipment, the tests about battery life time and data transmission range of the naked probe to this paper.



# Acknowledgements

As child, I liked to play in streams, constructing small dams and watching the water destroying them. More than twenty years later, I still construct dams and observe how the water erodes them. As I grew up, the size of my dams increased and the play turned into research, leading to this PhD.

Many people have advised, supported and motivated me during my PhD research and I am grateful to all of them. It has been a pleasure to meet and discuss riprap and dams with interested people and to delve into that topic.

I would like to thank my main supervisor Professor Leif Lia for his support, enthusiasm and engineering approach to science. Without his contacts in the hydropower industry, this PhD research would not have been possible. A special thanks goes to my co-supervisor Professor Jochen Aberle for the numerous discussions, advise related to physical modeling and for the valuable support in paper-writing. I also like to thank my mentor Hroar Klempe for our discussions and giving me the opportunity to see my PhD studies from a different perspective.

I am grateful for all the scientific, administrative and technical support at the Department of Hydraulic and Environmental Engineering and in the Hydraulic Laboratory. The collaboration with the contributing companies in the project 'PlaF' is acknowledged and thanks to Leif Basberg in Energy Norway who coordinated the project. A special thanks goes to Sira-Kvina Kraftselskap for providing access to the site at dam Svartevatn. Without their generous support, especially from Rolv Guddal and Per Magne Sinnes, the field tests would not have been possible. In connection with the field tests, I thank also Svein Rune Erland Skilnand for the video, the students Hans Edward Røer, Julia Caramanos, Fredrikke Kjosavik and Bastian Dost for their help with the tests and Geir Tesaker for technical assistance. Furthermore, I appreciated all the help with the model tests such as the students constructing riprap and assisting in running experiments, help with sorting and washing stones, company in picking the stones in the quarry and support in data analysis. Franzefoss Pukk AS kindly provided the stones for the model tests. The permissions to use the reports of Larsen et al. (1986) and Sommer (1997) by the Regierungspräsidium Karlsruhe and the Karlsruhe Institute of Technology are acknowledged.

The collaboration about the 'Smartstone' sensor with Trier University provided me insight into the research at the Department of Physical Geography

lead by Professor Markus Casper and I appreciated the discussions with the researchers, especially Dr. Oliver Gronz. The two month exchange at Colorado State University in Fort Collins were enriching and I valued the stay at the Engineering Research Center and Hydraulics Laboratory as well as the discussions with Professor Christopher Thornton, Dr. Steven R. Abt and Natalie Youngblood.

A big thank you goes to all my PhD fellows at the Department, the Norwegian Hydropower Centre and abroad for all the scientific discussions as well as talks about nothing and everything. A special thanks goes to Morten, Kaspar and my sister Rebecca for their constructive feedback on the draft of this thesis.

Last but not least I thank all my friends and family for supporting and motivating me when I needed it, as well as charging my batteries in social activities or on trips in the mountains. Merci vielmol, tusen takk!

---

If we wonder often,  
the gift of knowlege will come.  
(Arapaho proverb)

# Contents

<b>Abstract</b>	<b>i</b>
<b>Preface</b>	<b>vii</b>
<b>Acknowledgements</b>	<b>ix</b>
<b>Contents</b>	<b>xi</b>
<b>List of papers</b>	<b>xiii</b>
<b>List of supervised students</b>	<b>xv</b>
<b>1. Introduction</b>	<b>1</b>
<b>2. Background</b>	<b>5</b>
2.1. Erosion protection on embankment dams . . . . .	5
2.2. Riprap stability . . . . .	7
<b>3. Research methodology</b>	<b>15</b>
3.1. Research design . . . . .	15
3.2. Experimental setup . . . . .	18
3.3. Accelerometers and the Smartstone monitoring equipment . .	22
<b>4. Summary of results</b>	<b>25</b>
4.1. Paper I: Accumulating stone displacements as failure origin in placed riprap on steep slopes . . . . .	27
4.2. Paper II: Field and model tests of riprap on steep slopes exposed to overtopping . . . . .	29
4.3. Paper III: Smartstones: A small 9-axis sensor implanted in stones to track their movements . . . . .	30
4.4. Paper IV: Placed riprap as erosion protection on the down- stream slope of rockfill dams exposed to overtopping . . . . .	31
<b>5. Discussion</b>	<b>33</b>
<b>6. Conclusion</b>	<b>39</b>
<b>References</b>	<b>43</b>

A. Selected papers	49
B. Secondary papers	155
C. Permissions from journals and statements from co-authors	163

# List of papers

The results of this PhD research are presented in four selected papers which are printed in full-text in Appendix A. There are in addition six secondary papers whereof the abstracts are given in Appendix B.

## Selected papers

### **Paper I: Accumulating stone displacements as failure origin in placed riprap on steep slopes**

Priska H. Hiller, Jochen Aberle, Leif Lia

*In press: Journal of Hydraulic Research, doi: <http://dx.doi.org/10.1080/00221686.2017.1323806>*

### **Paper II: Field and model tests of riprap on steep slopes exposed to overtopping**

Priska H. Hiller, Leif Lia, Jochen Aberle

*In review: Journal of Applied Water Engineering and Research*

### **Paper III: Smartstones: A small 9-axis sensor implanted in stones to track their movements**

Oliver Gronz, Priska H. Hiller, Stefan Wirtz, Kerstin Becker, Thomas Iserloh, Manuel Seeger, Christine Brings, Jochen Aberle, Markus C. Casper, Johannes B. Ries (2016)

*CATENA: 142, 245-251, doi: <http://dx.doi.org/10.1016/j.catena.2016.03.030> (Open Access)*

### **Paper IV: Placed riprap as erosion protection on the downstream slope of rockfill dams exposed to overtopping**

Priska H. Hiller, Leif Lia

*25th Congress on Large Dams  
Stavanger, Norway, 2015*



## Secondary papers

### **Dam Svartevatn - An example of challenging upgrading of a large rockfill dam**

Priska H. Hiller, Leif Lia, Per Magnus Johansen, Rolv Guddal

*ICOLD Annual Meeting and Symposium*

*Bali, Indonesia, 2014*

### **Riprap design on the downstream slope of rockfill dams**

Priska H. Hiller, Leif Lia, Jochen Aberle, Stefan Wirtz, Markus C. Casper

*Mitteilungen - Leichtweiss-Institut für Wasserbau der Technischen Universität*

*Braunschweig Vol. 161, 39-44, 2014*

### **Large-scale overtopping tests - Practical challenges and experience**

Priska H. Hiller, Leif Lia

*1st International Seminar on Dam Protections against Overtopping and Accidental Leakage*

*Madrid, Spain, 2014*

### **Practical challenges and experience from large-scale overtopping tests with placed riprap**

Priska H. Hiller, Leif Lia (2015)

*In M. Á. Toledo, R. Morán, E. Oñate (Eds.), Dam Protections against Overtopping and Accidental Leakage, 151-157. London: CRC Press/ Balkema*

### **Field tests of placed riprap as erosion protection against overtopping and leakage**

Priska H. Hiller, Fredrikke Kjosavik, Leif Lia, Jochen Aberle

*United States Society on Dams - Annual Meeting and Conference*

*Denver CO, USA, 2016*

### **Kartlegging av plastring på nedstrøms skråning av fyllingsdammer**

[Survey of placed riprap on the downstream slopes of rockfill dams]

Priska H. Hiller

*NTNU Report B1-2016-1, ISBN-10: 978-827598-095-1*

*Trondheim, Norway, 2016*

# List of supervised students

**Ellen Bogfjellmo (2013)** *Nedstrøms skråning av steinfyllingsdammer - Analyse av eksisterende plastringer.*

Development of a method to survey placed riprap on rockfill dams, (Semester project).

**Hans Edward Røer (2014)** *Nedstrøms skråning av steinfyllingsdammer - Modellforsøk av plastring under ulike strømningsforhold.*

Scaled model tests of placed riprap exposed overtopping, through flow and a combination, (Master thesis).

**Ragnhild Sørliæ Meaas (2014)** *Plastring av elvebunn med sterk strøm.*

Scaled model tests of placed riprap exposed to supercritical flow, (Master thesis).

**Johannes Kobel (2014)** *Smartstones.*

Testing out the Smartstone sensors and evaluate its application properties, (Semester project).

**Jens Jakobsen (2015)** *Plastring av fyllingsdammer - Forskyving i plastring og anvendelse av Smartstone sensorer.*

Evaluating displacements in placed riprap and test the application of the Smartstone sensors, (Master thesis).

**Eirik Helgetun Pettersen (2015)** *Plastring av fyllingsdammer - Effekt av forband på styrken av plastringen.*

The effect of interlocking placement on the stability of placed riprap, (Master thesis).

**Wiebke Marie Zander (2015)** *Untersuchungen zur Genauigkeit von Smartstones - ein auf RFID-Technologie basierendes Tracersystem.*

Evaluating the accuracy of the Smartstone - a tracer system based on RFID technology, (Bachelor thesis).

**Fredrikke Kjosavik (2015)** *Plastring av fyllingsdammer - Forskyvingar i damkrona.*

Analysis of displacements on the dam crest with large-scale field tests and scaled model tests, (Master thesis).

**Guri Holte Veslegard (2016)** *Plastring av fyllingsdammer - Forskyvning i plastring.*

Analysis of displacements within placed riprap, (Semester project).

# List of Figures

1.1.	Dam Svartevatn was with its height of 129 m the largest dam in Northern Europe when it was finished in 1976. The picture shows the dam after rehabilitation in 2015. The downstream slope is covered with placed riprap (Photo: P. H. Hiller). . . .	2
2.1.	Rehabilitation work at the 129 m high dam Svartevatn. The excavator is setting the placed riprap on the downstream slope of 1:1.5 corresponding to $S = 0.67$ . The downstream slope and the inclination $\beta$ of the riprap stones are indicated. The field tests site (described in Section 3.2) is marked with a circle (Photo: NTNU). . . . .	10
2.2.	Existing data for the stability of dumped (a) and placed riprap (b) expressed through the critical stone-related Froude number $F_{s,c}$ relative to the slope $S$ . The marker size is proportional to the used stone diameter (the marker size used in the legend corresponds to $d = 0.1$ m). . . . .	11
3.1.	Schematic presentation of the scales and the performed studies. Field tests (F'year') and model tests (M'nr') are symbolized with rectangulars, papers (P'nr') with diamonds. Application and tests involving the Smartstone sensor 'SST' are indicated with rectangulars and labelled correspondingly. . . . .	17
3.2.	Grain size distribution curves for the riprap and support fill/filter for the field tests F13 and F15 and the model tests. . . .	19
3.3.	Test set-up for the experiments with placed riprap P01 - P04 with $L_s = 1.8$ m. The coordinate systems $xyz$ and $x'y'z'$ have their origin in the edge between the horizontal crest and the chute. The marked stones, which positions were tracked, are marked with 'MS' and their $x$ -coordinate. The inclination angle $\beta$ of the riprap stones is illustrated in the enlarged part in the top right. All dimensions in [mm]. . . . .	20
3.4.	Spillway outlet channel with a test dam covered with placed riprap (F15P2 in 2015). The crest of dam Svartevatn is visible in the upper right corner in the background. The discharge was provided from the reservoir impounded by the dam (Photo: NTNU). . . . .	21

3.5. Smartstone probe and accelerometer in model and field applications. . . . .	24
4.1. Development of the relative displacements with increasing discharge exemplarily for P02 in (a) and averaged values for the tests with placed riprap where riprap failure occurred in (b). The error bars in (b) mark the minimum and maximum values for $\Delta x_i L_i^{-1}$ included in the average $\overline{\Delta x_i L_i^{-1}}$ . . . . .	28
4.2. Video snaps of the field test F15P2 with placed riprap. Cascading flow for the lowest discharge in (a) and skimming flow for the highest discharge just before riprap failure in (b) (Video: S.R. Skilnand). . . . .	29

# List of Tables

3.1. Stone properties for the studies. The overline indicates mean values. . . . .	18
4.1. Summary of the model tests carried out with riprap stones with $d_{50} = 0.057$ m. Test P01 - P08 were carried out with placed riprap and D01 and D02 with dumped riprap. The boundary conditions are described by chute length covered with riprap $L_s$ and packing factor $P_c$ . The results of the experiments are presented with the critical discharge per unit width $q_c$ , the ratio between the unit discharges for erosion of the first stone $q_s$ and $q_c$ , and the critical stone-related Froude number $F_{s,c}$ . . . . .	25
4.2. Boundary conditions and results of the field tests in terms of the mean stone diameter $d_{50}$ , packing factor $P_c$ , the critical discharge per unit width $q_c$ , the ratio between the unit discharges for erosion of the first stone $q_s$ and $q_c$ , and the critical stone-related Froude number $F_{s,c}$ . The tests in 2013 were carried out with placed riprap (F13P1, F13P2). Three additional field tests were run in 2015, whereof two with placed riprap (F15P1, F15P2) and one with dumped riprap (F15D1). . . . .	26



# 1

## Introduction

Dams have been constructed all over the world for thousands of years. They are necessary in infrastructure to store and regulate water for irrigation, water supply, transport, flood control and hydropower production.

The industrial development and the availability of heavy construction equipment in the 20<sup>th</sup> century allowed the construction of higher and larger dam structures. The volumes of stored water increased and therewith the risk of potential dam failures. Theoretical assessments and case studies of dam failures have contributed to improve the design of dams. The most common dam type worldwide are embankment dams: 77 % according to the World Register on Dams (International Commission on Large Dams [ICOLD], 2016). A dam exceeding 15 m in height is considered a 'large dam' according to ICOLD. Embankment dams consist of an impervious layer, such as a slab covering the upstream slope, or a core consisting of either moraine, clay or asphalt. The embankment provides the required weight to withstand the water pressure. A rockfill dam is an embankment dam with more than 50 vol% of the filling obtained from rock quarry, rock excavation or natural stones and boulders (Kjærnsli, Valstad, & Høeg, 1992).

Overtopping is the most common reason for dam failure of embankment dams (ICOLD, 1995) and a protective layer on the crest and the downstream slope can prevent or delay erosion in case of accidental leakage, overtopping or violent attacks on the dam (e.g. Orendorff, Al-Riffai, Nistor, & Rennie, 2013; Toledo, Morán, & Oñate, 2015). Riprap is widely used as erosion protection and can be used to protect the downstream slopes of rockfill dams. Riprap consists of large elements, which can either be placed in an interlocking pattern or be randomly dumped. Figure 1.1 shows dam Svartevatn, a rockfill dam with a placed riprap on its downstream slope. The riprap stones were placed in an interlocking pattern and with their longest axes inclined towards the dam as described in Ministry of Petroleum and Energy (OED, 2009).





**Figure 1.1.:** Dam Svartevatn was with its height of 129 m the largest dam in Northern Europe when it was finished in 1976. The picture shows the dam after rehabilitation in 2015. The downstream slope is covered with placed riprap (Photo: P. H. Hiller).

Several countries face considerable investments to maintain their dams in the future. This is also the situation in Norway, where many (86%) of the 185 large rockfill dams were constructed before 1990 (Norwegian Water Resources and Energy Directorate [NVE], 2016). Since then, population and infrastructure located downstream of dams have grown. In combination with the revised dam safety regulations (OED, 2009) with full retroactive effect (see Midttømme, Grøttå, & Hyllestad, 2010, for details), considerable rehabilitations are required. An example of such a rehabilitation is described as case for dam Svartevatn in Hiller, Lia, Johansen, and Guddal (2014). The costs to upgrade the existing dams in Norway according to the dam safety regulation are estimated in the range of 8 billion NOK (approx. 900 million EUR) (Kjellesvig, Konow, Wiggen, & Stokseth, 2011). Upgrading works usually include reconstruction, rehabilitation or construction of the placed riprap on the downstream slope with a usual inclination of 1:1.5 (vertical: horizontal). The report about administrative practices in dam safety (Kjellesvig et al., 2011) therefore recommends further research about placed riprap to enhance methods and knowledge for an optimized riprap design.

It is against this background that a research project was initiated by Energy Norway and the Norwegian University of Science and Technology (NTNU) in 2011 to study the stability of placed riprap on the downstream slopes of rockfill dams. The present PhD research is part of this research project.

### **Scope and aim**

The scope of present PhD research is the stability of placed riprap on the downstream slopes of rockfill dams exposed to overtopping. The aim of the research is to optimize the design of placed riprap. Consequently, the important parameters in the riprap as well as in the flow have to be identified to describe how they affect the stability of placed riprap. Neither the overall geotechnical stability of the embankment, as for example summarized in Larsen et al. (1986), Morán and Toledo (2011), nor the breach formation and development (e.g., Müller, Frank, & Hager, 2016; Schmocker, Höck, Mayor, & Weitbrecht, 2013; EBL Kompetanse AS, 2005; Morris, Hassan, & Vaskinn, 2007; Løvoll, 2006) are part of the present research.

### **Thesis outline**

Following this introduction, there is an overview about riprap stability and erosion protections on the downstream slopes of embankment dams. Together with the scope and the aim presented above, the objectives are developed in Chapter 3. The research methodology is described including a presentation of the physical tests executed in a small-scale model in the hydraulic laboratory and large-scale tests at a temporary field site. The chapter also includes the description of a novel developed monitoring equipment to track stone movements, the so-called 'Smartstone'. The research results are presented as summary of four selected scientific papers in Chapter 4 and discussed in the subsequent chapter. The conclusion in the final Chapter 6 also includes recommendations for the design of placed riprap. The selected scientific papers are presented in full-text in Appendix A and the abstracts are given for the secondary papers in Appendix B.



# 2

## Background

In the following, erosion protection on embankment dams are discussed in general. Thereafter, riprap stability is discussed as a specific measure with focus on failure mechanisms, riprap parameters and available knowledge.

### 2.1. Erosion protection on embankment dams

Embankment dams need erosion protection on the upstream slope, i.e. on the impounded side, against the wear from waves, ice and the altering water level. The crest as well as the dry downstream slope are secured against run-off and potential additional loads. The relevant load scenarios as well as recommendations for the design are normally formalized in national regulations. In the 1960s and 70s, when many dams were constructed and the dam volume and heights increased, efforts were put in the optimization of the dam design to achieve more durable structures and a balanced cost-value ratio. A discussed possibility was to integrate the spillway into the dam construction, i.e., to overtop the embankment during floods (e.g. Olivier, 1967; Hartung & Scheuerlein, 1970). Practical recommendations focused on avoiding flow concentration either due to an uneven overflow section or due to the normally trapezoidal profile of a dam. Flow concentration would increase the discharge per unit width even though the total discharge remained constant. Scouring immediately downstream of the rockfill dam should be prevented to avoid retrogressive erosion. Physical model tests were carried out to investigate the flow through and over rockfill dams (e.g., Olivier, 1967; Linford & Saunders, 1967; Hartung & Scheuerlein, 1970). The main advantage of spilling the flood over the embankment was the reduced cost because of lower freeboard and no expenses for a spillway. An important requirement was that the embankment was highly permeable to avoid pore

pressures, which could cause global failure of the embankment, and the implementation was recommended for rockfill, but not for earthfill dams.

Overtoppable dams have not become accepted and detached spillways have become common practice. However, exceptional loads such as the probable maximum flood, clogged spillways, violent attacks or landslide-generated impulse waves can generate overtopping over a dam. In case of overtopping of the impervious core, the water will flow through the rockfill and exit the embankment further downstream. Solvik (1991) investigated through flow and overflow problems in rockfill dams based on solid rock foundations and presented design diagrams for the requested stone size for the crest, downstream face and the dam toe, which should be secured with stones of adequate size.

The development in the recent years tends to either secure the downstream slope against erosion of exceptional loads or to construct the spillway over dams where the overtoppable section is specifically secured. The measures against erosion of accidental leakage or overtopping are divided in soft protections such as overtopping-resistant dumped or placed riprap, and hard protections, such as concrete slabs, shaped blocks or articulated concrete blocks (Toledo et al., 2015).

In the context of flood retention, small earthfill dams (up to 10 m high) are constructed to delay and to flatten the peak of the flood hydrograph. Those dams are only periodically impounded and the inundation area is usually used as agricultural land or recreation area. Further, the dams and related structures such as spillways should fit well into the landscape. Hence, overtoppable dams or dam sections secured with natural material such as stone, grass or reinforced soil are favoured. Corresponding research was carried out mainly in Germany (e.g., Dornack, 2001; Rathgeb, 2001; Queisser, 2006; Siebel, 2013). Overtopping over earthfill dams is according to the aforementioned studies allowable because the low permeability of the fill, which will not become saturated during a flood event and consequently will remain stable. In addition, such dams are usually constructed with gentle slopes of up to 1:4, although steeper slopes of up to 1:1.5 were investigated in for example Dornack (2001).

In Norway, placed riprap is used as erosion protection on the downstream slopes of rockfill dams against accidental loads caused by overtopping and/or through flow. Details about the design of the placed riprap are included at the end of Section 2.2. Scenarios such as short-time overtopping due to

landslide-generated impulse waves, clogged spillway or extraordinary large floods can result in overtopping of a dam. Especially the latter scenario is of particular interest in the context of climate change as frequency and discharge of floods are expected to increase in most of the parts in Norway (Lawrence, 2016).

## 2.2. Riprap stability

Riprap consists of large elements which secure adjacent layers from erosion and is a common measure to protect hydraulic structures such as dams, bridge piers and abutments, streambeds and river banks (e.g., Abt & Johnson, 1991; CIRIA, CUR, & CETMEF, 2007; Abt, Thornton, Scholl, & Bender, 2013; Chanson, 2015; Jafarnejad, Franca, Pfister, & Schleiss, 2016). The riprap elements are either artificial or consist of natural stones. They are placed in an interlocking pattern or can be randomly dumped. The riprap protection is exposed to hydraulic wear of currents or waves.

### Failure mechanisms

Dumped and placed riprap exposed to overtopping are characterised by different failure mechanisms. Usually, failure of dumped riprap is considered when the adjacent filter layer is exposed to the flow because the randomly placed surface layer stones have been eroded (e.g., Linford & Saunders, 1967; Abt & Johnson, 1991; Robinson, Rice, & Kadavy, 1998; Peirson, Figlus, Pells, & Cox, 2008). Placed riprap typically consists of a single layer of stones placed in an interlocking pattern on top of the filter layer. Erosion of the first stone would result in riprap failure according to the failure criteria of dumped riprap as the filter would be exposed at that particular location. However, erosion of single stones from a placed riprap does not necessarily result in failure of the entire riprap layer (Larsen et al., 1986; Sommer, 1997; Dornack, 2001). The interlocking between the stones results in a bearing structure in the riprap layer and increases its stability. Consequently, critical conditions for placed riprap should rather be the occurrence of progressive bulk erosion (Larsen et al., 1986; Sommer, 1997; Dornack, 2001). The bearing structure furthermore allows the transfer of longitudinal forces within the placed riprap on steep slopes. These slopes do not allow continuous transfer of the flow forces into the adjacent filter and the embankment. If the flow forces exceed a critical level, they can cause either sliding or rupture of the riprap layer (Larsen et al., 1986; Sommer, 1997; Dornack, 2001; Siebel, 2007).

The reports by Larsen et al. (1986) and Sommer (1997) document small rearrangements of stones resulting in displacements and compaction in the downstream part of the riprap layer and a loosening upstream. Such loosening occurs at very steep slopes according to Larsen et al. (1986), and represents a sore point in the riprap. Bulk failure may be initiated due to flow attack of the exposed stones in the loosened part of the riprap. More details about the analyses by Larsen et al. (1986) and Sommer (1997) are presented in Paper I together with the identification of displacements as an additional failure mechanism for placed riprap on steep slopes.

A further indication for different failure mechanisms in dumped and placed riprap is the location, where the erosion starts. On the one hand, Abt et al. (2013) states that riprap failure along a slope began and propagated from the lower third of the embankment. Historical field and laboratory observations showed that at this point normal depth of flow is typically achieved. On the other hand, Dornack (2001) observed for placed riprap that the critical area for erosion is slightly upstream of the point where self-aeration started, i.e. in the zone of acceleration flow without aeration. This observation is supported by Robinson et al. (1998) who noted that the area most subject to failure was the upper reach of the chute just below the crest. Hence, the area where failure initiates is of particular interest.

## Riprap parameters

The riprap stability depends on the interaction between the riprap and the hydraulic forces. The parameters can be subdivided in riprap and hydraulic properties as well as the geometric boundary conditions characterized by the slope  $S$ , the extension of the slope covered with riprap exposed to overtopping  $L_s$  and the width of the channel or dam  $B$ .

The riprap stones are characterised by their size, which is expressed through either their diameter  $d$ , volume  $V_s$  or mass  $m_s$ . These parameters are related to each other through  $V_s = C_f d^3 = C_f m_s \rho_s^{-1}$  with the stone density  $\rho_s$  and the form factor  $C_f$  varying between 0.4 for schistous stones and 0.8 for more cubical ones (NVE, 2012). The diameter can be expressed as the equivalent spherical diameter  $d_s$ , i.e. the diameter of a sphere with the same volume as the corresponding stone, or the nominal diameter  $d = \sqrt[3]{abc}$  (Bunte & Abt, 2001). The factors  $a$ ,  $b$  and  $c$  denote the longest, intermediate and shortest axes of the stones, respectively. The grading of the stones is described by the particle size distribution curve where the index  $i$  in  $d_i$  gives the percentage by mass which is finer than  $d_i$ . The coefficient of uniformity  $C_u = d_{60}/d_{10}$

is a commonly used indicator for the grading. The shape of the stones influence the stability and Abt, Thornton, Gallegos, and Ullmann (2008) found that rounded stones need to be approximately 40% larger than angular stones to withstand similar flow conditions. Further parameters such as asperities, angle of repose, weathering resistance and geological composition (e.g., CIRIA et al., 2007) can be included to describe the stone material in more detail.

Stones are arranged into a riprap and its construction induces further properties such as packing density and the riprap layer thickness. The orientation of the stones within a placed riprap can be described with the inclination angle  $\beta$  between the surface and the longest axes of the stones (see sketch in Figure 2.1). There has not been found any common way to describe the quality of dumped and placed riprap. However, the packing density seems to be an appropriate indicator. The packing factor  $P_c$  was introduced by Linford and Saunders (1967) and Olivier (1967)

$$P_c = \frac{1}{Nd_s^2}, \quad (2.1)$$

with the amount of stones per  $m^2$ ,  $N$ , related to the stone area  $d_s^2$ , allows comparison of the packing density of ripraps with different stone sizes. A low packing factor  $P_c$  indicates a high packing density.

The flow velocity  $v$  is the key parameter to describe the hydraulic forces such as drag, lift and shear. The flow over riprap is driven by gravity and mainly characterized by the Froude number  $F = v(gh)^{-0.5}$ , the Reynolds number  $R = v\mu^{-1}$ , and the Weber number  $W = \rho_w h v^2 \sigma^{-1}$ , with the gravitational acceleration  $g$ , water level  $h$ , kinematic viscosity  $\nu$ , density of water  $\rho_w$  and the surface tension  $\sigma$ . The Reynolds number can be neglected if the flow in the model and prototype is turbulent. The Weber number is relevant to describe the transport of air. For high-speed air-water flow scaled with Froude similitude, Pfister and Chanson (2012) recommend  $W^{0.5} > 140$  or  $R > 2$  to  $3 \times 10^5$  to prevent significant scale effects.

The Froude number  $F$  can be combined with the relative submergence  $hd^{-1}$  to the stone-related Froude number  $F_s = q(gd^3)^{-0.5}$  with the discharge per unit width  $q = vh$ . Using the stone-related Froude number  $F_s$  instead of the Froude number  $F$  eases the comparison of results from tests at different scales. Furthermore, the determination of  $v$  and  $h$  is often hampered in supercritical flow due to fluctuating stage and air mixed into the flow, whereas their





**Figure 2.1.:** Rehabilitation work at the 129 m high dam Svartevatn. The excavator is setting the placed riprap on the downstream slope of 1:1.5 corresponding to  $S = 0.67$ . The downstream slope and the inclination  $\beta$  of the riprap stones are indicated. The field tests site (described in Section 3.2) is marked with a circle (Photo: NTNU).

product  $q$  remains constant as long as the geometry does not change. At critical conditions, i.e. riprap failure, with the critical unit discharge  $q_c$ , the stone-related Froude number becomes

$$F_{s,c} = \frac{q_c}{\sqrt{gd^3}} \quad (2.2)$$

The density term  $(\rho_s - \rho_w)\rho_w^{-1}$  can be included in Equation 2.2 to compare data points obtained with stones of considerable different densities.

The critical stone-related Froude number has traditionally been used to describe riprap stability, as described in more detail in the following section. The parameter  $F_{s,c}$  does not include the duration of the hydraulic loading. In case of time-dependent or -limited processes, incorporation of time  $t$  should be considered for example as the water volume which passed over the riprap per unit width ( $qt$ ). However, studies including time-dependency in riprap stability are rare and have only been found in Jafarnejad et al. (2016) addressing riverbed riprap exposed to flow perpendicular to the slope.

## Available data and stability approaches for riprap design

Riprap stability has mainly been studied for dumped riprap on gentle slopes with  $S < 0.2$  as apparent in Figure 2.2a, which uses the critical stone-related Froude number  $F_{s,c}$  as measuring unit for riprap stability. The figure contains data points of multiple studies (Abt et al., 1987; Abt & Johnson, 1991; Wittler, 1994; Mishra, 1998; Robinson et al., 1998; Peirson & Pells, 2005; Siebel, 2007; Thornton, Cox, & Turner, 2008; Thornton, Abt, Clopper, Scholl, & Cox, 2012), which were summarized and evaluated in Abt et al. (2013). The majority, about 75%, of the data points, come from studies with

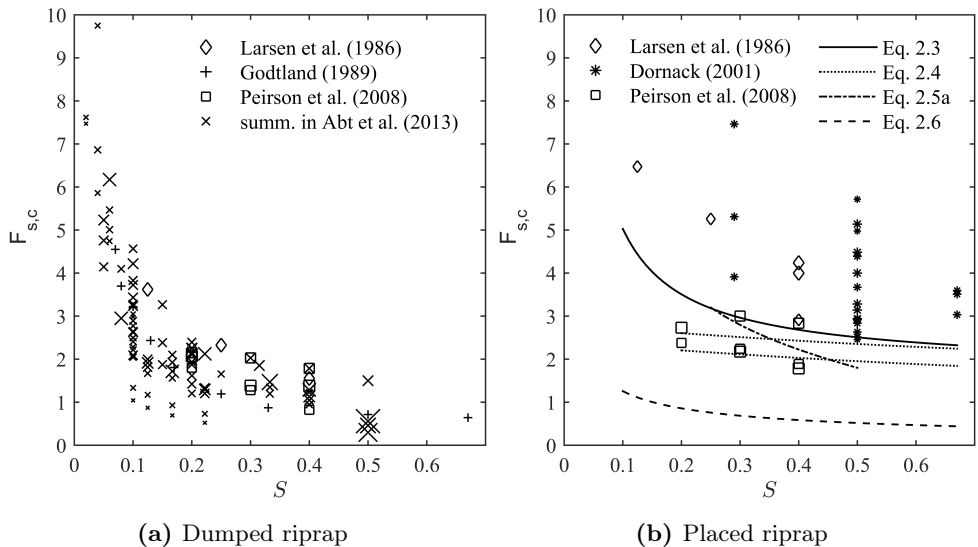


**Figure 2.2.:** Existing data for the stability of dumped (a) and placed riprap (b) expressed through the critical stone-related Froude number  $F_{s,c}$  relative to the slope  $S$ . The marker size is proportional to the used stone diameter (the marker size used in the legend corresponds to  $d = 0.1$  m).

stones  $d < 0.1$  m, and only four of the presented 96 data points are for  $d > 0.2$  m. Riprap stones in prototype applications are usually larger than 0.2 m. In addition to the collected data points, Abt et al. (2013) contains an evaluation of 21 overtopping riprap design relationships. Thornton, Abt, Scholl, and Bender (2014) applied multivariable power regression analysis to the data points presented in Abt et al. (2013) and presented an empirical design relationship. However, they related  $d_{50}$  to the riprap layer thickness, expressed as a multiple of  $d_{50}$ , and the relationship may hence be affected

by spurious correlation. The same applies for the empirical relationship developed by Khan and Ahmad (2011). In general, overtopping flow should not exceed the interstitial flow through the riprap layer for dumped riprap as recommended by Frizell, Ruff, and Mishra (1998) and Eli and Gray (2008).

Data for dumped riprap in Figure 2.2a were extended with a study covering steeper slopes of up to  $S = 1$  (Godtland, 1989) and two studies which include data for both dumped and placed riprap (Peirson et al., 2008; Larsen et al., 1986). Comparing Figure 2.2b for placed riprap with Figure 2.2a for dumped riprap demonstrates that placing riprap stones in an interlocking pattern increases riprap stability. However, the values for  $F_{s,c}$  scatter more for placed riprap. The stability gain of placed riprap compared to dumped riprap was quantified to approximately 30% in Peirson et al. (2008) and 80% in Larsen et al. (1986). The different stability gain can be explained by the packing factors of  $P_c = 0.94$  and  $P_c = 0.65$ , respectively. The stabilizing effect is especially distinct on steep slopes as shown by Dornack (2001) who investigated placed riprap on steep slopes of  $0.29 \leq S \leq 0.67$ . His study was the only found including data of placed riprap on slopes as steep as the downstream slopes of rockfill dams of  $S = 0.67$ . Based on his data, Dornack (2001) developed a design equation for placed riprap applicable for  $0.10 \leq S \leq 0.67$ :

$$F_{s,c} = (0.649 \tan \alpha^{-0.6} + 1.082 \tan \alpha^{0.4})^{5/4} \cdot \sqrt{\left(\frac{\rho_s}{\rho} - 1\right) \cos \alpha}, \quad (2.3)$$

with  $\tan \alpha = S$  (plotted in Figure 2.2b). The second slope term in Equation 2.3 accounts for the stabilizing friction forces due to the inclination. In addition, Dornack points out that a loss of stones of 0.5 % is allowable without leading to failure of placed riprap. A further relationship is presented by Knauss (1979) including the packing factor  $\Phi$  in the equation:

$$F_{s,c} = 1.9 + 0.8\Phi - 3 \sin \alpha, \quad (2.4)$$

valid for stone densities of  $\rho_s = 2700 \text{ kg m}^{-3}$  and packing factors of  $0.625 \leq \Phi \leq 1.125$ , corresponding to approximately  $1.2 \geq P_c \geq 0.8$  (the boundaries correspond to the two dotted lines in Figure 2.2b). The  $\Phi$ -factor was defined by Scheuerlein (1968) as the ratio of the mean vertical roughness height to the mean horizontal width of the roughness elements. Knauss (1979) combined the data of the studies by Hartung and Scheuerlein (1970), Linford and Saunders (1967), Olivier (1967), Scheuerlein (1968) in Equation 2.4, which is

applicable for  $0.2 \leq S \leq 0.67$ . The above presented relationships are based on  $F_{s,c}$  and do not include the duration of overtopping. However, overtopping events are usually related to flood events and the discharge varies with time. Sommer (1997) indirectly included time-dependency in his three-step design approach for  $0.25 \leq S \leq 0.50$

$$F_{s,c} = 2.25 - 2.25S + 0.3S^{-7/6}, \quad (2.5a)$$

$$\frac{\Delta x_i}{d_s} = 0.048 \sin \alpha \cdot \left( \frac{L_i}{d_s} - 1 \right) \leq 0.5, \quad (2.5b)$$

with the displacement of a stone  $\Delta x_i$  at the location  $i$  and the corresponding allowable distance  $L_i$  to a downstream fixed structure. Step one in Equation 2.5a gives the relation between slope, discharge and stone size (plotted in Figure 2.2b). In step two, the extension  $L_i$  of the riprap has to be limited by constructing fixed cross-structures to restrict the displacements to  $\Delta x_i d_s^{-1} \leq 50\%$  (Equation 2.5b). Geotechnical considerations of the embankment are included in the third step. Sommer's approach is based on model tests where the placed riprap could not be destroyed with the available discharge of  $q_{\max} \approx 0.5 \text{ m}^2\text{s}^{-1}$ , corresponding to  $F_s = 3.3$ .

The remaining line in Figure 2.2b reflects a specific recommendation for the sizing of riprap stones used as erosion protection on the downstream slopes of embankment dams in Norway:

$$d_{\min} = 1.0 \cdot S^{0.43} \cdot q^{0.78} \quad (\text{NVE, 2012}) \quad (2.6)$$

The equation includes a safety factor and is based on the results of tests with dumped riprap and on recommendations of a research project focusing on the breach development of rockfill dams (EBL Kompetanse AS, 2005). The discharge to determine the minimal stone size  $d_{\min}$  depends on the consequence class of a dam. The Norwegian dams are classified into five classes (Class IV to Class 0) according to the consequences of a potential dam failure. The most severe Class IV implies that more than 150 households, important infrastructure and/or high environmental values are at risk (OED, 2009). The guideline for embankment dams (NVE, 2012) recommends to set the discharge per unit width in Equation 2.6 not lower than  $q \geq 0.5 \text{ m}^2\text{s}^{-1}$  for dams in consequence Class III and II and  $q \geq 0.3 \text{ m}^2\text{s}^{-1}$  for dams in Class I. For dams in the most severe class IV, the riprap stones need a minimum volume of  $V_{s,\min} = 0.15 \text{ m}^3$ . This volume corresponds to  $d_{\min} \approx 0.63 \text{ m}$ , which was used in combination with Equations 2.6 and 2.2 to construct

the corresponding line in Figure 2.2b. In addition to the recommendation for the stone size, there is the requirement to place the riprap stones in an interlocking pattern with their longest axes inclined towards the dam slope (OED, 2009).

The research project about the riprap stability on the downstream slopes of rockfill dams initiated in 2011 including this PhD study aims to increase the knowledge of placed riprap exposed to overtopping and through flow. The current recommendations are based on data of dumped riprap and data of placed riprap is needed. In the period 2011-2012, the effect of the embankment slope and of the inclination of the riprap stones  $\beta$  on the riprap stability was investigated in the framework of student projects, before this PhD study started in 2013. Furthermore, field tests with prototype-sized riprap were carried out in 2012 and documented in Lia, Vartdal, Skoglund, and Campos (2013). A summary of their result is included in Paper II of this thesis and an evaluation is presented in Paper IV.

# 3

## Research methodology

The scope and aim for the research project was to improve the design of placed riprap on the downstream slopes of rockfill dams. The objectives of the present research were derived based on the already available knowledge summarized in Chapter 2. Additionally, this chapter focuses on the specific methodologies to address the objectives.

### 3.1. Research design

Only a single study investigated the stability of placed riprap for steep slopes of 1:1.5 corresponding to  $S = 0.67$ . Hence, additional studies for placed riprap on slopes of  $S = 0.67$ , i.e., as steep as the downstream slopes of rockfill dams, are needed. Studies of placed riprap exposed to overtopping are limited. To quantify the stability gain compared to dumped riprap, both types of riprap need to be assessed. The force propagation within a placed riprap structure is not fully understood yet and small-scale laboratory experiments with natural stones were chosen to simulate the interstone connection as realistic as possible. To evaluate laboratory and scaling effects, field experiments at large- to prototype-scale are needed for result validation. These considerations are expressed in the following six research objectives.

#### Objectives:

1. Identify the important parameters of the riprap material and the hydraulics on the downstream slope.
2. Perform physical model tests to improve the data basis for dumped and placed riprap on slopes of  $S = 0.67$ .
3. Perform large-scale model tests to validate the results of the small-scale model tests.

4. Describe the failure of the ripraps qualitatively and as far as possible quantitatively. Identify the most exposed parts of the riprap.
5. Detect and describe the main hydraulic forces on the riprap with special focus on riprap failure.
6. Recommend properties for the design of placed riprap on the downstream slopes of rockfill dams and compare these to the effective guidelines and existing engineering practice.

The objectives were addressed in the subsequent described studies whereof two were at model-scale, two at large-scale, and one as prototype investigation. A detailed description of the experimental setups is included in Section 3.2. A considerable effort was made in testing a novel developed monitoring equipment to detect stone movements. These findings are presented in a separate study.

## **Studies:**

### **Model A (MA): Stability investigation of riprap**

Dumped and placed ripraps were exposed to increasing discharges. The discharge was stopped between each discharge increment to monitor the position of marked stones within the riprap. Some of them were equipped with Smartstone sensors (see description in Section 3.3).

### **Model B (MB): Scaled field tests**

The ripraps were exposed to the scaled discharges of the field tests in 2015 (see F15 below). Those were scaled based on the proportion between the stone sizes in the field and the model of 1:6.5.

### **Field 2013 (F13): Stability of placed riprap**

Placed riprap was exposed to overtopping to confirm findings of tests run at model-scale and to include more monitoring equipment compared to the tests in 2012 by Lia et al. (2013).

### **Field 2015 (F15): Validation of Model A**

The experiments were performed with smaller stones compared to F13. The monitoring equipment was extended as described below and the Smartstones were tested.

### **Sensor development (SST):**

Aiming to monitor the forces on a riprap stone at the moment of failure to improve the understanding of the erosion process.

### Prototype survey: Survey of constructed placed riprap

Placed ripraps constructed on the downstream slopes of 33 rockfill dams in Norway were investigated. The results were compared to the recommendations in the guideline for embankment dams (NVE, 2012) and the requirements in the dam safety regulation (OED, 2009). The summary of the report about the survey is included as secondary paper in this thesis.

Paper I presents the results of the model tests MA and MB and describes displacements as potential failure mechanism for placed riprap on steep slopes. The comparability of small-scale model tests and large-scale field tests is discussed in Paper II. Sensors to detect stone movements were tested during F13, F15 and MA. A novel developed monitoring equipment was tested. Its functionality as well as a first application are described in Paper III. The results of F13 are presented in Paper IV and accompanied with a brief literature review as well as a discussion of the field test results in 2012 (Lia et al., 2013). The prototype survey of placed riprap resulted in a report in Norwegian and is hence included as secondary paper in Appendix B. The connections between the scales, studies and papers are illustrated in Figure 3.1.

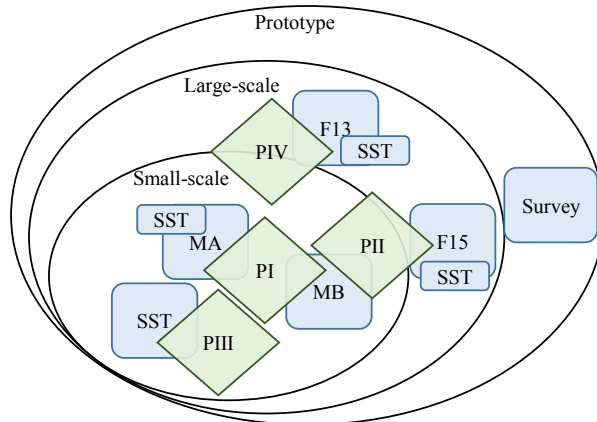


**Figure 3.1.:** Schematic presentation of the scales and the performed studies. Field tests (F'year') and model tests (M'nr') are symbolized with rectangles, papers (P'nr') with diamonds. Application and tests involving the Smartstone sensor 'SST' are indicated with rectangles and labelled correspondingly.



## 3.2. Experimental setup

All the experiments were designed to achieve riprap failure to evaluate the stability. As large stones as possible were used to reduce laboratory and scale effects. Experience from the tests described in literature and the field tests carried out by Lia et al. (2013) were used as a basis for the design. The scaling between the prototype, the large-scale field tests and the model-scale tests in the laboratory was based on Froude similarity. The range of the scales is assessable from the stone sizes presented in Table 3.1 and the grain size distribution curves in Figure 3.2. Prototype stones as used in placed riprap on the downstream slopes of rockfill dams in Norway are in the magnitude of 0.3 to 0.7 m in diameter, dependent on the consequence class of a specific dam and on the local available stone quality. The recommendation for the highest Class IV corresponds to  $d \approx 0.63$  m as described in Section 2.2. That reveals an approximate scale of 1:1.2 and 1:1.7 between the prototype and the field tests F13 and F15, respectively. The ratio between the stone size in the prototype and the model is 1:11. Owing the variation in available stone size for prototype riprap the conceptual model-scale is set to 1:10.

The discharge per unit width at the time when the first stone was eroded, is indicated with  $q_s$ , if the erosion of the stone was possible to observe. Progressive erosion of the riprap layer was considered as riprap failure. The corresponding critical discharge per unit width is given as  $q_c$ . The stone-related Froude numbers corresponding to erosion of the first stone and riprap failure are  $F_{s,s}$  and  $F_{s,c}$ , respectively.

**Table 3.1.:** Stone properties for the studies. The overline indicates mean values.

Study	$\bar{a}$ (m)	$\bar{b}$ (m)	$\bar{c}$ (m)	$\bar{d}$ (m)	$d_{50}$ (m)	$C_u$ (-)	$\rho_s$ ( $\text{kg m}^{-3}$ )
F13	0.71	0.48	0.34	0.48	0.54	1.58	2750
F15	0.53	0.35	0.23	0.35	0.37	1.24	2750
MA, MB	0.091	0.053	0.038	0.056	0.057	1.17	2710

### Physical model tests with small-scale riprap

The hydraulic model was specifically planned and constructed in the hydraulic laboratory at NTNU. The model consisted of a horizontal crest and an inclined chute with  $S = 0.67$ , whereof a length of  $L_s$  was covered with riprap (see Figure 3.3). The setup was designed to carry out destructive

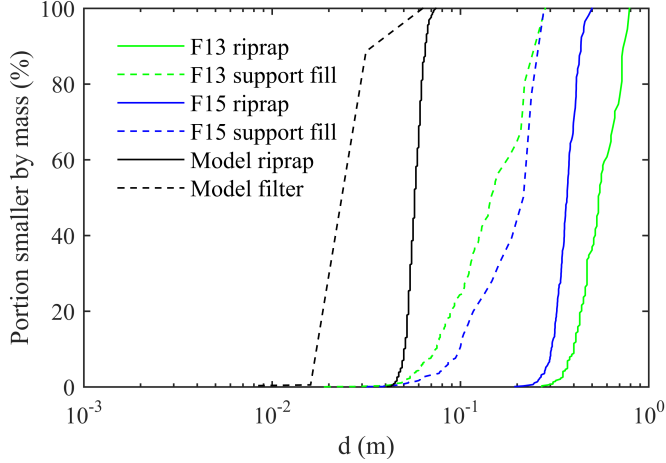


**Figure 3.2.:** Grain size distribution curves for the riprap and support fill/ filter for the field tests F13 and F15 and the model tests.

riprap tests to investigate the stability of dumped and placed riprap. Hence, the riprap stones were chosen to be small enough that the ripples should fail with the available discharge. The stone size was furthermore chosen as large as possible to avoid scale effects and follow the recommendations for the Reynolds and Weber number as described in Section 2.2. These two contradicting requirements for the stone size were balanced for the final choice. The critical stone-related Froude numbers were expected to be in a range of  $2 < F_{s,c} < 8$  for placed riprap, similar to the range of the existing data points in Figure 2.2b. The nominal diameter of 500 riprap stones was determined by measuring their  $a$ ,  $b$  and  $c$ -axes as well as their mass  $m$ , revealing in  $d_{50} = 0.057$  m and slight oblong stones with  $a/b = 1.7$  (see Table 3.1 for further details and Figure 3.2 for the grain size distribution curve). Placed riprap was constructed by placing the riprap stones by hand on the filter layer from down- to upstream. The stones were placed in an interlocking pattern with a target inclination of the longest axes towards the dam of  $\beta = 60^\circ$ . They were intentionally not placed with their longest axes perpendicular to the slope (most stable arrangement) to resemble a realistic inclination angle as in prototype riprap on rockfill dams (Hiller, 2016). Approximately 1200 riprap stones were required to cover the crest and the chute for  $L_s = 1.8$  m with placed riprap. Dumped riprap was constructed by placing the stones with

random orientation and without interlocking pattern. The stones could not be dumped and spread because of the steep slope.

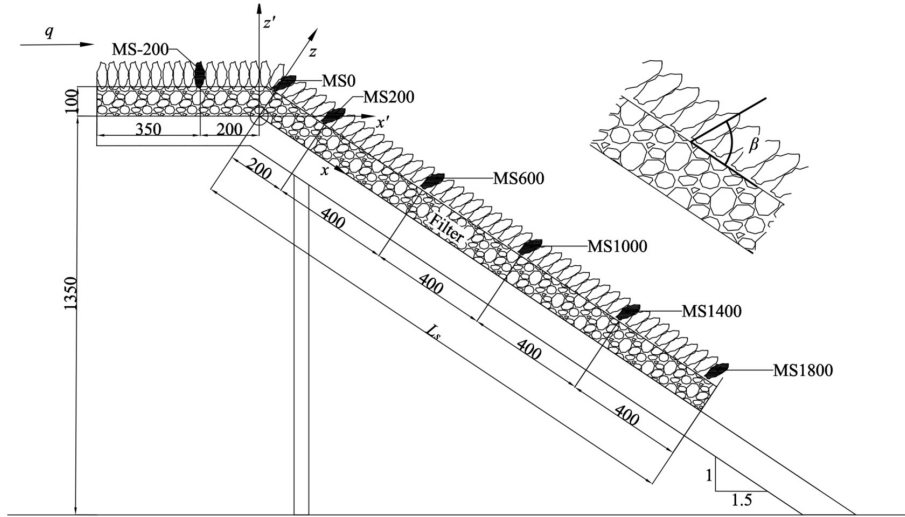


**Figure 3.3.:** Test set-up for the experiments with placed riprap P01 - P04 with  $L_s = 1.8$  m. The coordinate systems  $xyz$  and  $x'y'z'$  have their origin in the edge between the horizontal crest and the chute. The marked stones, which positions were tracked, are marked with 'MS' and their  $x$ -coordinate. The inclination angle  $\beta$  of the riprap stones is illustrated in the enlarged part in the top right. All dimensions in [mm].

Some riprap stones were marked at specific locations to monitor their position, see 'MSxx' in Figure 3.3, where 'xx' indicates the distance in flow direction from the edge between the horizontal crest and the chute. The riprap was loaded with step-wise increased discharges and the discharge was stopped between each step to inspect the riprap and to measure the positions of the marked stones. Consequently, valuable data about displacements within placed riprap could be gained. Displacements  $\Delta$  denote the difference in position compared to the original location of a stone. They can be divided in  $\Delta x$ ,  $\Delta y$  and  $\Delta z$  according to the coordinate system in Figure 3.3. Due to the regular discharge stops to determine the positions of the stones, the effort for running tests became more time consuming. A detailed description of the model setup, the monitoring equipment and the loading procedure can be found in Paper I.

For the study MA, four tests were carried out with placed riprap (P01-P04) and one with dumped riprap (D01). The study MB comprises of three tests with placed (P05-P08) and one with dumped riprap (D02). The boundary conditions in terms of the chute length covered with riprap  $L_s$  and the achieved packing factors  $P_c$  are presented in Table 4.1, which also contains the results.

### Field tests with large-scale riprap

The field tests with large-scale riprap stones were executed at a temporary site in Sirdal, Southwestern Norway. The site had already been used for tests with prototype-scale riprap in 2012 (Lia et al., 2013). The tests were supported by the site owner, Sira-Kvina power company, which provided the discharge and the opportunity to use the temporary infrastructure from the upgrading work of the nearby dam Svartevatn. The dimensions of the test dams (approximately 3 m high and 12 m wide on the top) were given by the dimensions of the spillway outlet channel where the dams were tested (see Figure 3.4). The discharge was regulated by a gate connected to the Svartevatn reservoir. A detailed description of the setup and the monitoring installations is presented in Paper II.



**Figure 3.4.:** Spillway outlet channel with a test dam covered with placed riprap (F15P2 in 2015). The crest of dam Svartevatn is visible in the upper right corner in the background. The discharge was provided from the reservoir impounded by the dam (Photo: NTNU).

The dimensions of the test dams and riprap stones as well as the expected high discharges were challenging for the selection of monitoring equipment. The conditions in the field were rough and equipment installed in the riprap was even exposed to the devastating conditions during the riprap failure and erosion of the test dams. Therefore, the equipment had to be either sufficiently robust to endure riprap failure and relocatable after the tests, or disposable, transferring the data before it was damaged or lost. The equipment not directly located in the flow, had to be robust enough for field conditions in terms of battery life-time and weather resistance. In addition, the safety of the operators had to be ensured.

The study F13 was conducted during one week in 2013 and comprised two tests with placed riprap (F13P1, F13P2). The used monitoring equipment is described and evaluated in Hiller and Lia (2015). For the tests in 2015 the monitoring equipment was enhanced compared to 2013 and two tests with placed (F15P1, F15P2) and one with dumped riprap (F15D1) were carried out within three weeks. The boundary conditions for both studies in terms of stone size  $d_{50}$  (detailed properties in Table 3.1 and Figure 3.2) and packing factors  $P_c$  are included in Table 4.2, which also contains the corresponding results.

### 3.3. Accelerometers and the Smartstone monitoring equipment

In order to optimize riprap design and quantify riprap stability, it is necessary to know the forces acting on a stone in the moment of erosion and to quantify those forces. The challenge is to measure the forces on a riprap stone within placed riprap without disturbing the interlocking placement pattern or the flow. To isolate a stone would mean to remove the contact forces to the neighbouring stones and therewith decrease the retention.

The concept to measure the forces in the moment of erosion of a riprap stone is based on Newton's law  $F = m \cdot a$ , which relates the force  $F$  to the product of mass  $m$  and the acceleration  $a$ . If it is possible to find a sensor to measure the acceleration in the moment of failure, the retaining force can be back-calculated. This allows to quantify the extra stability caused by the interlocking. The requirements for a suitable sensor to measure  $a$  were: (1) size (sufficient small to fit into the stones used for the model tests with  $d = 0.057$  m); (2) data transfer (preferably also during the tests to prevent data

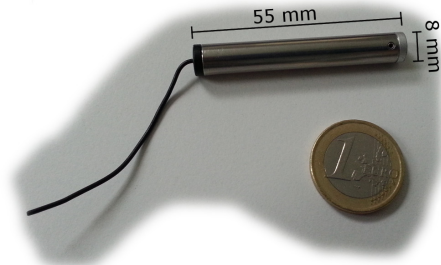
loss in case of sensor damage); (3) low cost (potential loss or damage during riprap failure and possibility to equip many stones with sensors).

In the course of the flourishing smartphone industry, the size and price of accelerometers have decreased considerably in the recent years. A couple of sensors already equipped with data loggers were evaluated for being mounted in riprap stones during the above described experiments: the Texas Instruments CC2541 SensorTag (Texas Instruments, 2013), the MSR 165 Data Logger (MSR Electronics GmbH, 2013) and the 'Messsystem Deckwerkstein' developed by the Federal Waterways Engineering and Research Institute in Germany (Mittelbach, Pohl, & Konietzky, 2014). All of them did not fulfill the requirements as they were too large to fit inside the stones used in the model. Additionally, MSR 165 was too expensive and CC2541 SensorTag used Bluetooth technology for data transmission that is not suitable for signal transfer through water.

A solution with a triaxial accelerometer, ADXL325 (Analog Devices, 2009), was tested during the field tests in 2013. Two stones were equipped for test F13P2 with one accelerometer each, which was casted in a waterproof enclosure and connected with cables to a computer for data acquisition and power supply (see Figure 3.5a). During the test, the sensors were registering no accelerations until dam failure, when the registration suddenly changed to noise caused by damage of the cable. Hence, the initial acceleration could not be registered and transmitted. Predetermined breaking points in the cables prevented the computer from being dragged into the water. The conclusion of the trial was that accelerometers were promising, but the solution had to be wireless.

In the following, a novel developed monitoring equipment with a sufficiently small probe was tested in collaboration with the Department of Physical Geography at Trier University. The hardware and software were engineered by the company SST (Smart Sensor Technologies) in Rheinberg, Germany. Incorporating smartphone technology in stones resulted in the name 'Smartstone'. The cylindrical probe (0.055 m long, 0.008 m in diameter and a mass of 0.0075 kg, Figure 3.5b), has a 0.07 m long flexible antenna and was mounted in a bored hole into stones, see Figure 3.5c. The probe contains a BMX055 sensor module (Bosch Sensortec, 2013) including a triaxial accelerometer, a triaxial gyroscope and a geomagnetic sensor; an active radio frequency identification (RFID) tag; a data logger with 262 kB memory; a chronometer; a thermometer and two silver-oxide button cells (1.55 V, 20 mAh) for power supply. The sensed data are transferred with radio to a gateway, which sends

the data over LAN or WLAN to a computer. A detailed description of the Smartstone monitoring equipment and its functions is presented in Paper III (Gronz et al., 2016). The Smartstones were tested in Study MA in the model stones as shown in Figure 3.5c. The probe was inserted in a marked stone and the hole closed with a rubber plug. For the field tests in 2015, one riprap stone was equipped with a Smartstone probe during the test F15P2, see Figure 3.5d.



(a) Accelerometer removed from a riprap stone after the field experiment F13P2 (Photo: NTNU) (b) Smartstone probe with size indication (Photo: O. Gronz)



(c) Smartstone probe mounted in a stone used for the model tests (Photo: NTNU) (d) Riprap stone equipped with a Smartstone probe (left) and a pressure cell (right) (Photo: NTNU)

**Figure 3.5.:** Smartstone probe and accelerometer in model and field applications.

# 4

## Summary of results

The results of the present PhD research are presented as summaries of four selected papers. The full papers are available in Appendix A.

The results of ten model tests and five field tests with large-scale riprap provided the data basis for the papers. The boundary conditions and the results are summarized in Table 4.1 for the model tests and in Table 4.2 for the field tests. A video of the field test F13P1 is available on: <http://www.iahrmedialibrary.net/overtopping-test-ntnu-sira-kvina/>.

**Table 4.1.:** Summary of the model tests carried out with riprap stones with  $d_{50} = 0.057$  m. Test P01 - P08 were carried out with placed riprap and D01 and D02 with dumped riprap. The boundary conditions are described by chute length covered with riprap  $L_s$  and packing factor  $P_c$ . The results of the experiments are presented with the critical discharge per unit width  $q_c$ , the ratio between the unit discharges for erosion of the first stone  $q_s$  and  $q_c$ , and the critical stone-related Froude number  $F_{s,c}$ .

Test	$L_s$ (m)	$P_c$ (-)	$q_c$ ( $\text{m}^2\text{s}^{-1}$ )	$q_s q_c^{-1}$ (-)	$F_{s,c}$ (-)
P01	1.8	0.56	0.24	0.42	5.6
P02	1.8	0.55	0.36	0.28	8.4
P03	1.8	0.52	0.25	1.00	5.9
P04	1.8	0.53	0.40	0.50	9.4
P05	1.0	0.48	> 0.49	n/a	> 11.5
P06	0.8	0.50	> 0.49	< 0.73	> 11.5
P07	0.8	0.56	> 0.49	n/a	> 11.5
P08	1.8	0.55	0.24	0.81	5.6
D01	1.8	1.05	0.04	1.00	0.9
D02	0.8	0.83	0.05	1.00	1.2



**Table 4.2.:** Boundary conditions and results of the field tests in terms of the mean stone diameter  $d_{50}$ , packing factor  $P_c$ , the critical discharge per unit width  $q_c$ , the ratio between the unit discharges for erosion of the first stone  $q_s$  and  $q_c$ , and the critical stone-related Froude number  $F_{s,c}$ . The tests in 2013 were carried out with placed riprap (F13P1, F13P2). Three additional field tests were run in 2015, whereof two with placed riprap (F15P1, F15P2) and one with dumped riprap (F15D1).

Test	$d_{50}$ (m)	$P_c$ (-)	$q_c$ ( $\text{m}^2\text{s}^{-1}$ )	$q_s q_c^{-1}$ (-)	$F_{s,c}$ (-)
F13P1	0.54	n/a	6.5	n/a	5.2
F13P2 <sup>a</sup>	0.54	n/a	2	1.00	1.6
F15P1	0.37	0.75	6.1	0.74	8.7
F15P2	0.37	0.64	7.5-8.0	0.84-0.79	10.6-11.3
F15D1	0.37	0.84	0.4-0.8	1.00	0.6-1.2

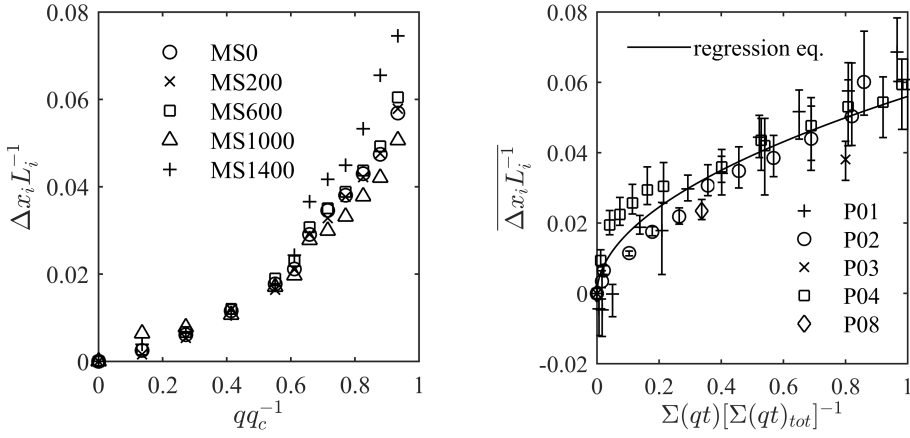
<sup>a</sup> failed due to an instability in the dam toe, i.e. not riprap failure

The packing factors  $P_c$  in Table 4.1 varied slightly between the tests and turned lower for the tests P03 - P06 with the increasing experience of experimentalists in setting the riprap stones. To counteract this effect, riprap stones were randomly picked and placed interlocking with the neighbouring stones without further optimization in the subsequent tests. The  $P_c$  value consequently increased again for P07 and P08. The packing factors for dumped riprap were considerably higher. Furthermore,  $P_c$  for placed riprap was lower in the model than in the field. The placed riprap in P05 - P07 did not fail with the maximum possible discharge of  $q_{\max} = 0.49 \text{ m}^2\text{s}^{-1}$  and  $q_c$  is in Table 4.1 given as  $q_c > 0.49 \text{ m}^2\text{s}^{-1}$ . The corresponding critical stone-related Froude numbers are  $F_{s,c} > 11.5$ . The erosion of the first stone could not be observed for P05 and P07 and is indicated with 'n/a' in Table 4.1. The ripples in the field tests F15P2 and F15D1 failed while increasing the discharge and therefore, the corresponding results are given as ranges in Table 4.2. Erosion of the first stone did usually not coincide with riprap failure for placed riprap, i.e.  $q_s q_c^{-1} < 1$ , except for P03 and F13P2. Erosion of the first stone in dumped riprap corresponded to riprap failure. The critical stone-related Froude numbers for placed riprap were on average seven times higher than for dumped riprap (see Tables 4.1 and 4.2), not included in the average are the tests P05 - P07 (no riprap failure) and F13P2 (instability in dam toe).

## 4.1. Paper I: Accumulating stone displacements as failure origin in placed riprap on steep slopes

The paper addresses failure mechanisms and stability for dumped and placed riprap. It includes the data of the studies MA and MB consisting of two tests with dumped (D01, D02) and eight with placed riprap (P01 - P08). The stability in terms of the critical stone-related Froude number  $F_{s,c}$  of placed riprap was in average five times higher than for dumped riprap, based on the aforementioned tests. The main finding is that accumulating stone displacements have to be considered as potential failure mechanism for placed riprap on steep slopes.

During the tests with placed riprap, a developing gap was observed on the downstream edge of the crest. The overtopping flow compacted the placed riprap on the downstream part of the chute, resulting in loosening further upstream. Stones adjacent to the gap gradually lost their interlocking and the riprap finally failed. Riprap failure started at the gap, where aeration was absent for the discharges at riprap failure and the velocity was close to the critical velocity corresponding to  $F = 1$ . The displacements were related to the distance between the marked stones and the downstream fixed end of the riprap, resulting in  $\Delta x_i L_i^{-1}$ . The relative displacements were independent of the location in the riprap as apparent in Figure 4.1a for the marked stones MS0, MS200, MS600, MS1000 and MS1400 and developed in the same way with increasing discharge. The maximum absolute displacements were observed at MS0 where  $L_i$  was maximal,  $L_i \approx 1.8$  m. The relative displacements of the marked stones were averaged, i.e.  $\overline{\Delta x_i L_i^{-1}}$ , to facilitate the comparison between the different tests (Figure 4.1b). To include time-dependency, the averaged relative displacements were related to the water volume per unit width that had passed over the riprap  $\Sigma(qt)$  relative to the total volume of water passed over the riprap before riprap failure  $\Sigma(qt)_{tot}$  (Figure 4.1b). In this way, time could be included in the stability analysis as  $F_{s,c}$  is independent of the exposure time. A regression analysis was carried out and the resulting equation is shown as line in Figure 4.1b. The regression equation in combination with the fact that the maximum displacements were observed for MS0 where  $L_i = 1.8$  m is maximal, revealed a 95% confidence interval for  $\Delta x_{max} = [0.090 \text{ m}, 0.115 \text{ m}]$ . This interval overlaps the range for the longest axes of the stones  $a = [0.069 \text{ m}, 0.115 \text{ m}]$ , with an average of  $\bar{a} = 0.091$  m. Consequently, placed riprap became unstable when the gap



(a) Relative displacements for the marked stones in test P02 (b) Averaged relative displacements relative to the water volume per unit width that had passed over the riprap

**Figure 4.1.:** Development of the relative displacements with increasing discharge exemplarily for P02 in (a) and averaged values for the tests with placed riprap where riprap failure occurred in (b). The error bars in (b) mark the minimum and maximum values for  $\Delta x_i L_i^{-1}$  included in the average  $\overline{\Delta x_i L_i^{-1}}$ .

exceeded one stone length. The displacements are therefore recommended to be limited to a stone length  $a > \Delta x_{\max} = 0.056L_s$ .

The observations revealed furthermore that the chute length covered with riprap  $L_s$  and the packing density  $P_c$  influence the displacements. The riprap in tests P05, P06 and P07, which were run with shorter  $L_s$  than P01 - P04 and P08 (see values in Table 4.1) did not fail with the maximum possible discharge of  $q_{\max} = 0.49 \text{ m}^2 \text{ s}^{-1}$ . In addition, the ripples in P05 and P06 were densely packed and had corresponding low  $P_c$  values.

Studies including displacement measurements within placed riprap are rare. However, there were two project reports (Sommer, 1997; Larsen et al., 1986) including comparable results for the observed displacements in the tests P01 - P04 and P08. This indirectly confirmed that displacements have to be considered as possible failure mechanism in placed riprap on steep slopes. The results of the two reports, written in German and not necessarily accessible to international researchers, are summarized in the paper.

Dornack (2001) and Larsen et al. (1986) recommended the construction of horizontal cross-structures perpendicular to the overtopping flow to limit the accumulation of longitudinal forces within the riprap and to prevent rupture of the riprap. This countermeasure would also limit the potential displacements and therefore contribute to an increased stability of the riprap. Nevertheless, further investigations are needed with focus on aeration and flow development, spatial characteristics of the displacements and exposed locations (crest, toe, abutments) to develop more precise recommendations.

## 4.2. Paper II: Field and model tests of riprap on steep slopes exposed to overtopping

The comparability of tests with large-scale riprap and model-scale riprap was investigated in terms of riprap stability expressed through the critical stone-related Froude number, packing factors and visual observed flow pattern. The scale between the field and model tests was 1:6.5 based on the ratio between the respective stone diameters. The paper is based on the studies F15 and MB. It contains the results of two large-scale riprap tests with placed riprap (F15P1 and F15P2) and one with dumped riprap (F15D1). The flow pattern over the riprap in test F15P2 is shown in Figure 4.2 for the lowest and highest applied discharge. The paper additionally includes five tests in model-scale, whereof four carried out with placed riprap (P05 - P08) and one with dumped riprap (D02).

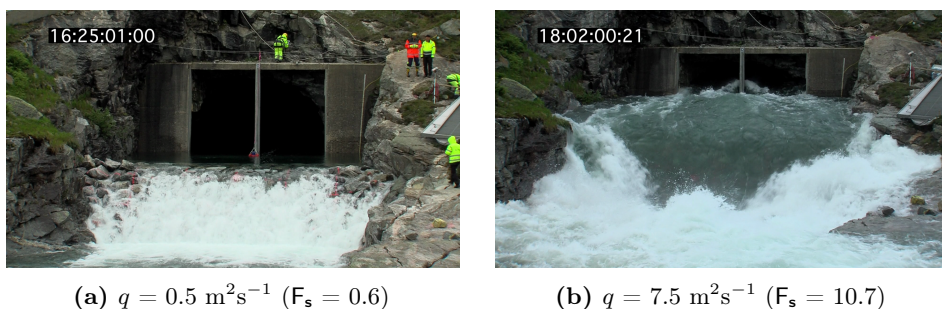


**Figure 4.2.:** Video snaps of the field test F15P2 with placed riprap. Cascading flow for the lowest discharge in (a) and skimming flow for the highest discharge just before riprap failure in (b) (Video: S.R. Skilnand).

The results for dumped riprap complied well between the field and the model tests in terms of the critical stone-related Froude number, packing

factors and flow pattern. The tests with placed riprap agreed well in the visual observed flow pattern as apparent when comparing Figure 5 with Figure 6 in Paper II (Appendix A). The relative overtopping height monitored upstream of the overtopped ripraps showed also good comparability. However, the riprap in the model tests P06 - P07 did not fail with the maximum possible discharge of  $q_{\max} = 0.49 \text{ m}^2\text{s}^{-1}$  corresponding to  $F_s > 11.5$ . They were carried out with a chute length of  $L_s = 0.8 \text{ m}$  corresponding to that of the downscaled field test dams. Therefore,  $L_s$  was extended for P08 to  $L_s = 1.8 \text{ m}$ . The riprap failed in P08 at  $F_{s,c} = 5.6$ . The packing factors for the placed riprap in the field were in average 33% higher than for the ripraps in the model tests. The denser packed riprap stones in the model are another possible explanation for the higher critical stone-related Froude numbers.

### **4.3. Paper III: Smartstones: A small 9-axis sensor implanted in stones to track their movements**

This paper was written as a Technical Note and presents the novel Smartstone monitoring equipment. The measuring principle is described in the paper as well as preliminary tests addressing technical features and the applicability of the Smartstones. The Smartstone monitoring equipment consists of the Smartstone probe, a gateway, and a computer for data communication. The core of the probe consists of a sensor module with a triaxial accelerometer, gyroscope and geomagnetic sensor. The technical specifications of the Smartstone were included in Section 3.3. The probe operates in three different modes: recording, standby and configuration. The sensor switches between recording and standby mode depending on impacts to optimize power consumption. The configuration mode allows active communication between the probe and the computer to set the sensor configuration depending on a specific application, e.g. measuring accuracy.

The preliminary tests revealed a maximum communication range of 280 m in case of intervisibility between the gateway and the naked probe. By inserting the sensor probe into a pebble, the range was reduced to approximately 50 m. One set of batteries lasted for about three to four cycles with continuous data acquisition at 10 Hz for 15 minutes and subsequent downloading and deleting of the data.

The capabilities and present limitations of the monitoring equipment were evaluated with the following experiment: A Smartstone probe was mounted

into a pebble and rolled down a laboratory flume. The movement of the sensor was calculated from the recorded sensor data. For comparison, the exact position was tracked by a high speed camera. The distance moved, derived by the Smartstone data, differed with 63.2% as mean absolute deviation compared to the trajectory captured with the high speed camera in a sample application with five runs on a distance of 1.5 m. In the online version of the paper a video of the experiment is included. It shows the data detected by the accelerometer and the geomagnetic sensors together with slow motion of the high speed-frames and a simulation of the moving pebble. The main sources of the differences were identified to be (given in increasing order of magnitude): quantisation error of the data due to limited precision, signal noise, integration error due to numerical integration, orientation error of the magnetometer data and clipping error in the accelerometer data. These errors can be reduced with more sophisticated data analysis and by adapting the sensor settings depending on the application. The errors are not independent. For example, an increased range of the accelerometer will on the one hand reduce the clipping error, but on the other hand increase the quantisation error because the resolution of the sensor decreases with increasing range.

The Technical Note concludes with recommendations for the further development, remaining accuracy tests, and potential applications within geomorphology and hydraulic engineering.

#### **4.4. Paper IV: Placed riprap as erosion protection on the downstream slope of rockfill dams exposed to overtopping**

This paper was written in an early stage of the present PhD research with the objective to summarize available data about placed riprap on steep slopes and to present preliminary results of the field study F13. The focus is on riprap in context of dams as the paper was presented at the 25<sup>th</sup> Congress on Large Dams and includes a brief presentation of the current requirements and recommendations of the Norwegian dam safety authorities.

Beside a brief literature study, an experimental study on stability of placed riprap is included that bases on results of model and field tests carried out in advance of this PhD research, but within the same research project. The inclination of the riprap stones against the dam surface  $\beta$  was identified as an important riprap parameter. Placed riprap with a stone inclination of

$\beta$  close to  $90^\circ$  was most stable (Lia et al., 2013). Moreover, the qualitative results of a Master's thesis showed that riprap loaded with through flow failed at lower discharges than riprap loaded with either through flow and overtopping or solely overtopping.

Studies with slopes comparable to the one on Norwegian rockfill dams and placed riprap were only found for spillway design of small embankment dams constructed for flood retention. The only study, which was found about placed riprap and  $S = 0.67$ , gives a formula for the design of the stone size dependent of the slope and the discharge. The formula was compared with the stone size and discharge recommended by the Norwegian guideline for embankment dams for a dam in consequence Class IV with  $S = 0.67$ . The formula revealed a stone size of  $d = 0.34$  m (including a safety factor of 1.6) and accorded to half of the stone size recommended in the guideline. Placing riprap with an interlocking pattern increases its stability compared to randomly dumped stones. Recommendations for dumped riprap can be used to design placed riprap. However, the design will be conservative with a large factor of safety and eventually result in oversized riprap stones. For example, placed riprap tested in large-scale field tests withstood a unit discharge of up to  $8 \text{ m}^2\text{s}^{-1}$  which was more than 10 times the recommendation in the guideline for embankment dams.

The paper concludes that recommendations for the design of placed riprap are rare and additional data are needed, especially for steep slopes. Furthermore, there is need for a consistent way to describe the pattern of placed riprap to facilitate comparison of different studies. A suitable description might also be used as a quality criteria for riprap exposed to overtopping.

# 5

## Discussion

The results presented in the papers are discussed. Moreover, the findings concerning riprap stability are related to erosion protection on the downstream slopes of rockfill dams. Finally topics for further research are recommended.

### Experiments

The tests carried out with dumped and placed riprap in small-scale model and large-scale field tests contribute valuable data about the riprap stability on steep slopes with  $S = 0.67$ . The results presented in Paper I, II and IV comply with the need for additional data based on large stone sizes and for steep slopes as corresponding data in the literature is scarce (cf. Figure 2.2). The stability gain of placed riprap compared to dumped riprap is found to be larger than previously supposed by Larsen et al. (1986) and Peirson et al. (2008). The more densely packed riprap in the presented study might contribute to the increased stability. Furthermore, the steep slope was close to the angle of repose of the riprap material and the stability of dumped riprap was therefore low.

The high stability of the placed riprap caused challenges because the setup of the model tests was designed for  $F_{s,c}$  up to 10 based on data available in literature. The combination of a short part of chute covered with riprap, short  $L_s$ , and low packing factors  $P_c$  resulted in placed ripraps, which did not fail in the test P05 - P07 with the maximum possible discharge. These ripraps finally failed when stones were manually removed from the riprap under overtopping. The tendency of increasing packing density was overcome by establishing and following rules for the construction of placed riprap as described in Paper I. The placed riprap in the field was looser packed than in the model. The difference in  $P_c$  indicates laboratory effects due to the more accurate placement of stones by hand (Pardo, Herrera, Molines, & Medina, 2014). A detailed comparison of placed riprap with other studies



was hampered because of the different ways describing placed riprap and its construction, if this information was included at all. The packing factor  $P_c$  was found to be an appropriate parameter to describe the packing density, but can only be determined post-construction. To allow comparison of studies, it is recommended to include information about the angularity of the stones, the stone shape in terms of the main axes, and their orientation within the riprap such as the inclination angle  $\beta$ , in addition to packing factor  $P_c$ .

The identification of accumulating displacements as failure mechanism for placed riprap on steep slopes in Paper I is a main contribution to the understanding of riprap behavior under overtopping. Stone displacements developed gradually during overtopping and formed a gap. Therefore, time must be incorporated in analyses of riprap stability. This was done in Paper I by relating the displacements to the discharge, and the water volume which had passed over the dam per unit width (integral of discharge over time). The critical size of the gap lead to a stability criteria. The displacements can be reduced by limiting the distance to the downstream end of the riprap. In case of a long chute, fixed cross-sections can be constructed to limit the distance over which displacements can accumulate as recommended by e.g., Dornack (2001), Larsen et al. (1986). The development of displacements is related to  $L_s$  and  $P_c$  because they affect the potential for small rearrangements of the riprap stones that are a source for the displacements.

The field tests with large-scale riprap gave a valuable validation of the results in the model tests and Paper II discusses the comparability between the two scales. The field tests in 2013 served mainly to test and evaluate different monitoring equipment (described in Hiller & Lia, 2015) and were essential for the preparation and successful realization of the tests in 2015. The height of the tests dams was limited due to the terrain and the downstream slope covered with riprap was relatively short. Nevertheless, results of tests with large riprap stones ( $d > 0.2$  m) are rare in the literature and the results of the field tests are a unique contribution to the knowledge about riprap stability.

## **Smartstone monitoring equipment**

The Smartstone monitoring equipment was a considerable improvement compared to the wired accelerometers used in the field tests in 2013. The advantages included the smaller size of the probe, wireless data transfer and identification with RFID. The triaxial magnetometer and gyroscope in

addition to the accelerometer allowed for monitoring of the orientation and rotating speed.

The sample application of tracking a Smartstone embedded in a pebble rolling down a flume, described in Paper III, reflects the focus on geomorphological processes of the collaborating research group at Trier University. The tracking of the entire erosion path is not necessary for addressing riprap stability. In order to quantify the acting force during erosion, the initial acceleration needs to be captured only, as described in Section 3.3. However, the current version of the Smartstones did not switch fast enough from standby to recording mode to record the initial acceleration, when it was tested in the model study MA and the field tests in 2015.

Further improvements are needed to successfully apply Smartstones in riprap stability studies. Based on the first experience with the novel equipment, it is recommended to extend the battery life time and to increase the measuring range for the accelerometers to  $\pm 16$  g to reduce clipping error. Furthermore, the software should be modified to allow faster switching between standby and recording mode in case of an impact, and to add the function to manually activate the recording mode over wireless communication. The focus of the present thesis is riprap design and the improvement of the Smartstones was left to the collaborators at Trier University after the field tests in 2015.

## **Riprap on the downstream slopes of rockfill dams**

From an engineering point of view dumped and placed riprap can be used to increase the stability of a dam slope against erosion from overtopping flow. It is important for both types of riprap to avoid flow concentration for example due to an unlevelled overtopping section or a trapezoidal dam profile resulting in an increase of the discharge per unit width, which can exceed the design discharge. For large dams, it is difficult to guarantee a constant elevation of the impervious core because settlements will occur over time. Moreover, the downstream end of the riprap has to be locked and the adjacent terrain sufficiently secured against erosion in order to guarantee the stability of the dam toe.

The highest stability in placed riprap is achieved by packing the stones as dense as possible (low packing factor  $P_c$ ) with their longest axes perpendicular to the dam slope. The critical stone-related Froude numbers presented in this thesis for slopes of  $S = 0.67$  and placed riprap are larger than the

corresponding existing data points in Figure 2.2b. However, for the design of placed riprap it is recommended to use the relationship in Equation 2.3 (Dornack, 2001) to determine the required stone size dependent on the design discharge and the slope, because the slope was varied in Dornack (2001).

The recommended equation in the guideline for embankment dams (NVE, 2012) should be revised accordingly as it is based on data for dumped riprap. The results for dumped riprap in the present thesis would plot above the line corresponding to the recommendation in the guideline in Figure 2.2b confirming the use of Equation 2.6 for dumped riprap with the inclusion of a safety factor. A recommended adaptation would allow the use of smaller stones. However, if larger stones are available at the site, they should preferably be used for the riprap. Larger stones withstand higher discharges and the construction of the riprap will take less time.

The revision of the guideline should also focus on the practicability of the recommendations. For example, the ratio between the smallest and the largest stone is not met by any of the 33 dams which were part of a survey of placed riprap on Norwegian rockfill dams (Hiller, 2016). Displacements as failure mechanism have so far not been considered and might be crucial for the stability of placed riprap. Assuming that there are no fixed cross-sections in a placed riprap with stones of  $d = 0.63$  m (corresponding to the recommendation for a Class IV dam, see Section 2.2), the length covered with riprap should not exceed 17 m to limit the displacements to one stone length,  $a$ -axis (see recommendations Paper I, Appendix A). This length of the slope corresponds to a dam height of 10 m, if  $S = 0.67$ . However, the displacements might develop slowly over time and would not exceed the critical level during a flood hydrograph, but further research is needed to clarify the time-dependency of displacements.

Technically speaking, the results of this PhD research show that dumped riprap exposed to overtopping complies with the recommended relation between slope, discharge and stone size in the guideline for embankment dams (NVE, 2012). However, dumped riprap does not fulfill the requirement in the dam safety regulation (OED, 2009) about an interlocking placement pattern. As a consequence, the question raises whether it is necessary to secure the downstream slopes of rockfill dams with placed riprap. A similar recommendation to protect the surface of the entire downstream slope from overtopping has not been found for other countries. A possible compromise is to limit the extra protection with placed riprap to the most exposed parts

of the downstream slope such as the dam toe, along the abutments and on the crest.

### **Recommendations for further research**

Before describing topics for further research, there are recommendations referring to optimise the experimental setup. A test facility to carry out model tests with placed riprap should have a sufficient chute length to allow complete flow development. Based on the results of this thesis the test facility needs a capacity corresponding to stone-related Froude numbers of up to 15. Placement rules are needed to balance the  $P_c$  values over several experiments. An arrangement to monitor the position of stones is required to gather data about displacements within the riprap layer. Valuable data can be gathered by running some tests with dumped riprap for comparison with literature and to quantify the stability gain of placed riprap.

Topics for further research:

**Statistical analysis about the effect of the packing factor  $P_c$  and the chute length  $L_s$  on the displacements  $\Delta$ :** The parameters  $P_c$  and  $L_s$  should be varied systematically in further model tests with placed riprap to quantify their effect on the displacements. Additional model tests similar to P01 - P04 will also increase the number of data points and hence allow for an extended statistical analysis of riprap stability in terms of the critical stone-related Froude number. The number of displacement monitoring points can preferably be increased to include the spatial development of the displacements over the entire slope.

**Time-dependency of riprap stability and erosion:** Systematic tests to quantify the effect of overtopping time on the riprap stability. The tests can be carried out by either varying fixed time intervals or by overtopping the riprap until a specific size of displacement is monitored. Scaled flood hydrographs can be applied to investigate the effect of overtopping on the riprap in relation to certain flood scenarios.

**Permeability of the rockfill:** The field tests revealed that the rockfill is not very permeable. Furthermore, the permeability of the rockfill might be inhomogeneous and have changed after the dam was built. In case of overtopping of the impervious core of a rockfill dam, the water will flow internally in the dam body before exiting on the lowest part of the slope. Increased knowledge about the permeability of the rockfill

would allow more accurate estimates of the flow through and over the riprap.

Moreover, a work group should address the questions about the necessity of placed riprap on the downstream slopes of Norwegian rockfill dams. The group should consist of the different stakeholders such as dam safety authorities, dam owners, engineers, entrepreneurs and politicians. They should revise the current requirement for placed riprap on the entire downstream slope and the recommendations for the corresponding discharges and stone sizes. The result should include practically achievable recommendations to comply with relevant load scenarios for socio-economic acceptable risks and costs. For complex hydropower systems consisting of several dams and reservoirs, there might be promising solutions where a measure on one component can have a positive effect for the entire system. Increasing the volume of a reservoir for example, will delay and reduce the peaks of a flood hydrograph for reservoirs located further downstream in the catchment. Another possibility for reservoirs with several dams is to construct one of the minor dams intentionally lower or as a fuse plug. Such structures will serve as emergency spillways in case of extraordinary floods and prevent overtopping of the main dam. Fortunately, a research project was initiated in 2015 to analyse dam safety on an overall perspective (Energy Norway AS, 2016) and will hopefully address the question of placed riprap on the downstream slopes of rockfill dams.

# 6

## Conclusion

The present PhD study increases the knowledge of riprap on steep slopes exposed to overtopping flow. The stability and design of dumped and placed riprap made of natural stone were studied. Dumped riprap consists of randomly oriented and dumped stones, whereas for placed riprap, the stones are placed one by one in an interlocking pattern. Most data is available for dumped riprap on gentle slopes and the literature review revealed that data for placed riprap and riprap on steep slopes of 1:1.5 corresponding to  $S = 0.67$  are scarce. The research objectives described in Section 3.1 were consequently developed and addressed.

The important parameters of the riprap and the hydraulics were identified. The riprap material is described with the size of the stones, their shape and grain size distribution. The dimensionless packing factor  $P_c$  was identified as a further important parameter to describe riprap. The  $P_c$  value quantifies the packing density and thereby reflects the different types of riprap, dumped or placed, as well as the orientation of the riprap stones. The hydraulics of the overtopping flow, can be characterised with the Froude number. Combining the parameters of the riprap material with the hydraulics results in the stone-related Froude number. As a consequence, riprap stability can be expressed through the critical stone-related Froude number, which is calculated with the the critical discharge at riprap failure and the size of the riprap stones.

Physical experiments were carried out with small-scale riprap stones in a model and with large-scale stones on a field site to investigate the riprap stability. The results provide additional data points for dumped and placed riprap on a slope of  $S = 0.67$ . A comparison between the results of the field and model tests revealed good agreement for dumped riprap in terms of the critical stone-related Froude number, packing factor, overtopping height and the visual observed flow pattern. Placed riprap showed good comparability for the flow pattern and the overtopping height, whereas the riprap in the

model tests were denser packed than in the field and represent an explanation for the higher critical stone-related Froude numbers in the model tests.

The position of selected stones within placed riprap were monitored during the model tests to describe riprap failure as detailed as possible. Small rearrangements of the riprap stones were detected and quantified with the stone monitoring. The measured stone displacements increased with increasing discharge and loading time. The size of the displacements were proportional to the distance between the corresponding monitored stone and the downstream end of the riprap. The displacements accumulated over the chute and an increasing gap developed in the transition between the horizontal crest and the chute. The stones adjacent to the gap were gradually losing their interlocking pattern, became unstable and caused finally riprap failure. A regression analysis of the stone displacements relative to the water volume which had passed over the riprap, revealed a confidence interval for the maximum displacements, which coincided with the range of the size of the longest stone axes. The model tests consequently revealed that accumulating displacements are a relevant failure mechanism for placed riprap on steep slopes. Comparing the results of dumped riprap with placed riprap, showed that placing the riprap stones in an interlocking pattern increased the stability and resulted in on average seven times higher critical stone-related Froude numbers.

In order to detect and describe the hydraulic forces on a specific riprap stone at the moment of failure, the novel 'Smartstone' monitoring equipment was tested in collaboration with Trier University. A Smartstone probe equipped with a triaxial accelerometer, gyroscope and magnetometer, aimed to detect the acceleration of the stone at the moment of riprap failure. However, the current version of the Smartstones did not yet allow the desired monitoring. Further development is needed to comply with the requirements for this specific application.

The observations of the accumulating displacements and the riprap failure resulted in a corresponding design criteria to limit displacements to the size of one  $a$ -axis of the riprap stones. Due to the gradual development of the gap, time-dependency has to be integrated in riprap stability analyses as proposed in the present research. Moreover, it is recommended to study the permeability of the rockfill below the riprap layer to get more accurate estimates for the portion of the discharge, which flows through the rockfill. The presented results were furthermore compared with the recommendations and requirements for placed riprap on the downstream slopes of rockfill dams

in Norway. The comparison indicated a generous safety factor as all the tests carried out with dumped riprap complied with the design recommendations for placed riprap. Hence, placed riprap as stability measure should be reevaluated in an interdisciplinary group with consideration of relevant loading scenarios to find a socio-economic optimized riprap design. Technically speaking, the highest riprap stability is achieved when placing large stones with proper interlocking and as dense as possible, i.e. oblong stones are placed with their longest axes perpendicular to the slope. However, dumped riprap might provide sufficient stability for certain applications. From an engineering point of view, the required stability has to be met balancing the stone size and packing density with the associated costs for construction as well as ensuring practical feasibility.





# Bibliography

- Abt, S. R. & Johnson, T. L. (1991). Riprap design for overtopping flow. *Journal of Hydraulic Engineering*, 117(8), 959–972. doi:10.1061/(ASCE)0733-9429(1991)117:8(959)
- Abt, S. R., Khattak, M. S., Nelson, J. D., Ruff, J. F., Shaikh, A., Wittler, R. J., ... Hinkle, N. (1987). *Development of riprap design criteria by riprap testing in flumes: phase 1* (Report No. NUREG/CR-4651). Nuclear Regulatory Commission.
- Abt, S. R., Thornton, C. I., Gallegos, H. A., & Ullmann, C. M. (2008). Round-Shaped riprap stabilization in overtopping flow. *Journal of Hydraulic Engineering*, 134(8), 1035–1041. doi:10.1061/(ASCE)0733-9429(2008)134:8(1035)
- Abt, S. R., Thornton, C. I., Scholl, B. A., & Bender, T. R. (2013). Evaluation of overtopping riprap design relationships. *Journal of the American Water Resources Association*, 49(4), 923–937. doi:10.1111/jawr.12074
- Analog Devices. (2009). Small, Low Power, 3-Axis  $\pm 5$  g Accelerometer, ADXL325. Data sheet.
- Bosch Sensortec. (2013). BMX055. Data sheet.
- Bunte, K. & Abt, S. R. (2001). *Sampling surface and subsurface particle-size distributions in wadable gravel- and cobble-bed streams for analyses in sediment transport, hydraulics, and streambed monitoring* (Report No. RMRS-GTR-74). United States Department of Agriculture.
- Chanson, H. (2015). Embankment overtopping protection systems. *Acta Geotechnica*, 10(3), 305–318. doi:10.1007/s11440-014-0362-8
- CIRIA, CUR, & CETMEF. (2007). *The Rock manual. The use of rock in hydraulic engineering* (2nd). London: CIRIA.
- Dornack, S. (2001). *Überströmbare Dämme - Beitrag zur Bemessung von Deckwerken aus Bruchsteinen [Overtoppable dams - design criteria for riprap]* (PhD Thesis, Technische Universität Dresden).
- EBL Kompetanse AS. (2005). *Stability and breaching of embankment dams, Report on Sub-project 2, Stability of downstream shell and dam toe during large through-flow*. Oslo: EBL Kompetanse AS.
- Eli, R. N. & Gray, D. D. (2008). Hydraulic performance of a steep single layer riprap drainage channel. *Journal of Hydraulic Engineering*, 134(11), 1651–1655. doi:10.1061/(ASCE)0733-9429(2008)134:11(1651)

- Energy Norway AS. (2016). Damsikkerhet i et helhetlig perspektiv [Dam safety in a overall perspective]. <https://www.energinorge.no/energiforskning/fornybar-energiproduksjon/vannkraft/dam/damsikkerhet-i-et-helhetlig-perspektiv/>. (Online; accessed 23 January 2017). Energy Norway.
- Frizell, K. H., Ruff, J. F., & Mishra, S. (1998). Simplified design guidelines for riprap subjected to overtopping flow. In *Association of State Dam Safety Officials*. Las Vegas.
- Godtland, K. (1989). *Steinfyllingsdammer: dimensjonering av nedstrøms plastringstein unntatt damfoten [Rockfill dams: design of riprap stones on the downstream slope except the dam toe]* (Report No. 82-595-5892-0). Norsk hydroteknisk laboratorium.
- Gronz, O., Hiller, P. H., Wirtz, S., Becker, K., Iserloh, T., Seeger, M., . . . Ries, J. B. (2016). Smartstones: A small 9-axis sensor implanted in stones to track their movements. *CATENA*, *142*, 245–251. doi:10.1016/j.catena.2016.03.030
- Hartung, F. & Scheuerlein, H. (1970). Design of overflow rockfill dams. In *10th Congress on Large Dams* (Vol. Q36, pp. 587–598). International Commission on Large Dams.
- Hiller, P. H. (2016). *Kartlegging av plastring på nedstrøms skråning av fyllingsdammer [Survey of placed riprap on the downstream slopes of rockfill dams]* (Report No. ISBN-10: 978-827598-095-1). Norwegian University of Science and Technology.
- Hiller, P. H. & Lia, L. (2015). Practical challenges and experience from large-scale overtopping tests with placed riprap. In M. Á. Toledo, R. Morán, & E. Oñate (Eds.), *Dam Protections against Overtopping and Accidental Leakage* (pp. 151–157). London: CRC Press/ Balkema.
- Hiller, P. H., Lia, L., Johansen, P. M., & Guddal, R. (2014). Dam Svartevatn - An example of challenging upgrading of a large rockfill dam. In *ICOLD Annual Meeting and Symposium*.
- International Commission on Large Dams. (1995). *Dam failures statistical analysis*. Bulletin 99. Paris: ICOLD.
- International Commission on Large Dams. (2016). World register on dams, general synthesis. (Online; accessed 28 October 2016). ICOLD.
- Jafarnejad, M., Franca, M. J., Pfister, M., & Schleiss, A. J. (2016). Time-based failure analysis of compressed riverbank riprap. *Journal of Hydraulic Research*, 1–12. doi:10.1080/00221686.2016.1212940
- Khan, D. & Ahmad, Z. (2011). Stabilization of angular-shaped riprap under overtopping flows. *World Academy of Science, Engineering and Technology*, *59*, 774–779.

- Kjærnsli, B., Valstad, T., & Høeg, K. (1992). *Rockfill dams: design and construction*. Trondheim: Norwegian Institute of Technology.
- Kjellesvig, H. M., Konow, T., Wiggen, T., & Stokseth, S. (2011). *Forvaltningspraksis ved norsk damsikkerhet - et sammenlignende studium av regelverk og forvaltningspraksis rundt damsikkerhet i Norge [Administrative practices in Norwegian dam safety - a comparative study about the regulations and administrative practices concerning dam safety in Norway]* (Report No. RA 684931-01). Energy Norway.
- Knauss, J. (1979). Computation of maximum discharge at overflow rockfill dams (a comparison of different model test results). In *13th Congress on Large Dams* (Vol. Q50, pp. 143–159).
- Larsen, P., Bernhart, H. H., Schenk, E., Blinde, A., Brauns, J., & Degen, F. P. (1986). *Überströmbare Dämme, Hochwasserentlastung über Dammscharten [Overtoppable dams, spillways over dam notches]*. (Unpublished report prepared for Regierungspräsidium Karlsruhe). Universität Karlsruhe.
- Lawrence, D. (2016). *Klimaendring og framtidige flommer i Norge [Climate change and future floods in Norway]* (Report No. 2016-81). Norwegian Water Resources and Energy Directorate.
- Lia, L., Vartdal, E. A., Skoglund, M., & Campos, H. E. (2013). Rip rap protection of downstream slopes of rock fill dams - a measure to increase safety in an unpredictable future climate. In *9th ICOLD European Club Symposium*. Italian Committee on Large Dams.
- Linford, A. & Saunders, D. H. (1967). *A hydraulic investigation of through and overflow rockfill dams* (Report No. RR888). British Hydromechanics Research Association.
- Løvoll, A. (2006). Breach formation in rockfill dams - results from Norwegian field tests. In *22nd Congress on Large Dams* (Vol. Q86, pp. 35–51). International Commission on Large Dams.
- Midttømme, G. H., Grøttå, L., & Hyllestad, E. (2010). New Norwegian dam safety regulations. In *8th ICOLD European Club Symposium* (pp. 351–355). Austrian National Committee on Large Dams.
- Ministry of Petroleum and Energy. (2009). Forskrift om sikkerhet ved vassdragsanlegg (Damsikkerhetsforskriften) [Dam safety regulation]. Legal Rule or Regulation.
- Mishra, S. K. (1998). *Riprap design of overtopped embankments* (PhD Thesis, Colorado State University).
- Mittelbach, L., Pohl, M., & Konietzky, H. (2014). A coupled DEM-CFD simulation of rip-rap revetements in tidal areas. In *11th International*

- Conference of Hydrosience and Engineering*. Federal Waterways Engineering and Research Institute.
- Morán, R. & Toledo, M. A. (2011). Research into protection of rockfill dams from overtopping using rockfill downstream toes. *Canadian Journal of Civil Engineering*, 38(12), 1314–1326. doi:10.1139/111-091
- Morris, M. W., Hassan, M. A. A. M., & Vaskinn, K. A. (2007). Breach formation: Field test and laboratory experiments. *Journal of Hydraulic Research*, 45(SPEC. ISS.), 9–17.
- MSR Electronics GmbH. (2013). MSR 165 Data Logger for shock and vibration. Data sheet.
- Müller, C., Frank, P.-J., & Hager, W. H. (2016). Dyke overtopping: effects of shape and headwater elevation. *Journal of Hydraulic Research*, 1–13. doi:10.1080/00221686.2016.1170072
- Norwegian Water Resources and Energy Directorate. (2012). Veileder for fyllingsdammer [Guideline for embankment dams]. NVE.
- Norwegian Water Resources and Energy Directorate. (2016). Database SIV [Norwegian dam register]. (Database; data extracted 31 October 2016). NVE.
- Olivier, H. (1967). *Through and overflow rockfill dams - New design techniques*. Institution of Civil Engineers.
- Orendorff, B., Al-Riffai, M., Nistor, I., & Rennie, C. D. (2013). Breach outflow characteristics of non-cohesive embankment dams subject to blast. *Canadian Journal of Civil Engineering*, 40(3), 243–253. doi:10.1139/cjce-2012-0303
- Pardo, V., Herrera, M., Molines, J., & Medina, J. (2014). Placement test, porosity, and randomness of cube and cubipod armor layers. *Journal of Waterway, Port, Coastal, and Ocean Engineering*, 04014017. doi:10.1061/(ASCE)WW.1943-5460.0000245
- Peirson, W. L., Figlus, J., Pells, S. E., & Cox, R. J. (2008). Placed rock as protection against erosion by flow down steep slopes. *Journal of Hydraulic Engineering*, 134(9), 1370–1375.
- Peirson, W. L. & Pells, S. E. (2005). *Steady state testing of scour protection options for Penrith Lakes weirs* (Report No. Technical report 2005/11). The University of New South Wales Water Research Laboratory.
- Pfister, M. & Chanson, H. (2012). Scale effects in physical hydraulic engineering models By VALENTIN HELLER, *Journal of Hydraulic Research*, Vol. 49, No. 3 (2011), pp. 293–306. *Journal of Hydraulic Research*, 50(2), 244–246. doi:10.1080/00221686.2012.654671

- Queisser, J. (2006). *Entwicklung landschaftsverträglicher Bauweisen für überströmbare Dämme [Development of landscape compatible construction methods for overtoppable dams]* (PhD Thesis, Universität Karlsruhe).
- Rathgeb, A. (2001). *Hydrodynamische Bemessungsgrundlagen für Lockerdeckwerke an überströmbarren Erddämmen [Hydro-dynamical design of riprap on overtoppable earthfill dams]* (PhD Thesis, Universität Stuttgart).
- Robinson, K. M., Rice, C. E., & Kadavy, K. C. (1998). Design of rock chutes. *Transactions of the American Society of Agricultural Engineers*, 41(3), 621–626.
- Scheuerlein, H. (1968). *Der Rauherinneabfluss [Macroturbulent flow]* (PhD Thesis, Technische Hochschule München).
- Schmocker, L., Höck, E., Mayor, P., & Weitbrecht, V. (2013). Hydraulic model study of the fuse plug spillway at Hagneck canal, Switzerland. *Journal of Hydraulic Engineering*, 139(8), 894–904. doi:10.1061/(ASCE)HY.1943-7900.0000733
- Siebel, R. (2007). Experimental investigations on the stability of riprap layers on overtoppable earthdams. *Environmental Fluid Mechanics*, 7(6), 455–467. doi:10.1007/s10652-007-9041-8
- Siebel, R. (2013). *Experimentelle Untersuchungen zur hydrodynamischen Belastung und Standsicherheit von Deckwerken an überströmten Erddämmen [Experimental investigations of the hydro-dynamic loading and stability of erosion protection on overtoppable earthfill dams]* (PhD Thesis, Universität Stuttgart).
- Solvik, Ø. (1991). Throughflow and stability problems in rockfill dams exposed to exceptional loads. In *17th Congress on Large Dams* (Vol. Q67, pp. 333–343). International Commission on Large Dams.
- Sommer, P. (1997). *Überströmbare Deckwerke [Overtoppable erosion protections]* (Unpublished report No. DFG-Forschungsbericht La 529/8-1). Institut für Wasserbau und Kulturtechnik, Versuchsanstalt für Wasserbau, Universität Karlsruhe.
- Texas Instruments. (2013). CC2541 Sensortag development kit. Data sheet. Texas Instruments.
- Thornton, C., Abt, S. R., Clopper, C., Scholl, B. N., & Cox, A. L. (2012). *Rock stability testing in overtopping flow*. Engineering Research Center, Colorado State University.
- Thornton, C., Abt, S., Scholl, B., & Bender, T. (2014). Enhanced stone sizing for overtopping flow. *Journal of Hydraulic Engineering*, 140(4), 06014005. doi:10.1061/(ASCE)HY.1943-7900.0000830

- Thornton, C., Cox, A. L., & Turner, M. D. (2008). *Las Vegas wash sloped rock-weir study*. Report prepared for the Southern Nevada Water Authority.
- Toledo, M. Á., Morán, R., & Oñate, E. (2015). *Dam protections against overtopping and accidental leakage*. London: CRC Press/ Balkema.
- Wittler, R. J. (1994). *Mechanics of riprap in overtopping flow* (PhD Thesis, Colorado State University).



## Selected papers





## Paper I

---

### **Accumulating stone displacements as failure origin in placed riprap on steep slopes**

Priska H. Hiller, Jochen Aberle, Leif Lia

In press: Journal of Hydraulic Research  
doi: <http://dx.doi.org/10.1080/00221686.2017.1323806>

---



## Displacements as failure origin of placed riprap on steep slopes

PRISKA H. HILLER, PhD Student, *Department of Civil and Environmental Engineering, NTNU, Norwegian University of Science and Technology, Trondheim, Norway*

*Email: priska.hiller@ntnu.no (author for correspondence)*

JOCHEN ABERLE (IAHR Member), Professor, *Department of Civil and Environmental Engineering, NTNU, Norwegian University of Science and Technology, Trondheim, Norway*

*Email: jochen.aberle@ntnu.no*

LEIF LIA (IAHR Member), Professor, *Department of Civil and Environmental Engineering, NTNU, Norwegian University of Science and Technology, Trondheim, Norway*

*Email: leif.lia@ntnu.no*

*Running Head: Displacements as failure origin of placed riprap*

# Displacements as failure origin of placed riprap on steep slopes

## ABSTRACT

This paper presents results from a scale model study related to the stability of dumped and placed riprap on steep slopes of 1: 1.5 (vertical: horizontal) exposed to overtopping. The experiments showed that small rearrangements of the stones in placed riprap, quantified as displacements of particular stones, led to a compaction in the lower part of the riprap and to loosening in the upstream part. The riprap became unstable when the maximum displacements exceeded the size of the longest axes of the riprap stones. The experimental data were used to develop a relationship to describe the development of the displacements taking the load-history into account. The obtained results were indirectly confirmed by comparison with findings of two reports which are described in the present paper. Moreover, placing the riprap stones in an interlocking pattern resulted in five times higher critical discharges compared to randomly dumped riprap.

*Keywords:* Displacements, erosion control, flow-structure interactions, hydraulic models, interlocking pattern, riprap stability

## 1 Introduction

Riprap is a common measure to protect shorelines, streambeds, river banks, dams, bridge piers and abutments as well as other hydraulic structures against erosion (e.g. Abt & Johnson, 1991; Abt, Thornton, Scholl, & Bender, 2013; Chanson, 2015; CIRIA, CUR, & CETMEF, 2007; Jafarnejad, Franca, Pfister, & Schleiss, 2016). It is defined as a permanent and erosion-resistant ground cover of large elements such as natural rocks or artificial elements to secure subjacent layers against the impact of hydrodynamic forces due to currents and waves. Riprap can be exposed to wave action or currents either perpendicular or parallel to the slope, and the elements forming the riprap can either be dumped or placed one by one in a specific pattern. These two construction methods define dumped riprap and placed riprap, respectively. Compared to dumped riprap, placed riprap is both more cost- and labour-intensive during construction. On the other hand, placed riprap offers specifically at steep slopes a higher stability in comparison to dumped riprap (Dornack, 2001).

A special application of placed riprap is to protect the downstream slopes of rockfill dams against erosion due to leakage, overtopping and violent attacks (e. g. Orendorff, Al-Riffai, Nistor, & Rennie, 2013; Toledo, Morán, & Oñate, 2015). Moreover, dependent on the dam-height, a specific area of the dam downstream side may be used as spillway by specifically creating a notch in the dam (e.g. Dornack, 2001; Larsen et al., 1986). In order to protect dams, dam safety regulations in Norway prescribe to protect the downstream slope with a placed riprap built with an interlocking pattern and the stones placed with their longest axes inclined towards the dam (Fig. 1; Ministry of Petroleum and Energy, OED, 2009). The typical downstream slopes of Norwegian rockfill dams are 1: 1.5 (vertical: horizontal) corresponding to a slope of  $S = 0.67$ , which is usually covered with a single-layered placed

riprap. Studies about riprap stability on such steep slopes with overtopping flows parallel to the slope are rare as most of the existing studies were carried out for milder slopes. It is against this background and the fact that many Norwegian dams need to be upgraded in the near future, including the construction or upgrade of placed riprap, that a research project was initiated to investigate the stability of placed riprap on steep slopes with the objective to improve corresponding design approaches. The project focuses on both small-scale laboratory investigations as well as large-scale field tests and further details on the project can be found in e.g. Hiller, Kjosavik, Lia, and Aberle (2016), Hiller and Lia (2015) and Lia, Vartdal, Skoglund, and Campos (2013).

In this paper, we present results from laboratory tests related to the stability and failure mechanisms of placed riprap due to stone displacement as a consequence of overtopping. Section 2 provides an overview over existing design relationships and summarizes findings of two reports related to stone displacement due to overtopping. Section 3 describes the physical model tests of which the results are presented in Section 4 and discussed in Section 5. Geotechnical stability criteria concerning the dam structure, as for example summarized in Larsen et al. (1986) and Morán and Toledo (2011), are beyond the scope of this paper.

## **2 Riprap stability on steep slopes**

Dumped and placed riprap are characterized by different failure mechanisms when being exposed to overtopping. The failure of dumped riprap is usually defined as the moment when the adjacent filter layer is exposed to the flow which occurs when the randomly placed surface layer stones are eroded (e. g. Abt & Johnson, 1991; Linford & Saunders, 1967; Peirson, Figlus, Pells, & Cox, 2008; Robinson, Rice, & Kadavy, 1998). Placed riprap, on the other hand, consists typically of a single surface layer of stones, which are placed in an interlocking pattern on top of a filter. The failure criteria for placed riprap has also been associated with filter exposure. For single-layer riprap, this means that erosion of the first riprap stone defines failure due to the exposition of the filter at this particular location. However, Dornack (2001), Larsen et al. (1986) and Sommer (1997) reported that the erosion of single stones in a placed riprap does not necessarily result in the loss of the structural integrity of the single-layer placed riprap structure. This is due to the fact that interlocking of stones results in a bearing structure increasing the stability compared to that of a single stone. In this context, Peirson et al. (2008) distinguish between ‘initial displacement of a single stone’, ‘significant rock motion’ (dislocation of five rocks over a distance of more than five stone diameters) and ‘armour failure’ when the filter layer is exposed. In the study of Peirson et al. (2008), erosion of the first stone out of placed riprap did not result in ‘armour failure’ as their dumped and placed riprap consisted of two layers of stones. Consequently, critical conditions can be defined at the discharge when progressive (bulk) erosion occurs (Dornack, 2001; Larsen et al., 1986; Sommer, 1997).

The interlocking of riprap stones allows for the transfer of longitudinal forces within the placed riprap. If these forces become large enough, they can cause either sliding or rupture of the riprap layer (Dornack, 2001; Larsen et al., 1986; Siebel, 2007; Sommer, 1997). Moreover, as will be described below, the longitudinal forces can cause a compaction at the lower end of the riprap layer resulting in a loosening of the riprap in the upper part. According to Larsen et al. (1986), such loosening can occur at very steep slopes and it represents a sore point in the riprap at which bulk failure may be initiated due to flow attack of the stones, which gradually lose their interlocking.

Although existing approaches for the determination of the stability of steep riprap take into account geometrical and flow boundary conditions, riprap material characteristics and fluid properties, they neglect the failure mechanism due to the combination of compaction and loosening. This may be due to the fact that most approaches have been developed for dumped riprap and slopes  $S < 0.2$  (see e.g. the summary of Abt et al., 2013) for which the failure mechanism 'displacement' is not of importance.

The surface layer of dumped riprap is usually parameterized by the stone density  $\rho_s$ , stone size  $d$ , grain size distribution, and the embankment slope  $S$ . For placed riprap an additional parameter, the packing factor, needs to be introduced to describe the quality of the placement as described further below. The flow over the riprap surface can be characterized by the Froude number  $F = v(gh)^{-0.5}$  with  $v$  = flow velocity,  $g$  = gravitational acceleration and  $h$  = water depth. When a riprap structure is overtopped, both  $v$  and  $h$  vary along the dam downstream slope until the flow is fully developed, meaning that  $F = 1$  at the crest and  $F > 1$  further downstream. However, the definition of  $v$  and  $h$  is hampered due to the rough bed conditions requiring the definition of an arbitrary bed level. This limits the applicability of  $F$  to investigate riprap stability. An alternative way is to use a so called "Schoklitsch-type" approach by combining  $F$  and the relative submergence  $h/d$  to a stone-related Froude number  $F_s = q(gd^3)^{-0.5}$  with  $q$  = discharge per unit width. At critical conditions (i.e. riprap failure) this Froude number becomes thus:

$$F_{s,c} = \frac{q_c}{(gd^3)^{0.5}} \quad (1)$$

where  $q_c$  = critical discharge per unit width at riprap failure.

Equation (1) allows for a direct comparison of experimental data from different studies at critical conditions. Figure 2a shows  $F_{s,c}$  as a function of the slope  $S$  for different studies carried out with dumped riprap. The data in Fig. 2a were extracted from Abt et al. (2013), who summarized experimental data of various investigations as described in the figure caption, as well as Godtland (1989), Larsen et al. (1986) and Peirson et al. (2008). The figure shows that the stability of dumped riprap decreases significantly with increasing slope due to the destabilizing effect of gravitational forces at larger slopes (e.g., Graf, 1991). Moreover, the comparison of the dumped riprap data with data for placed riprap reported by Dornack (2001), Larsen et al. (1986) and Peirson et al. (2008),

shown in Fig. 2b, verifies that placed riprap offers a higher stability at steep slopes. In fact, the data in Fig. 2b show that for the slope range covered by the placed riprap studies ( $S > 0.125$ ) the critical stone-related Froude number is generally  $F_{s,c} > 2$  while  $F_{s,c} < 2$  for the dumped riprap studies. In addition to the experimental data, Fig. 2b visualizes existing approaches derived for the sizing of riprap stones (excluding potential safety factors). The figure reveals differences between these approaches, which will be briefly highlighted in the following.

The placed riprap study of Dornack (2001) had the objective to optimize erosion protection of spillways on small earthfill dams constructed for flood retention. The investigation was based on experiments carried out with stones of a density  $\rho_s = 2610 \text{ kg m}^{-3}$ , an equivalent diameter  $d_s$  (diameter of a sphere having the same volume as an average stone) in the range of  $0.030 \text{ m} \leq d_s \leq 0.050 \text{ m}$ , slopes ranging from  $0.29 \leq S \leq 0.67$  and lengths covered with riprap of  $3.5 \text{ m} \geq L_s \geq 1.8 \text{ m}$ , respectively. Based on these data, Dornack (2001) developed a design equation for placed riprap applicable for  $0.1 \leq S \leq 0.67$ :

$$F_{s,c} = (0.649 \tan \alpha^{-0.6} + 1.082 \tan \alpha^{0.4})^{5/4} \cdot [(\frac{\rho_s}{\rho} - 1) \cos \alpha]^{1/2} \quad (2)$$

with  $\tan \alpha = S$ , where  $\alpha$  = slope angle, and  $\rho$  = density of water. In this equation, stabilizing friction forces due to the large inclination are indirectly taken into account by the second slope term. Equation (2) represents the lower boundary of Dornack's experimental data and its application would result in an adequate riprap design for the boundary conditions used by Dornack (2001) and Larsen et al. (1986) (see Fig. 2b). However, the formula does not describe the data of Peirson et al. (2008) (experimental parameters: two-layer riprap with  $0.076 \text{ m} \leq d_{50} \leq 0.109 \text{ m}$  where  $d_{50}$  = median stone size,  $2290 \text{ kg m}^{-3} \leq \rho_s \leq 2640 \text{ kg m}^{-3}$ ,  $0.2 \leq S \leq 0.4$  and  $8.4 \text{ m} \geq L_s \geq 4.2 \text{ m}$ , respectively). The latter data points are closer to the line defined by the approach developed by Knauss (1979)

$$F_{s,c} = 1.9 + 0.8\Phi - 3 \sin \alpha \quad (3)$$

which is valid in the range of  $0.1 \leq S \leq 0.67$  and was derived for stone densities of  $\rho_s = 2700 \text{ kg m}^{-3}$  and a packing factor  $\Phi$  ranging between  $0.625 \leq \Phi \leq 1.125$  (the two values are reflected by the two curves in Fig. 2b). According to Scheuerlein (1968), the  $\Phi$ -factor is defined as the ratio of mean vertical roughness height to the mean horizontal width of the roughness elements. Developing the approach, Knauss (1979) combined results from Hartung and Scheuerlein (1970), Linford and Saunders (1967), Olivier (1967) and Scheuerlein (1968). However, Peirson and Cameron (2006) found that the approach by Hartung and Scheuerlein (1970) was not conservative for design and revised the formula for the critical velocity accordingly. Their approach applicable for dumped riprap was further revised in Peirson et al. (2008).

The packing factor  $\Phi$  used in Eq. (3) is similar to a roughness density parameter, but may be difficult to determine in field situations. However, the above  $\Phi$ -factor range defined by the boundaries



0.625 and 1.125, respectively, can also be expressed in terms of a packing factor ( $1.2 \geq P_c \geq 0.8$ , respectively), with  $P_c$  being defined by Linford and Saunders (1967) and Olivier (1967) according to:

$$P_c = \frac{1}{N \cdot d_s^2} \quad (4)$$

where  $N$  = number of stones per  $m^2$ . Typical values for  $P_c$  range from 0.8 (stones placed on edge) to 1.2 (dumped stones), i.e.  $P_c$  is lower for a densely packed riprap compared to loosely packed or dumped riprap. Note that the placed riprap data of Dornack (2001) and Larsen et al. (1986) shown in Fig. 2b were characterized by  $P_c = 0.80$  and  $P_c = 0.63$ , respectively, which might explain some of the deviation in  $F_{s,c}$  compared to the Peirson et al. (2008) data for which  $P_c = 0.94$  (assuming  $d_s = d_{50}$  to calculate  $P_c$ ).

The stability criteria outlined above do neither reflect the effect of a potential compaction of the riprap layer due to flow forces nor consider a potential time-dependency of the erosion process as mentioned for example by Jafarnejad et al. (2016) in their time-based failure analysis of riprap exposed to flow perpendicular to the slope. The literature review carried out in the framework of the presented research project revealed reports of Larsen et al. (1986) and Sommer (1997) in regard to the significance of displacements for the stability of placed single-layer riprap composed of angular quarry stones. These reports were prepared in German and have thus not necessarily been available for international researchers. Although some findings of these studies become already apparent from the above considerations, some more details are presented in the following.

Larsen et al. (1986) studied the stability of both dumped and placed riprap (see data in Fig. 2). The majority of the tests with placed riprap were carried out with stones of  $d_s = 0.074$  m and  $P_c = 0.63$  with a length of the placed riprap of  $L_s = 2.34$  m at slopes of  $S = 0.125$ ,  $S = 0.25$  and  $S = 0.4$ . The single-layer riprap was placed below a chute section with fixed roughness elements. Larsen et al. (1986) found that the successive overtopping of the riprap with increasing discharges resulted in a compaction of the downstream part of the placed riprap at slopes of  $S = 0.25$  and  $S = 0.4$ . This compaction caused a loosening of the riprap further upstream close to the fixed chute part. The compaction was quantified by manual measurements of the displacement  $\Delta x$  (i.e. stone movement in flow direction compared to the initial location) of five individual stones following each discharge step. Larsen et al. (1986) normalized  $\Delta x$  with  $L_i$ , the distance between the measured stone and the downstream fixed point of the riprap, and observed a reasonable collapse of the individual displacement curves  $\Delta x_i/L_i$  when these were plotted vs. the applied discharges. The observed maximum relative displacements of the five stones ranged between 1.6 – 2.0% for  $S = 0.25$  and 1.3 – 2.0% for  $S = 0.4$ .

The experiments carried out with  $S = 0.125$ , on the other hand, resulted in smaller and more evenly distributed displacements which caused no significant loosening of the riprap. Larsen et al. (1986) hypothesized that in the latter case, the shear force by the overtopping water could, to a large extent, be transferred through friction into the filter layer (and hence into the embankment) while this

force-transfer mechanism was not as efficient for the steeper slopes. Larsen et al. (1986) recommended consequently that transverse cross-structures should be considered when designing steep ripraps to facilitate force transfer into the embankment and to limit displacements.

Sommer (1997) investigated single-layer, placed riprap with  $d_s = 0.134$  m and an average packing factor of  $P_c = 0.77$  at slopes of  $S = 0.25$ ,  $S = 0.33$  and  $S = 0.5$  in a 4.7 m long and 0.97 m wide chute. In comparison to Larsen et al. (1986), the experiments were carried out without a fixed upstream chute section. Moreover, Sommer (1997) added compressed air to the flow at the inlet section to mitigate effects arising from the short flow development zone upstream of the measurement section (approx. 0.7 m). The experiments were carried out by increasing the discharge in a stepwise manner and displacements were measured following each discharge increment. Displacements were quantified with a laser displacement meter along three longitudinal profiles of 2.7 m length (measured from the downstream fixed point). These profiles covered also a drag force measurement device installed in the riprap downstream region, which was protected by a rigid fence (for the analysis of drag forces see Sommer, 1997). Note that further details on individual displacement measurements as well as the loading history in terms of  $q$  and time reported by Sommer (1997) were available from one of the authors' project-thesis (Aberle, 1995).

Sommer (1997) reported difficulties to reach critical conditions for the tested ripraps, as they withstood the maximum possible discharge in the flume of  $q \approx 0.5 \text{ m}^2\text{s}^{-1}$ , i.e. for these experiments  $F_{s,c} > 3.25$ . The riprap remained stable due to the interlocking mechanism even if parts of the filter layer were eroded or if a gap developed at the upstream end of the riprap. In fact, failure in the experiments could only be achieved through manual manipulation of the riprap. The maximum relative displacements  $\Delta x_i/L_i$  found in the experimental series ranged between 0.5-2.4% for  $S = 0.33$  and 0.6-1.7% for  $S = 0.25$ .

Based on the experimental results, Sommer (1997) derived a three step recommendation for the design of placed riprap taking into account stone displacements. The first step includes the determination of the required stone diameter for a given discharge and embankment slope using Eq. (1) and

$$F_{s,c} = 2.25 - 2.25S + 0.3S^{-7/6} \quad (5)$$

Equation (5) may be interpreted as an intermediate approach between the approaches by Dornack (2001) and Knauss (1979) (Fig. 2b). Even though Sommer (1997) noted the gradual development of displacements in his tests, the time-dependency of the displacements was not incorporated in the design approach. In step 2, Sommer (1997) recommended the limitation of the riprap compaction to  $0.5d_s$ , i.e.  $\Delta x_i/d_s \leq 50\%$  through the construction of fixed cross-structures in the placed riprap. The corresponding allowable riprap length  $L_s$  upstream of such a cross-structure can be determined from the relationship

$$\frac{\Delta x_i}{d_s} = 0.048 \sin \alpha \cdot \left( \frac{L_s}{d_s} - 1 \right) \quad (6)$$

We note that the third step included geotechnical considerations, which are not in the focus of the present paper.

It is interesting to note that the application of Eq. (6) to estimate the relative stone displacements  $\Delta x_i/d_s$  for the data presented by Dornack (2001) and Peirson et al. (2008) results in intervals of [94%, 158%] and [67%, 113%], respectively. The lower limits of both intervals are larger than the value  $\Delta x_i/d_s \leq 50\%$  recommended by Sommer (1997) indicating that displacements may have been contributing to riprap failure, although details in regard to this issue have not been reported in these studies.

The above considerations show that stone displacements can be an important factor concerning the stability of placed riprap, especially on steep slopes. However, corresponding data are scarce and further investigation of displacements as failure mechanism requires additional data. The focus of the following sections is to determine and quantify stone displacements in placed riprap on steep slopes of  $S = 0.67$  exposed to overtopping and to relate the displacements to discharge and time.

### 3 Experimental setup and procedure

Experiments were carried out in a 25 m long, 2 m high and 1 m wide horizontal flume in the hydraulic laboratory of the Norwegian University of Science and Technology (NTNU). A conceptual 1:10 scale model of the downstream section of a dam was constructed along a 4 m long window section at the upstream part of the flume assuming Froude similarity. The base frame of the model consisted of a 0.55 m long horizontal crest and a 2.43 m long chute (along flow direction) with an inclination of 1:1.5 ( $S = 0.67$ ; see Fig. 3). The base frame was constructed from expanded metal which was sealed by a polyethylene mat and silicon at the transitions to the flume walls. The discharge to the flume was delivered by two pipes equipped with Siemens Sitrans Mag 5000 discharge meters and controlled by valves. The model was located sufficiently downstream of the inflow section to guarantee calm flow conditions at the crest of the model dam when testing the ripraps as described below. The upstream water level was monitored with a Microsonic mic +340 sensor located 1.6 m upstream of the crest corresponding to 3-4 times the overtopping depth at high discharges.

An automated 3D-traverse system at the top of the flume spanned the model section and allowed for the determination of coordinates of individual points along the model dam by an attached laser displacement meter with an accuracy of  $\pm 0.1$  mm in  $x$ - and  $y$ -direction and  $\pm 1$  mm in  $z$ -direction. Two Cartesian coordinate systems with the origin at the transition from the horizontal crest to the chute were defined to account for the horizontal and the sloped section, respectively (see Fig. 3). The  $x$ -axis of the first coordinate system  $xyz$  was aligned with the bottom of the chute while the second coordinate system ( $x'y'z'$ ) was rotated through  $-33.7^\circ$  with the  $x'$ -axis parallel to the horizontal

crest. The  $z$ - and  $z'$ -coordinate described the height perpendicular to the model base frame. Two video cameras were used to provide video footage of the tests. One camera was facing the dam while the second camera was filming through the flume window.

The tested riprap structures covered the 0.55 m long horizontal crest and a chute length  $L_s$  ranging between 0.8 - 1.8 m (see below for details). The adjustable downstream end of the riprap section was used to lock the riprap and constructed by an expanded metal sheet perpendicular to the chute. The downstream end of the riprap was elevated against the flume bottom to avoid backwater effects as the focus of the investigations was on erosion of the riprap due to overtopping and not failure due to scour development at the transition to the tail water area.

The tests were carried out with both placed and dumped riprap, which were installed on a filter layer (Fig. 3). The latter consisted of a geotextile and a 0.1 m thick layer of angular stones with a diameter  $d_{50,F} = 0.025$  m and a density of  $\rho_{s,F} = 3050$  kg m<sup>-3</sup>. The thickness of the filter layer was chosen in agreement with the Norwegian guidelines for the construction of embankment dams (Norwegian Water Resources and Energy Directorate, NVE, 2012). The riprap surface layer consisted of quarry stones of rhyolite with a diameter of  $d_{50} = 0.057$  m, a density of  $\rho_s = 2710$  kg m<sup>-3</sup> and an average mass of 0.24 kg. The  $d_{50}$  was derived from the grain size distribution (by mass) of the nominal diameter  $d = (abc)^{1/3}$  (Bunte & Abt, 2001) of 500 stones, where  $a$ ,  $b$  and  $c$  denote the longest, intermediate and shortest axis of the stones, respectively. The  $a$ ,  $b$ , and  $c$  axes were manually measured with a calliper and the mean values corresponded to 0.091 m, 0.053 m, and 0.038 m, respectively. The stones were angular to subangular and slightly oblong ( $a/b = 1.7$  in average) and, although individual stones varied in size, the grain size distribution of the surface stones could be classified as uniform ( $d_{60}/d_{10} = 1.17$  with  $d_{\min} = 0.041$  m and  $d_{\max} = 0.074$  m). The friction angle was evaluated with a tilting box to 50° and 52° for the filter and dumped riprap stones, respectively.

Placed riprap was constructed manually by placing stones from down- to upstream in an interlocking pattern. For the tests with  $L_s = 1.8$  m approximately 1200 stones were needed. The stones were placed at an angle of  $\beta \approx 60^\circ$  between the chute-bottom and the stones  $a$ -axis (see enlarged part in Fig. 3) and  $\beta \approx 90^\circ$  on the horizontal crest as these values are characteristic for existing ripraps at Norwegian dams (Hiller, 2016; Lia et al. 2013). Dumped riprap consisted of a layer with a thickness of approximately  $1.5 d_{50}$  and was constructed by randomly placing the riprap stones with an arbitrary orientation and without any interlocking pattern. Placing rather than dropping and spreading the stones was necessary due to the steep slope of  $S = 0.67$ . The number of placed or dumped stones was used to determine the packing factor  $P_c$  with Eq. (4) in Tab. 1 for both the placed and dumped riprap, respectively.

In the following, results from ten experiments are presented of which eight were carried out with placed riprap (tests P01–P08) and two with dumped riprap (tests D01 and D02). Tab. 1 summarizes the experimental boundary conditions for the tests. Five of the placed riprap tests were carried out with  $L_s = 1.8$  m (P01–P04 and P08), one with  $L_s = 1.0$  m (P05), and two with  $L_s = 0.8$  m

(P06 and P07). The tests with dumped riprap (D01 and D02) were carried out with  $L_s = 1.8$  and  $0.8$  m, respectively, and served for a direct comparison of the stability of dumped and placed riprap. We note that the reason for the different riprap length  $L_s$  was to enable a direct comparison of tests P05-P07 and D02 with field tests described in Hiller et al. (2016) which were carried out using 12 m wide and 3 m high test dams with riprap stones of  $d_{50} = 0.4$  m. The results of this comparison will be presented in a separate paper, as stone displacement could not be determined in the field tests.

It is worth mentioning that  $P_c$  for the placed riprap varied slightly between the tests. The lower  $P_c$  values for the tests P03-P06 reflect that the experimentalists became more experienced in packing the riprap (lower  $P_c$  values in Tab. 1). The  $P_c$  value for P07 and P08 increased again because the riprap stones were placed into the interlocking pattern without carefully choosing and placing each stone. This procedure aimed at the reduction of the effect arising through the experience in placing riprap (see below) and to reduce model effects due to manual placement compared to machine placement as described in Pardo, Herrera, Molines, and Medina (2014) for concrete elements. For the present experiments, this meant that the stones were randomly picked and then placed interlocking with the neighbouring stones without further optimization measures (i.e. the stones were not put at other locations where they would have fitted better). It was the intention to achieve interlocking, but not to minimize the porosity in the model (i.e.  $\beta \approx 60^\circ$  and not  $\beta \approx 90^\circ$ ) in order to construct the placed riprap as similar as in prototype conditions where the riprap stones are placed with an excavator and the selection is limited to the number of stones delivered by a truck.

In the present laboratory tests, the displacements of particular stones were determined using the aforementioned positioning system. We focused on the determination of the displacement of individual stones by measuring the position of a point marker tagged to their top instead of the determination of the positions of all stones because a complete scan of the riprap was hampered due to shadowing of the oblong stones. The marked stones were located along the centreline ( $y = y' \approx 0.5$  m) at fixed initial positions of  $x' \approx -0.2$  m and  $x \approx 0, 0.2, 0.6, 1.0, 1.4$  and  $1.8$  m, respectively, for  $L_s = 1.8$  m. For the tests with a reduced length  $L_s$  the number of marked stones was reduced so that the displacements of only four stones located at  $x' \approx -0.2$  m and  $x \approx 0, 0.2, 0.6$  m were determined. The marked stones can be identified in Fig. 3 and were labelled with “MSxx” where “xx” denotes their initial position along the  $x$ -axis. In the following, stone displacements  $\Delta x$ ,  $\Delta y$  and  $\Delta z$  are defined for the marked stones as the difference in the marker position compared to its original position before the riprap was exposed to the flow. Note that due to the different nature of dumped riprap, displacements were not measured in the tests D01 and D02.

The tests P01 and D01 were used to determine the specific discharge per unit width  $q$  through the filter only ( $0.007$  and  $0.006$   $\text{m}^2\text{s}^{-1}$ , respectively) as well as through the filter and riprap layer ( $0.012$  and  $0.020$   $\text{m}^2\text{s}^{-1}$ , respectively). These flows were characterized by a water level over the horizontal crest reaching the top of the filter layer (i.e. at the boundary between the filter and the riprap stones) and the tips of the riprap stones, respectively. The subsequent tests were started with a higher initial

specific discharge ranging between  $q = 0.05$  and  $0.20 \text{ m}^2\text{s}^{-1}$ . Following the initial load period,  $q$  was stepwise increased in intervals ranging from  $\Delta q = 0.02 - 0.05 \text{ m}^2\text{s}^{-1}$ . Each discharge was maintained for a specific time interval  $\Delta t$  and, before the next increase in  $q$ , the flow was stopped and the positions of the marked riprap stones were determined. The critical discharge  $q_c$  corresponded to the discharge where a complete failure of the riprap, i.e. progressive erosion (bulk failure), occurred. The discharge when the first stone was eroded from the riprap was labelled  $q_s$  and this discharge did not necessarily correspond to  $q_c$ . Note that the flow through both the filter and the riprap layer (included filter) for the tests with placed riprap corresponded only to a small percentage of the observed  $q_c$  (3% and 5%, respectively).

Tab. 1 shows that the experimental boundary conditions varied slightly between the tests as they were carried out with a different number of experimental steps  $n$  in order to reduce the time-effort or to test the effect of specific load patterns. For example in P04, the discharge was stepwise increased to  $q = 0.40 \text{ m}^2\text{s}^{-1}$  for which the flume head tank was intermittently (but only slightly) overtopped. Although the maximum discharge was applied in this test, the riprap did not fail and it was therefore decided to continue this test with a slightly reduced discharge of  $q = 0.35 \text{ m}^2\text{s}^{-1}$  to avoid further overtopping of the head tank. However, as the riprap did not fail after 12.5 h overtopping with this discharge,  $q$  was increased again to  $q = 0.40 \text{ m}^2\text{s}^{-1}$  before the riprap failed 4.5 h later. This test was thus used to investigate the effect of a long-term load of the riprap. Stone displacements were determined several times by stopping the flow.

As indicated above, the experiments P05-P07 were scaled according to the experimental procedure in the field tests by Hiller et al. (2016). A similar load sequence was applied in test P08 which, however, was carried out with a larger length  $L_s$  of the riprap layer in order to investigate the effect of  $L_s$  on riprap failure. The discharge was therefore directly increased after each step without stopping the flow in order to keep similarity in the load-pattern between the laboratory and field tests. This means that stone positions were determined following overtopping with an initial discharge and after the field discharge sequence was completed and the maximum achievable discharge  $q_{\max}$  was reached. Note that  $q_{\max}$  was increased in these tests compared to P04 due to some modifications at the inlet tank to facilitate an increased maximum discharge without overtopping of the head tank. The erosion of the first stone could not be unambiguously related to the applied discharge in the experiments P05 and P07 because of the restricted visibility of the riprap surface due to wavy water surface and highly turbulent flow conditions. Moreover, the riprap did not fail in P05-P07 even if the maximum achievable discharge was applied following the load of the riprap with the scaled field hydrograph. Failure could only be achieved through manually removing stones from the riprap, being the reason for the unknown critical discharge in Tab. 1 indicated by  $q_c > 0.49 \text{ m}^2\text{s}^{-1}$ .

#### 4 Results and analysis

The direct comparison of the critical discharges for the placed and dumped riprap reveals that the placed riprap had, in average, a five times higher stability than dumped riprap. This is also evident through the critical stone-related Froude numbers because the stone size was not changed during the present study. The placed riprap was characterized by a lower  $P_c$ , i.e. it was more densely packed than the dumped riprap (Tab. 1). Table 1 furthermore shows that the erosion of a single stone did not necessarily affect the structural integrity of the placed riprap as in all cases  $q_s < q_c$ , except for P03. It was observed that individual stones within the riprap were or became loose during the tests, so that they could be more easily eroded. The combination of placing more than 500 stones / m<sup>2</sup> and the asperities and uneven shapes of angular stones resulted in some clearance between the stones, despite their placement in an interlocking pattern. In the experiments, the loose stones could be identified due to their trembling motion during water flow. However, not all of these stones were necessarily eroded and some stabilized again after some time due to the compaction of the riprap, i.e. they were stabilized due to minor movements of their neighbouring stones. Failure of the placed riprap was observed at the transition between the horizontal crest and the inclined chute as result of the formation of a gap spanning the flume width. The gap expanded with both increasing experimental time and discharge and was caused by the gradual displacement of the riprap layer on the chute in flow direction. The displacements were caused by flow induced vibrations resulting in compaction of the placed riprap. In addition, the shear-induced force of the flow could not be completely transferred from the riprap stones through the filter and into the embankment. Due to the steep slope of  $S = 0.67$  the forces accumulated within the riprap layer. The displacements accumulated with increasing distance to the downstream riprap end (see also below) and the uppermost riprap stones on the chute consequently lost their interlocking making them more prone to the flow attack than interlocked stones. Moreover, some riprap stones, which were located immediately upstream of the developing gap, turned gradually over and covered the gap, with their  $a$ -axes aligned to the flow.

The displacement of individual stones  $\Delta x_i$  (but also in transverse and vertical direction  $\Delta y_i$  and  $\Delta z_i$ , respectively) depends on stone characteristics, packing density, stone distance to the fixed downstream end, the applied discharge (flow forces) and load period. The riprap was physically stabilized at the downstream end of the chute and at this position the displacements were  $\approx 0$  m. The displacement of individual stones in  $x$ -direction depends thus on the distance to the fix-point and can be normalized according to Larsen et al. (1986) by  $\Delta x_i/L_i$ , where  $L_i = L_s - x_i$  and the subscript  $i$  denotes the position of a stone along the  $x$ -axis. The displacements developed gradually during the discharge steps indicating that the time-dependency of the displacements should be included into stability approaches in addition to maximum failure discharge and critical stone-related Froude number, respectively. The combined impact of load period and discharge can be expressed by the product of these parameters, i.e.  $qt$ . Considering subsequent steps,  $qt$  needs to be presented as a sum, i.e.  $\Sigma(q_j\Delta t_j)$

where the subscript  $j$  denotes a discharge step. Tab. 2 summarizes the results for the placed riprap tests in regard to the stone related Froude numbers for the erosion of a single stone ( $F_{s,s}$ ) and bulk failure ( $F_{s,c}$ ), the maximum displacement  $\Delta x_{\max}$  in the step before the failure occurred, and  $\Sigma(qt)_{\text{tot}}$ . The latter is the total volume of water per unit width which had passed over the riprap, i. e.  $\Sigma(qt)_{\text{tot}} = \sum_{j=1}^{n+1}(q_j \Delta t_j)$ , where  $(n+1)$  denotes the discharge step in which the riprap failed. Note that dumped riprap failed for critical stone-related Froude numbers of  $F_{s,c} = 0.9$  (D01) and  $F_{s,c} = 1.2$  (D02), respectively.

A closer inspection of the displacements in  $x$ -direction showed that, as expected, the maximum displacement  $\Delta x_{\max}$  was generally observed at the transition from the horizontal crest to the chute, i. e. at MS0. Exceptions were the tests P01 and P03 where  $\Delta x_{\max}$  occurred at MS200 with  $\Delta x_{\max} = 0.125$  m and  $\Delta x_{\max} = 0.068$  m, respectively. These displacements were similar to the ones observed for MS0 and the larger displacements for MS200 may result from a rotation of the stones during displacement. Some stones rearranged with small movements to a temporary more stable position and the rearrangement due to the trembling was often accompanied by an increase of the inclination angle  $\beta$ . The displacement was determined by the marker at the top of the stone and thus an increase in  $\beta$  results in positive  $\Delta z$ - and small negative  $\Delta x$ -values which were superimposed of the longitudinal displacement. For example, if a riprap stone with  $a = 0.091$  m does not move in  $x$ -direction but rotates through  $30^\circ$  (from  $\beta = 60^\circ$  to  $\beta = 90^\circ$ ) the resulting displacements are  $\Delta x = -0.046$  m and  $\Delta z = +0.012$  m. Note that in all tests, the displacements in  $y$ - and  $z$ -direction,  $\Delta y$  and  $\Delta z$ , were small compared to  $\Delta x$  ( $\Delta y \leq 0.014$  m and  $\Delta z \leq 0.034$  m).

Figure 4a exemplifies the development of the cumulative displacement for the marked stones as a function of  $q$  for test P02 which was carried out with constant time steps of  $\Delta t = 3600$  s. The stones MS-200 and MS1800, located on the horizontal crest upstream of the transition to the chute and at the downstream end of the riprap, respectively, moved only marginally during the experiments. MS1800 was partly pulled out of the riprap during P02 so that  $\Delta x_{\max}(\text{MS1800}) = 0.012$  m (see Fig 4a), even though this particular stone was located in the first row upstream of the locked end of the riprap. During all other tests  $\Delta x_{\max}(\text{MS1800}) \leq 0.005$  m. Figure 4a shows further that the magnitude of the displacement of the stones MS0-MS1400 depended on the distance of the measurement stones to the downstream fixed point. Plotting  $\Delta x_i/L_i$  vs.  $q/q_c$  (which is equal to  $F_s/F_{s,c}$ ) results, similar to the observations of Larsen et al. (1986), in a reasonably good collapse of the data points as indicated by Fig. 4b for the stones MS0-MS1400. Note that the deviations of the normalized displacements between the different tests in Fig. 4b increase for  $q/q_c > 0.6$ . The relative displacements for each step were also examined for all tests, but it was not possible to isolate a specific discharge that caused a major displacement compared to the other discharges. The near collapse of the  $\Delta x_i/L_i$  values for MS0-MS1400 (Fig. 4b) indicates the possibility to consider averaged  $\Delta x_i/L_i$  values for each test. Figure 5a



presents the averaged normalized displacements  $\overline{\Delta x_i / L_i}$  (the overbar denotes the averaging operator) as a function of  $q/q_c$  for the tests that failed without manual interference (indicated in Tab. 2). For the tests P01-P03 and P08, the  $\overline{\Delta x_i / L_i}$ -curves show a reasonable agreement despite some differences in load-history. However, the data points for P04 deviate due to the long-term load pattern as described in the experimental procedure. This means that only tests with similar load periods can be compared in this way. Note that for P01, small negative  $\Delta x$  were observed for the lowest discharges, which can be associated with the aforementioned rotation of stones. Moreover, Figs 4b and 5a show that maximum displacement was not necessarily observed for  $q/q_c = 1$ . The maximum relative displacements associated with  $q/q_c < 1$  are, however, an artefact of the experimental procedure as the displacements could not be measured after riprap failure. The riprap failed in a load period with increased discharge (i.e. in step  $n+1$ ) being the reason for values  $q/q_c < 1$  (see Tab. 1 for details).

The displacements resulted in the development of a gap at the transition from the crest to the chute over time. Consequently, the combined impact of load period and discharge as mentioned above was included into the further analysis by considering  $\Sigma(qt)_{\text{tot}}$  in order to compare the relative displacements  $\overline{\Delta x_i / L_i}$  of the different tests. This was also necessary because  $\Sigma(qt)_{\text{tot}}$  varied between 291 and 33023 m<sup>3</sup> (see Tab. 2) reflecting that the development of the displacements depends on the packing of the riprap stones, i.e. the packing density represents an initial boundary condition for the displacements. Figure 5b shows the relative displacements  $\overline{\Delta x_i / L_i}$  as a function of  $\Sigma(qt)/[\Sigma(qt)_{\text{tot}}]$ . For the preparation of the figure,  $\Sigma(qt)$  was determined according to  $\sum_{j=1}^k (q_j \Delta t_j)$ , where  $k$  denotes the step for which the displacement was measured ( $k \leq n+1$ ). The sum  $\Sigma(qt)$  was then normalized by  $\Sigma(qt)_{\text{tot}}$  as defined above. The time interval  $\Delta t_{n+1}$  for the step  $n+1$  where riprap failure occurred was different from  $\Delta t$  given in Tab. 1 and, as mentioned above, the displacements could not be determined for this last load period so that  $\Sigma(qt)/[\Sigma(qt)_{\text{tot}}] < 1$  in Fig. 5b. In general, the data points collapse reasonably well on a single line. Note that, compared to the other tests, more data points are plotted for P04 for  $\Sigma(qt)/[\Sigma(qt)_{\text{tot}}] < 0.3$  (see Fig. 5b) due to the long term load associated with this particular test. For this experimental series, the low discharge-steps contributed only marginally to  $\Sigma(qt)_{\text{tot}}$  compared to the multiple steps associated with  $q_c$ .

Neglecting data points for which  $\overline{\Delta x_i / L_i} \leq 0$  (which we associate with measurement errors and/or stone rotation), the data in Fig. 5b were fitted by a power law with a coefficient of determination  $R^2 = 0.85$  (see also Fig. 5b):

$$\overline{\Delta x_i L_i^{-1}} = 0.056 \left\{ \frac{\Sigma(qt)}{\Sigma(qt)_{\text{tot}}} \right\}^{0.51} \quad (7)$$

The 95% confidence interval for the relative displacement  $\overline{\Delta x_i / L_i}$  at  $\Sigma(qt)/[\Sigma(qt)_{\text{tot}}] = 1$  is [0.050, 0.064]. As mentioned above, the maximum displacement was generally observed at MS0 so that  $L_i$

can be replaced by  $L_s$  when considering the maximum displacement. Thus, it becomes possible to estimate a maximum displacement interval  $\Delta x_{\max} = [0.090 \text{ m}, 0.115 \text{ m}]$  for  $L_s = 1.8 \text{ m}$  in the present study. It is interesting to note that the size of the longest stone axis  $a$  falls in this interval (average  $a = 0.091 \text{ m}$ ;  $a_{\min} = 0.069 \text{ m}$  and  $a_{\max} = 0.115 \text{ m}$ ).

## 5 Discussion

The results of the present study confirm the displacement of riprap stones during overtopping as a relevant failure mechanism for placed riprap on steep slopes of  $S = 0.67$ . Thus it can be inferred that the stability of placed riprap depends on both discharge, the chute length  $L_s$  and the overtopping-time as the displacements were observed to be gradually developing. Details on the load history were, however, only available for the study of Sommer (1997), and the following comparison of the present results with results from other studies is therefore limited to the critical stone-related Froude number  $F_{s,c}$  and the boundary conditions.

The critical stone-related Froude numbers  $F_{s,c}$  for dumped riprap obtained in the present study are smaller than  $F_{s,c}$  obtained by Peirson et al. (2008) even though the interstitial flow was included in the total discharge. Furthermore, erosion of the first stone for dumped riprap coincided with riprap failure in the present experiments whereas Peirson et al. (2008) reported  $q_s/q_c < 1$  (i.e. the ratio between initial displacement and armour failure). The difference between the present and the Peirson et al. (2008) study is that the latter experiments were carried out with lower slopes providing an adequate explanation for these differences (see also Fig. 2a). The comparison of the obtained  $F_{s,c}$ -values for placed riprap with the data shown in Fig. 2b reveals larger  $F_{s,c}$ -values than previously reported for  $S = 0.67$  ( $F_{s,c} \geq 5.6$ ). Moreover,  $F_{s,c}$  is, for the present experiments, larger than the predicted values according to the approaches from Dornack (2001), Knauss (1979) and Sommer (1997). Although the formula of Knauss (1979) considers indirectly flow aeration, the failure of the riprap was not affected by air entrainment in the present experiments.

Visual observations during the experiments showed that air entrainment started between  $0.2 \text{ m} < x < 0.4 \text{ m}$  for  $q = 0.1 \text{ m}^2\text{s}^{-1}$  and that the point of aeration moved downstream with increasing discharge. For  $q \geq 0.3 \text{ m}^2\text{s}^{-1}$ , air entrainment could no longer be observed. It can therefore be assumed that aeration is not a key factor in regard to stability considerations for comparable prototype situations as verified in the field observations by Hiller et al. (2016). Scale effects due to air entrainment are consequently assumed to be negligible. However, the flow is at the borderline for scale effects according to Pfister and Chanson (2012) who recommended  $W^{0.5} \geq 140$  (Weber number  $W = \rho h v^2 / \sigma$ , with  $\sigma =$  surface tension) to avoid significant scale effects in two-phase air-water flows under Froude similitude as  $W^{0.5} \approx 45$  for  $q = 0.1 \text{ m}^2\text{s}^{-1}$  and  $W^{0.5} \approx 145$  for  $q = 0.4 \text{ m}^2\text{s}^{-1}$  in the present experiments. Note that the absence of flow aeration is an indicator that the flow was not fully developed due to the restricted riprap-length, which is the reason why detailed investigations

concerning the flow field and flow resistance were not carried out. Nonetheless, riprap failure could be initiated even though flow velocities in the flow development zone were lower than in the fully developed flow zone (which was not reached in the present experiments for large discharges). This observation is in agreement with Dornack (2001) who observed riprap failure always upstream of the point of air entrainment. Inspecting Figs 4b and 5a and bearing in mind that aeration was absent for  $q > 0.3 \text{ m}^2\text{s}^{-1}$  and that aeration was observed between  $0.2 \text{ m} < x < 0.4 \text{ m}$  for  $q = 0.1 \text{ m}^2\text{s}^{-1}$  results in an interesting observation. The gradient of the displacement curves changes at  $q \approx 0.2 \text{ m}^2\text{s}^{-1}$  (or  $q/q_c \approx 0.6$ ), except for P04 (Fig. 5a), and shows slight differences with increasing discharge for the different stones (see results for P02 in Fig. 4b). In fact, for the lower discharges where aeration was observed, the displacements did not develop as pronounced as for larger discharges where aeration was absent. Although the hydrodynamic forces are smaller at lower discharges, aeration may result in even lower flow forces due to the reduction of the fluid density. Aeration might therefore influence the development of the displacements. The critical displacement-length, however, is assumed to be independent of aeration. Further investigations are required to substantiate this observation.

Failure of the placed riprap was in all tests initiated at the transition between the horizontal crest and the chute. The flow velocities at the crest are close to the velocity corresponding to  $F = 1$  and are thus lower than the maximal velocity over the steep chute. This is a clear indication that the maximum velocity  $v_{\max}$  over a steep and placed riprap has only an indirect effect on stability as failure is not initiated at the location where  $v_{\max}$  occurs. However,  $v_{\max}$  will have an effect on the stone displacement as it is a governing parameter for the drag forces exerted by stones, but this issue could not be investigated in the present experiments.

The placed riprap tests can be directly compared with the data reported by Dornack (2001) for  $S = 0.67$  and  $L_s = 1.8 \text{ m}$  (see Fig. 2b). Dornack (2001) used slightly smaller stones with a 4% lower density  $\rho_s$ , and the ripraps tested in his experiments were characterized by larger packing factors (in average  $P_c$  was 50% larger in his experiments compared to the present tests). This rather significant difference in  $P_c$  provides an explanation of the observed average difference of approximately 50% for  $F_{s,c}$ . Furthermore, it highlights the significance of the packing density on stability and hence indirectly the significance of stone displacements. A direct comparison with the data from Peirson et al. (2008) is difficult due to different slopes, single- compared to double-layered riprap, and a significant larger packing factor of  $P_c = 0.94$  in Peirson et al. (2008). This  $P_c$ -value corresponds nearly to the  $P_c$ -value for dumped riprap in the present study.

A quantitative comparison of the displacement data with the data reported by Larsen et al. (1986) and Sommer (1997) is difficult due to the difference in boundary conditions and the lack of a general approach to link displacements with hydraulic parameters. Moreover, a significant difference in the experimental setup is that the present tests were carried out with a horizontal crest, which was not present in the experiments of Larsen et al. (1986) and Sommer (1997). Nevertheless, the development of the gap at the transition between the crest and the chute due to the compaction and

loosening in the riprap layer, is an agreement with the conclusions of Larsen et al. (1986) and Sommer (1997) that displacements are an important failure mechanism for steep riprap.

Two specific data sets of Sommer (1997) for which detailed data were available from Aberle (1995) can be used to support the findings of the present study. For  $F_s = 3.25$  and  $L_i = 2.7$  m, Aberle (1995) reported relative displacements of  $\Delta x_i/L_i \leq 0.024$  for a slope of  $S = 0.33$ , before the riprap was manually manipulated to induce failure. The riprap was loaded in steps of  $\Delta q = 0.1 \text{ m}^2\text{s}^{-1}$  up to a maximum achievable discharge of  $q = 0.5 \text{ m}^2\text{s}^{-1}$  with  $\Delta t = 1800$  s resulting in  $\Sigma(qt) = 2700 \text{ m}^2$  for stone related Froude-numbers up to  $F_s = 3.25$ . Assuming the applicability of Eq. (7), despite the fact that it has been derived for  $S = 0.67$ , yields  $\Sigma(qt)_{\text{tot}} = 14220 \text{ m}^2$  by inserting  $\overline{\Delta x_i / L_i} = \Delta x_i / L_i = 0.024$  and  $\Sigma(qt) = 2700 \text{ m}^2$ . Furthermore, assuming that the load pattern would be continued by increasing the discharge with  $\Delta q = 0.1 \text{ m}^2\text{s}^{-1}$  every  $\Delta t = 1800$  s until  $\Sigma(qt)/[\Sigma(qt)_{\text{tot}}] \approx 1$ , results in  $q_c \approx 1.2 \text{ m}^2\text{s}^{-1}$ . Applying the same calculations for the second data set for which  $\Delta x_i/L_i \leq 0.017$  on a slope of  $S = 0.25$  (Aberle, 1995), reveals  $\Sigma(qt)_{\text{tot}} = 27960 \text{ m}^2$  and  $q_c \approx 1.7 \text{ m}^2\text{s}^{-1}$ . The calculated  $q_c$  for  $S = 0.33$  and  $S = 0.25$  correspond to critical stone-related Froude numbers of  $F_{s,c} = 7.8$  and  $F_{s,c} = 11.1$ , respectively, and are in the same range as the  $F_{s,c}$  values of the present study.

Equation (7) can also be compared with Eq. (6). At riprap failure  $\Sigma(qt)/[\Sigma(qt)_{\text{tot}}] \approx 1$  and, as the maximum displacements  $\Delta x_{\text{max}}$  were observed at MS0 for which the distance to the fixed point corresponds to the chute length, i. e.  $L_i = L_s$ , the left hand side of Eq. (7) can be replaced by  $\Delta x_{\text{max}} / L_s$ , resulting in

$$\Delta x_{\text{max}} = 0.056L_s \quad (8)$$

This equation is valid for  $S = 0.67$  and  $P_c = 0.56$  (representing the average of  $P_c$  for P01-P04 and P08). Equation (6) can be rearranged so that

$$\Delta x = 0.048L_s \sin \alpha \quad (9)$$

assuming that  $L_s/d_s - 1 \approx L_s/d_s$  for large  $L_s/d_s$  values. The factor  $(0.048 \sin \alpha) = 0.027$  for  $S = 0.67$  and is thus 47.5% smaller than the factor in Eq. (8). However, the packing factors in the present study were different from the packing factor in Sommer (1997). The packing factor  $P_c$  affects the development of displacements because dense packing minimizes the amount of void between the riprap stones and thus the extent of the displacements. Sommer (1997) used  $\sin \alpha$  to include the effect of the slope in Eq. (6). For his data with  $S \leq 0.5$   $\sin \alpha \approx \tan \alpha$ , whereas for extrapolation to steeper slopes, we consider using  $\tan \alpha$  as more appropriate. Hence, using the inverse proportion of the packing factors  $0.8/0.56$  and  $\tan \alpha$  instead of  $\sin \alpha$  results in a factor of  $0.047$  for  $\tan \alpha = 0.67$ , which is reasonably close to  $0.056$ . Moreover, Sommer (1997) recommended a limitation of the maximum displacements to  $0.5d_s$  for the design of placed ripraps as discussed in Section 2. Sommer (1997) used stones for which  $a/b = 1.2$  which is smaller than the ratio of the slight oblong stones with  $a/b = 1.7$  in the present study. The placed riprap in the present study remained stable until the gap in the break-point between crest and chute spanned the size of an  $a$ -axis of a stone (i.e. larger than  $0.5 d_s$ ). Thus,

the proportions and shape of the stones as well as their variation in size might also influence the maximum achievable packing density and the limit for the maximum allowable displacement. Placing oblong stones with their longest axes normal to the slope will, for example, result in a higher packing density (lower  $P_c$  value) than placing cubical stones with the same volume. For dumped riprap, angular-shaped stones provide higher stability than round stones of the same size (Abt, Thornton, Gallegos, & Ullmann, 2008) and a similar effect can be assumed for placed riprap as the asperities will increase the interlocking forces between the stones.

Dornack (2001) recommended to construct cross-structures perpendicular to the flow direction in placed riprap to limit the accumulating longitudinal forces and a consequent disruption of the placed riprap. Furthermore, such structures can be used to limit the displacements (Larsen et al., 1986; Sommer, 1997). The present study supports the need of such cross-structures because the test series P05, P06 and P07, which were carried out with reduced  $L_s$ , did not fail compared to the tests with longer lengths. For steep ripraps of larger length  $L_s$  without cross-structures, the displacements are assumed to either accumulate at the upstream end of the riprap structure or the riprap will rupture due to inhomogeneity in the riprap and the subjacent filter so that several gaps may develop. The development of displacements is time-dependent and implies that the duration of overtopping has to be included in the design of placed riprap on steep slopes. A prerequisite for displacements as failure mechanism is that the flow forces will be large enough to initiate riprap failure, i.e. to erode stones and hence, a lower threshold value for the critical discharge exists. For the design of placed riprap on spillways or as extra safety against accidental overtopping, a flood hydrograph for the specific site with the required return period has to be chosen as a basis for design. In case of overtopping as an extraordinary load, certain displacements are acceptable because the riprap can be repaired after the flood event.

## 6 Conclusions

Results from physical model tests of placed riprap on steep slopes exposed to overtopping demonstrated that placing riprap stones in an interlocking pattern increased the stability in terms of the critical unit discharge for failure and the critical stone-related Froude number approximately five times in comparison to randomly dumped riprap. Erosion of the first stone did not necessarily cause failure and progressive erosion should be used as failure criteria. The results of the present study as well as the findings reported by Larsen et al. (1986) and Sommer (1997) identify displacements accumulating within the riprap as crucial for the stability of placed riprap on steep slopes. Consequently, displacements need to be considered as a failure mechanism for placed riprap in addition to the established failure mechanisms such as the stability in terms of the critical stone-related Froude number. The chute length  $L_s$  as well as the packing density affect the potential compaction of the riprap stones and hence the development of a gap as sore point within the riprap. Riprap stones located at the developing gap lost gradually their interlocking, and the riprap failed in

the present study when the maximum displacement exceeded the longest axes of the riprap stones. The displacements relative to the distance to the downstream fixed point developed quantitatively in the same way over the slope. Their development was related to the relative water volume, which had passed over the riprap layer. A regression formula was derived and combined with a maximum allowable displacement  $\Delta x_{\max}$  corresponding to the length of the  $a$ -axis of the riprap stones. This resulted in a stability criteria of  $a/L_s > 0.056 = \Delta x_{\max}/L_s$  based on the data from the present study. Additional data from independent studies are needed to evaluate and quantify the effect of the discharge magnitude as well as the time-dependency in the form of the passed water volume on the development of the displacements. Moreover, the slope, packing and chute length will also influence the development of the displacements but the aforementioned design criteria for the displacements is only dependent on the chute length.

Further investigations should also focus on the effect of aeration as well as flow development on displacements. Spatial characteristics of displacements should be considered as well as the stability at exposed locations such as the downstream end of the riprap and abutments, e.g. along the typical trapezoidal geometry of the downstream slopes of embankment dams. It is worth mentioning that advanced measuring equipment can allow for direct monitoring of riprap compaction in both the field and laboratory. For example, intelligent sensors with accelerometers and positioning systems as described by Gronz et al. (2016) may be used to directly monitor the movement of individual riprap stones over longer time-periods. Such information can subsequently be used to assess the quality of the riprap over time.

### **Acknowledgements**

The authors thank the Master students Eirik Helgetun Pettersen, Jens Jakobsen and Fredrikke Kjosavik for their help in carrying out the physical model tests and the staff in the NTNU hydraulic laboratory for technical assistance. The agreements to use the reports of Larsen et al. (1986) and Sommer (1997) by the Regierungspräsidium Karlsruhe and the Karlsruhe Institute of Technology are acknowledged. The authors appreciated the comments of the editor and reviewers which helped to improve this article.

### **Funding**

The financial support of the collaborators within the project “Placed riprap on rockfill dams” (PlaF) coordinated by Energy Norway, and the Research Council of Norway [project no. 235730] is kindly acknowledged.

## Notation

$a, b, c$	= main axes of a stone (longest, intermediate, shortest) (m)
$d$	= stone size (m)
$d_i$	= stone diameter of grain size distribution corresponding to $i$ % finer (m)
$d_s$	= equivalent stone diameter (m)
$F$	= Froude number (–)
$F_s$	= stone-related Froude number (–)
$F_{s,c}$	= critical stone-related Froude number at riprap failure (–)
$F_{s,s}$	= stone-related Froude number at erosion of first stone (–)
$g$	= gravitational acceleration ( $9.81 \text{ m s}^{-2}$ )
$h$	= water depth (m)
$L_i$	= distance to the downstream fixed point (m)
$L_s$	= slope length (m)
$m$	= stone mass (kg)
$n$	= number of steps (–)
$N$	= number of stones per unit area ( $\text{m}^{-2}$ )
$P_c$	= packing factor (–)
$q$	= unit discharge ( $\text{m}^2 \text{ s}^{-1}$ )
$q_c$	= critical unit discharge ( $\text{m}^2 \text{ s}^{-1}$ )
$q_s$	= unit discharge at erosion of the first stone ( $\text{m}^2 \text{ s}^{-1}$ )
$S = \tan(\alpha)$	= slope (–)
$t, \Delta t$	= time, time step (s)
$v$	= flow velocity ( $\text{m s}^{-1}$ )
$v_c$	= critical flow velocity ( $\text{m s}^{-1}$ )
$W$	= Weber number (–)
$xyz, x'y'z'$	= coordinates, $x$ and $x'$ in flow direction (m)
$\alpha$	= slope angle ( $^\circ$ )
$\beta$	= angle between the $a$ -axis of a stone and the slope ( $^\circ$ )
$\Delta x, \Delta y, \Delta z$	= displacement in $x$ , $y$ and resp. $z$ -direction (m)
$\rho$	= density of water ( $\text{kg m}^{-3}$ )
$\rho_s$	= density of stone ( $\text{kg m}^{-3}$ )
$\sigma$	= surface tension ( $\text{N m}^{-1}$ )
$\Phi$	= packing factor (–) (Knauss, 1979)

## References

- Aberle, J. (1995). *Stabilität ungebundener Deckwerke unter Berücksichtigung der Deckwerksverschiebung bei Überströmung* [Riprap stability considering displacements during overtopping] (unpublished thesis). Universität Karlsruhe.
- Abt, S. R., & Johnson, T. L. (1991). Riprap design for overtopping flow. *Journal of Hydraulic Engineering*, *117*, 959–972. doi: 10.1061/(ASCE)0733-9429(1991)117:8(959).
- Abt, S. R., Khattak, M. S., Nelson, J. D., Ruff, J. F., Shaikh, A., Wittler, R. J., ... Hinkle, N. (1987). *Development of riprap design criteria by riprap testing in flumes: phase I* (NUREG/CR-4651). Washington DC: Nuclear Regulatory Commission.
- Abt, S. R., Thornton, C. I., Gallegos, H. A., & Ullmann, C. M. (2008). Round-Shaped riprap stabilization in overtopping flow. *Journal of Hydraulic Engineering*, *134*, 1035-1041. doi:10.1061/(ASCE)0733-9429(2008)134:8(1035).
- Abt, S. R., Thornton, C. I., Scholl, B. A., & Bender, T. R. (2013). Evaluation of overtopping riprap design relationships. *Journal of the American Water Resources Association*, *49*, 923–937. doi: 10.1111/jawr.12074.
- Bunte, K., & Abt, S. R. (2001). *Sampling surface and subsurface particle-size distributions in wadable gravel- and cobble-bed streams for analyses in sediment transport, hydraulics, and streambed monitoring* (General Technical Report RMRS-GTR-74). Fort Collins CO: United States Department of Agriculture.
- Chanson, H. (2015). Embankment overtopping protection systems. *Acta Geotechnica*, *10*, 305-318. doi: 10.1007/s11440-014-0362-8.
- CIRIA, CUR, CETMEF (2007). *The rock manual: The use of rock in hydraulic engineering* (2nd ed.). C683, London: CIRIA.
- Dornack, S. (2001). *Überströmbare Dämme - Beitrag zur Bemessung von Deckwerken aus Bruchsteinen* [Overtoppable dams – a contribution to the design of riprap] (PhD thesis). Technische Universität Dresden.
- Godtland, K. (1989). *Steinfyllingsdammer: dimensjonering av nedstrøms plastringsstein unntatt damfoten* [Rockfill dams: design of riprap stones on the downstream slope except the dam toe] (STF60 A89121, ISBN: 82-595-5892-0). Trondheim: Norges hydrotekniske laboratorium.
- Graf, W. H. (1991). Flow resistance over a gravel bed: Its consequence on initial sediment movement. In A. Armanini, & G. Di Silvio (Eds.), *Lecture Notes on Earth Sciences, Fluvial Hydraulics of Mountain Regions* (pp. 17-32). Berlin: Springer.
- Gronz, O., Hiller, P. H., Wirtz, S., Becker, K., Iserloh, T., Seeger, M., . . . Ries, J. B. (2016). Smartstones: A small 9-axis sensor implanted in stones to track their movements. *CATENA*, *142*, 245-251. doi: 10.1016/j.catena.2016.03.030.



- Hartung, F., & Scheuerlein, H. (1970). Design of overflow rockfill dams. *10th Congress on Large Dams, Q36*, 587-598.
- Hiller, P. H. (2016). *Kartlegging av plastring på nedstrøms skråning av fyllingsdammer* [Survey of placed riprap on the downstream slope of rockfill dams] (B1-2016-1, ISBN-10: 978-827598-0951). Trondheim: Norwegian University of Science and Technology.
- Hiller, P. H., Kjosavik, F., Lia, L., & Aberle, J. (2016). *Field tests of placed riprap as erosion protection against overtopping and leakage*. Poster presented at the meeting of the United States Society on Dams, Denver CO.
- Hiller, P. H., & Lia, L. (2015). Practical challenges and experience from large-scale overtopping tests with placed riprap. In M. Á. Toledo, R. Morán, & E. Oñate (Eds.), *Dam Protections against Overtopping and Accidental Leakage* (pp. 151-157). London: CRC Press/ Balkema.
- Jafarnejad, M., Franca, M. J., Pfister, M., & Schleiss, A. J. (2016). Time-based failure analysis of compressed riverbank riprap. *Journal of Hydraulic Research*, 1-12.  
doi:10.1080/00221686.2016.1212940
- Knauss, J. (1979). Computation of maximum discharge at overflow rockfill dams (a comparison of different model test results). *13th International Congress on Large Dams, Q50*, 143-159.
- Larsen, P., Bernhart, H. H., Schenk, E., Blinde, A., Brauns, J., & Degen, F. P. (1986). *Überströmbare Dämme, Hochwasserentlastung über Dammscharten* [Overtoppable dams, spillways over dam notches] (unpublished report prepared for Regierungspräsidium Karlsruhe). Karlsruhe: Universität Karlsruhe.
- Lia, L., Vartdal, E. A., Skoglund, M., & Campos, H. E. (2013). *Rip rap protection of downstream slopes of rock fill dams - a measure to increase safety in an unpredictable future climate*. Paper presented at the European Club Symposium of the International Commission on Large Dams, Venice.
- Linford, A., & Saunders, D. H. (1967). *A hydraulic investigation of through and overflow rockfill dams* (RR. 888). The British Hydromechanics Research Association.
- Ministry of Petroleum and Energy (OED, 2009). *Forskrift om sikkerhet ved vassdragsanlegg (damsikkerhetsforskriften)* [Dam safety regulation] (FOR 2009-12-18-1600). Ministry of Petroleum and Energy.
- Mishra, S. K. (1998). *Riprap design of overtopped embankments* (PhD thesis). Colorado State University, Fort Collins CO.
- Morán, R., & Toledo, M. A. (2011). Research into protection of rockfill dams from overtopping using rockfill downstream toes. *Canadian Journal of Civil Engineering*, 38, 1314-1326.  
doi:10.1139/I11-091.
- Norwegian Water Resources and Energy Directorate (NVE, 2012). *Veileder for fyllingsdammer* [Guidelines for embankment dams] (Guideline 4/2012). Oslo: Norwegian Water Resources and

- Energy Directorate. Retrieved January 27, 2014, from:  
[http://publikasjoner.nve.no/veileder/2012/veileder2012\\_04.pdf](http://publikasjoner.nve.no/veileder/2012/veileder2012_04.pdf).
- Olivier, H. (1967). *Through and overflow rockfill dams - new design techniques* (Paper No. 7012). Institution of Civil Engineers.
- Orendorff, B., Al-Riffai, M., Nistor, I., & Rennie, C. D. (2013). Breach outflow characteristics of non-cohesive embankment dams subject to blast. *Canadian Journal of Civil Engineering*, *40*, 243-253. doi:10.1139/cjce-2012-0303.
- Pardo, V., Herrera, M., Molines, J., & Medina, J. (2014). Placement Test, Porosity, and Randomness of Cube and Cubipod Armor Layers. *Journal of Waterway, Port, Coastal, and Ocean Engineering*, *140*, 04014017. doi:10.1061/(ASCE)WW.1943-5460.0000245.
- Peirson, W. L., & Cameron, S. (2006). Design of rock protection to prevent erosion by water flows down steep slopes. *Journal of Hydraulic Engineering*, *132*, 1110-1114.
- Peirson, W. L., Figlus, J., Pells, S. E., & Cox, R. J. (2008). Placed rock as protection against erosion by flow down steep slopes. *Journal of Hydraulic Engineering*, *134*, 1370-1375. doi: 10.1061/(ASCE)0733-9429(2008)134:9(1370).
- Peirson, W. L., & Pells, S. E. (2005). *Steady state testing of scour protection options for Penrith Lakes weirs* (Technical report 2005/11). The University of New South Wales Water Research Laboratory.
- Pfister, M., & Chanson, H. (2012). Discussion - "Scale effects in physical hydraulic engineering models" by Heller, V. *Journal of Hydraulic Research*, *50*, 244-246. doi: 10.1080/00221686.2012.654671.
- Robinson, K. M., Rice, C. E., & Kadavy, K. C. (1998). Design of rock chutes. *Transactions of the American Society of Agricultural Engineers*, *41*, 621-626.
- Scheuerlein, H. (1968). *Der Rauherinneabfluss* [Flow in rough channels] (PhD thesis). Technische Hochschule München.
- Sommer, P. (1997). *Überströmbare Deckwerke*. [Overtoppable erosion protections] (unpublished report). Institut für Wasserbau und Kulturtechnik, Versuchsanstalt für Wasserbau, Universität Karlsruhe.
- Siebel, R. (2007). Experimental investigations on the stability of riprap layers on overtoppable earthdams. *Environmental Fluid Mechanics*, *7*, 455-467. doi: 10.1007/s10652-007-9041-8.
- Thornton, C., Abt, S. R., Clopper, C., Scholl, B. N., & Cox, A. L. (2012). *Rock stability testing in overtopping flow - 2012* (Hydraulics Laboratory Technical Report 2012-1). Fort Collins CO: Engineering Research Center, Colorado State University.
- Thornton, C., Cox, A. L., & Turner, M. D. (2008). *Las Vegas wash sloped rock-weir study* (Report). Las Vegas NV: Report prepared for the Southern Nevada Water Authority.
- Toledo, M. Á., Morán, R., & Oñate, E. (Eds.). (2015). *Dam protections against overtopping and accidental leakage*. London: CRC Press/ Balkema.

Wittler, R. J. (1994). *Mechanics of riprap in overtopping flow* (PhD thesis). Colorado State University, Fort Collins CO.

Tab. 1 Experimental boundary conditions for the tests including slope length  $L_s$ , packing factor  $P_c$ , discharge  $q$  given as range, number of discharge steps  $n$ , time intervals  $\Delta t$ , and unit discharges  $q_s$  and  $q_c$  corresponding to erosion of the first stone and bulk erosion of the riprap, respectively. For placed riprap only boundary conditions for  $q \geq 0.05$  ( $\text{m}^2\text{s}^{-1}$ ) are given in the table. The discharge range includes the  $n$  discharge steps which were run for complete time intervals  $\Delta t$ . If the riprap failed during step  $(n + 1)$  before  $\Delta t$  was reached,  $q_s$  or  $q_c$  exceeds the discharge range.

Test	$L_s$ (m)	$P_c$ (-)	$q$ ( $\text{m}^2\text{s}^{-1}$ )	$n$ (-)	$\Delta t$ (s)	$q_s$ ( $\text{m}^2\text{s}^{-1}$ )	$q_c$ ( $\text{m}^2\text{s}^{-1}$ )
P01 <sup>a</sup>	1.8	0.56	0.05 – 0.24	9	1800	0.10	0.24
P02	1.8	0.55	0.05 – 0.34	11	3600	0.10	0.36
P03	1.8	0.52	0.20 – 0.20	1	3600	0.25	0.25
P04 <sup>b</sup>	1.8	0.53	0.10 – 0.40, 0.35, 0.40	6	3600, 17h	0.20	0.40
P05 <sup>c</sup>	1.0	0.48	0.10, 0.10 – 0.49	1, 18	1020, 130	< 0.49 <sup>d</sup>	> 0.49
P06 <sup>c</sup>	0.8	0.50	0.10, 0.10 – 0.49	1, 18	1020, 130	0.36	> 0.49
P07 <sup>c</sup>	0.8	0.56	0.10, 0.10 – 0.49	1, 18	1020, 130	< 0.49 <sup>d</sup>	> 0.49
P08 <sup>e</sup>	1.8	0.55	0.10, 0.10 – 0.21	1, 7	1020, 130	0.19	0.24
D01	1.8	1.05	0.006 – 0.02	2	3600	0.04	0.04
D02 <sup>f</sup>	0.8	0.83	0.015 – 0.03	2	900, 690	0.05	0.05

<sup>a</sup> Two lower discharges  $q = 0.007$  and  $0.012 \text{ m}^2\text{s}^{-1}$  were run for  $\Delta t = 3600$  s;  $q = 0.05 \text{ m}^2\text{s}^{-1}$  was run for  $\Delta t = 3600$  s; <sup>b</sup> Long term experiment: after increasing the discharge stepwise in  $n = 6$  steps to  $0.4 \text{ m}^2\text{s}^{-1}$  the discharge was reduced to  $q = 0.35 \text{ m}^2\text{s}^{-1}$  for 12.5 h due to capacity issues with the flume. The final 4.5 h were run with  $q = 0.40 \text{ m}^2\text{s}^{-1}$ . <sup>c</sup> Hydrograph scaled using Froude model law to enable direct comparison with field tests of Hiller et al. (2016); initial load period with  $q = 0.10 \text{ m}^2\text{s}^{-1}$  for  $\Delta t = 1020$  s, inspection of the riprap without water, then  $q = 0.03 \text{ m}^2\text{s}^{-1}$  for  $\Delta t = 872$  s,  $q = 0.10 \text{ m}^2\text{s}^{-1}$  for  $\Delta t = 386$  s, increasing discharge with  $\Delta q = 0.023 \text{ m}^2\text{s}^{-1}$  every  $\Delta t = 130$  s until failure or  $q_{\text{max}}$  without stopping the flow. <sup>d</sup> The erosion of the first stone was not observed and the given value corresponds to  $q$  when the first missing stone was detected. <sup>e</sup> Discharge scaled as for P05 – P07, but with  $L_s = 1.8$  m; <sup>f</sup>  $q = 0.015 \text{ m}^2\text{s}^{-1}$  for  $\Delta t = 900$  s and  $q = 0.03 \text{ m}^2\text{s}^{-1}$  for  $\Delta t = 690$  s according to the discharges scaled from the field tests.

Tab. 2 Summary table of the results for placed riprap including the packing factor  $P_c$ , the stone-related Froude numbers for erosion of the first stone  $F_{s,s}$  and riprap failure  $F_{s,c}$ , the maximum displacements  $\Delta x_{\max}$  observed at MS0 as well as the total volume of water which passed over the riprap per width during the test  $\Sigma(qt)_{\text{tot}}$ .

Test	$P_c$ (-)	$F_{s,s}$ (-)	$F_{s,c}$ (-)	$\Delta x_{\max}$ (m) <sup>a</sup> at MS0	$\Sigma(qt)_{\text{tot}}$ (m <sup>2</sup> )
P01	0.56	2.3	5.6	0.110	4535
P02	0.55	2.3	8.4	0.106	11423
P03	0.52	5.9	5.9	0.066	1061
P04 <sup>b</sup>	0.53	0.9	9.4	0.108	33023
P05	0.48	< 11.5	> 11.5	0.012 <sup>c</sup>	7205 <sup>c</sup>
P06	0.50	8.4	> 11.5	0.013 <sup>c</sup>	4418 <sup>c</sup>
P07	0.56	< 11.5	> 11.5	0.023 <sup>c</sup>	4627 <sup>c</sup>
P08	0.55	4.5	5.6	0.038	291

<sup>a</sup> last measurement before failure; <sup>b</sup> long term load; <sup>c</sup> last measurement before destroying the riprap manually



Fig. 1 Reconstruction of a placed single-layer riprap on the downstream slope of the 129 m high rockfill dam Svartevatn in Southwestern Norway. The riprap stones are placed one by one in an interlocking pattern and form with the adjacent filter layer an erosion protection against accidental leakage and overtopping. (Photo: NTNU)

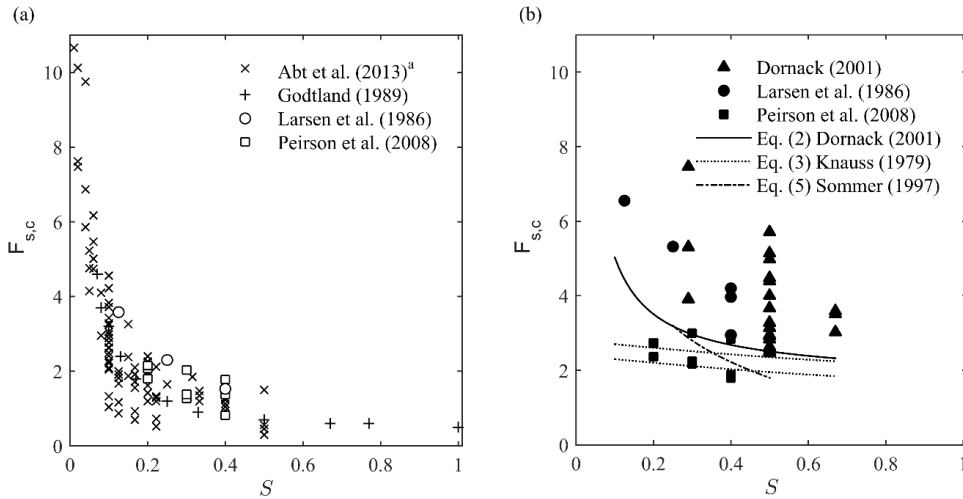


Fig. 2 Existing data points for dumped riprap (a) and placed riprap and design curves (b). Most data are available for dumped riprap on gentle slopes. The studies by Larsen et al. (1986) and Peirson et al. (2008) include data of dumped and placed riprap made of the same stones and show that placed riprap is more stable than dumped riprap.

<sup>a</sup>The data summarized in Abt et al. (2013) contain data points from Abt et al. (1987); Abt and Johnson (1991); Mishra (1998); Peirson and Pells (2005); Robinson et al. (1998); Siebel (2007); Thornton, Cox, and Turner (2008); Thornton, Abt, Clopper, Scholl, and Cox (2012); and Wittler (1994). Note that no distinction is made in terms of stone size, density or roundness for the presented data.

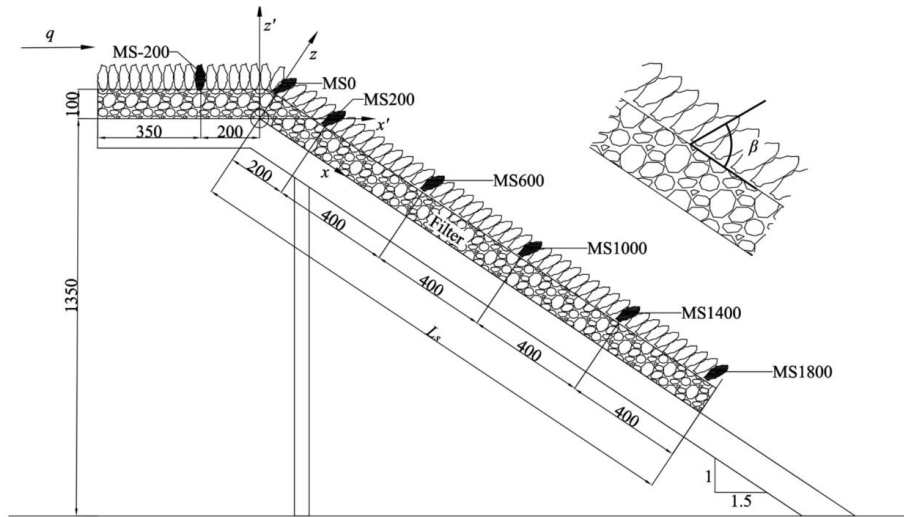


Fig. 3 Model setup with  $L_s = 1.8$  m and definition of the coordinate systems  $xyz$  and  $x'y'z'$  with the origin at the break-point between the crest and the chute. The marked stones MS are placed in the middle of the flume  $y = y' \approx 0.5$  m. All measures in (mm), flow direction from left to right. The inclination of the riprap stones is indicated with  $\beta$  in the enlarged part.



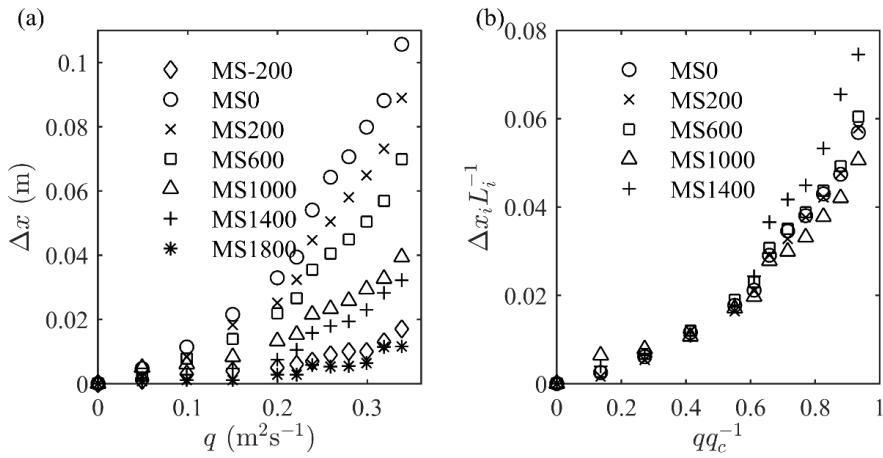


Fig. 4 Measured displacements at the marked stones for test P02 in absolute values (a) and dimensionless (b). MS-200 and MS1800 are omitted in (b) as they displaced differently compared to the other marked stones. Note that the riprap failed at  $q/q_c = 1$  and the maximum displacements were determined after the prior discharge step, i.e. for  $q/q_c < 1$ .

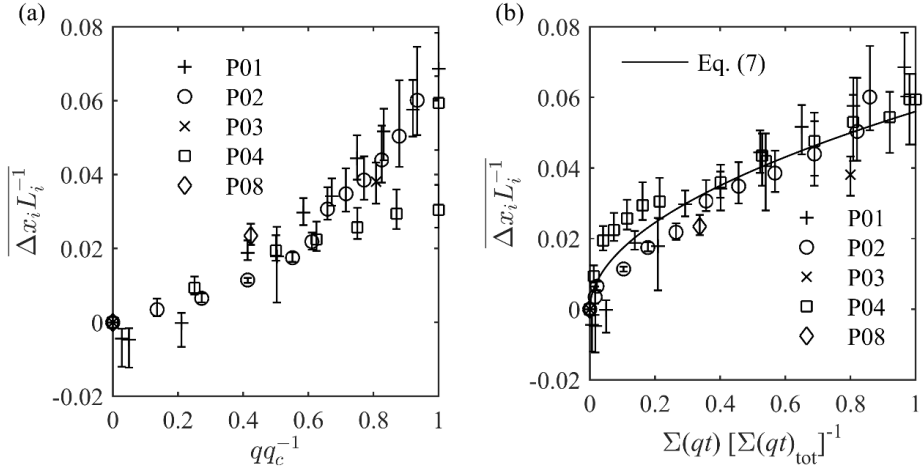


Fig. 5 Averaged dimensionless displacements over MS0 to MS1400 compared to the relative discharge in (a) and relative to the volume of water passed over the riprap in (b), including the regression Eq. (7). The vertical bars show the minimum and maximum values for the displacements included in the average. For P04 only the smallest and largest value for  $\overline{\Delta x_i / L_i}$  are plotted for  $q/q_c = 1$  in (a).



## Paper II

---

**Field and model tests of riprap on steep slopes exposed to  
overtopping**

Priska H. Hiller, Leif Lia, Jochen Aberle

In review: Journal of Applied Water Engineering and Research

---



# **Field and model tests of riprap on steep slopes exposed to overtopping**

Priska H. Hiller, Leif Lia, Jochen Aberle

*Department of Civil and Environmental Engineering, NTNU Norwegian University of Science and Technology, Trondheim, Norway*

S. P. Andersens veg 5, 7491 Trondheim, Norway

Corresponding author email: [priska.hiller@ntnu.no](mailto:priska.hiller@ntnu.no)

Priska H. Hiller holds a MSc in Civil Engineering from the Swiss Federal Institute of Technology ETH Zurich. She worked as a consultant in hydraulics and hydrology at Sweco Norway AS before she started in her current position as a PhD Candidate at the Norwegian University of Science and Technology (NTNU) in Trondheim in 2013. She chairs currently the Young Engineers Forum of the International Commission on Large Dams (ICOLD). (<https://orcid.org/0000-0002-7639-5358>)

Leif Lia graduated from Norges tekniske høyskole (NTH) in 1993 and his PhD was completed in 1998 at NTNU. He worked for Grøner/ Sweco Norway AS consulting company for 11 years, seven years as head of the Hydropower department and simultaneously nine year as assistant professor (20%) in Dam Safety at NTNU. Since 2009, he has been Professor in hydropower structures in the Department of Civil and Environmental Engineering at NTNU. He is currently Vice President of ICOLD in 2014 - 2017.

Jochen Aberle received his education in civil engineering from the University of Karlsruhe (TH), Germany, with a diploma in 1996 and the PhD title in 2000. After a two years postdoctoral stay at the National Institute of Water and Atmospheric Research (NIWA) in Christchurch NZ, he joined the Leichtweiss-Institute for Hydraulic Engineering and Water Resources (LWI) at the Technische Universität Braunschweig in 2003. In 2012 he joined NTNU in Trondheim as a full Professor. (<https://orcid.org/0000-0002-5435-2832>)

This work was supported by the Research Council of Norway under Grant [project number 235730]; Energy Norway under [project PlaF].

# Field and model tests of riprap on steep slopes exposed to overtopping

The comparability of large-scale field tests of dumped and placed riprap with a stone diameter of 0.37 m and corresponding model tests in a scale of 1:6.5 was investigated in terms of stability, packing density and visually observed flow pattern. The tested riprap protections were exposed to overtopping on a slope of 1:1.5 (vertical: horizontal). The results for dumped riprap revealed similarity between the field and model tests based on the critical stone-related Froude number as a measure for the stability, packing density, flow pattern and overtopping depth. The field and model tests with placed riprap showed good agreement in regard to flow pattern and overtopping depth. However, the placed riprap in the model tests were denser packed and more stable than in the field indicating laboratory effects. Placed riprap withstood up to ten times higher unit discharges than dumped riprap, 6 to 8 m<sup>2</sup>s<sup>-1</sup> in the field tests.

Keywords: field and model tests; overtopping; riprap; steep slope

## Introduction

Riprap consisting of large natural rocks or artificial elements is widely used to protect river banks, streambeds, bridge piers and abutments, dams, shorelines and other hydraulic structures against the impact of currents and waves (e.g., Abt and Johnson 1991; CIRIA et al. 2007; Abt et al. 2013; Chanson 2015; Jafarnejad et al. 2016). There exist two general riprap types, dumped and placed, which are constructed by either dumping the riprap elements or placing them in an interlocking pattern. The construction of placed riprap is more cost- and labour-intensive than simply dumping elements (Peirson et al. 2008), but placed riprap can withstand higher discharges than dumped riprap constructed with the same stone size (Larsen et al. 1986; Peirson et al. 2008; Hiller et al. 2017), especially on steep slopes (Dornack 2001).

An application of placed riprap within dam engineering is to protect the downstream slopes of embankment dams against erosion due to accidental leakage or

overtopping (Toledo et al. 2015). Embankment dams fail statistically more often than concrete dams, and the most common cause for dam failure is overtopping (ICOLD 1995). Overtopping is mainly associated with the inadequate design of spillways (Harris 2015), and enhancing the resistance of embankment dams against erosion from overtopping will thus increase their safety. Additionally, a specifically lowered part on small embankment dams (dam height lower than 10 m), secured with placed riprap, can be an alternative and cost-effective spillway solution (e.g. Larsen et al. 1986; Dornack 2001; Siebel 2007).

In order to increase the resistance against erosion from accidental leakage and overtopping, the downstream slopes of rockfill dams in Norway are secured by a single layer of placed riprap. For this purpose, the riprap stones are placed in an interlocking pattern with their longest axes inclined towards the dam, as shown in Figure 1 and prescribed by OED (2009). The typical downstream slope of embankment dams in Norway is 1:1.5 (vertical: horizontal), corresponding to a slope of  $S = 0.67$ , and the recommended stone size for the placed riprap is in the range of 0.3 m to 0.7 m, dependent on the consequences in case of dam failure (NVE 2012). In the near future, many Norwegian dams need to be upgraded because they were constructed in the period of 1960 – 1990, and periodical reassessments often reveal that they do no longer comply with the current dam safety regulation (OED, 2009), which applies retroactively. If required, the upgrade includes a new construction or rebuilding of placed riprap on the downstream slope of dams. This aspect has triggered the present research project with the aim to evaluate existing stability approaches of placed riprap on steep slopes and to optimise the design of placed riprap.

[Figure 1 somewhere here]



Almost all available approaches for the sizing of riprap stones exposed to an overtopping flow have been developed on the basis of physical model tests. However, most of the corresponding studies focused on milder slopes, and data for steep slopes of up to  $S = 0.67$  are rare. In addition, most tests were executed with riprap stones smaller than 0.1 m, and data from experiments with large stones are desirable for the validation of existing design approaches (Abt et al. 2013; Peirson and Cameron 2006).

Furthermore, a comparison between prototype and laboratory tests can provide information to what extent construction-related properties of placed riprap such as placement density and internal friction affect riprap stability. Those properties may moreover be prone to laboratory effects (Pardo et al. 2014).

Facilities offering the possibility to carry out prototype-scale riprap tests are rare due to the required boundary conditions (e.g. steep slopes, dam height, discharge, stone size) and are normally located outdoors (e.g. at the Engineering Research Center of the Colorado State University in Fort Collins). In the framework of the present study, a temporary site became available in Norway, and the opportunity was used to conduct riprap stability test with large stones in order to address the aforementioned challenges.

The objective of the present paper is to investigate the comparability of stability tests with placed riprap at large-scale and equivalent model tests at a smaller scale. Results from additional tests with dumped riprap at both scales will be used to consider the stability gain by placing riprap stones in an interlocking pattern, and to facilitate cross-comparison of the results with outcomes from existing studies. Note that in the present study, the riprap structures were solely exposed to overtopping (i.e. the current was parallel to the slope).

## Background

### *Riprap parameters*

The parameters affecting riprap stability can be subdivided in geotechnical riprap properties, properties of the overtopping flow, and geometric boundary conditions.

Riprap properties are typically characterised by the stone size  $d$ , stone density  $\rho_s$ , the grain size distribution and the riprap layer thickness. Construction-related properties such as packing densities (i.e. number of stones per unit area) are used to describe the quality of the placement. The dimensionless packing factor  $P_c$  defined by Linford and Saunders (1967) and Olivier (1967)

$$P_c = \frac{1}{Nd_s^2} \quad (1)$$

relates the number of stones per  $m^2$ ,  $N$ , to the squared stone size of the equivalent stone diameter  $d_s$  (diameter of a sphere having the same volume as an average riprap stone).

The packing factor  $P_c$  is scale-independent, and typical values range from 0.8 (stones placed on edge) to 1.2 (dumped stones);  $P_c$  is smaller for a densely packed riprap compared to a dumped riprap. Dependent on the shape and arrangement of the riprap stones, low packing factors can be achieved, for example  $P_c \approx 0.4$  when placing oblong stones with a ratio of  $a/b_s = 2.0$  on edge (Linford and Saunders 1967;  $a$  denotes the longest axis of the stone and  $b_s$  the average of the intermediate and shortest stone axis  $b$  and  $c$ , respectively).

The overtopping flow can be characterised by the Froude number  $F = v/(gh)^{0.5}$  where  $v$  denotes the flow velocity,  $g$  the gravitational acceleration, and  $h$  the water depth. During overtopping, the flow accelerates from the crest along the downstream slope until the flow is fully developed, meaning that  $F = 1$  at the dam crest and  $F > 1$  further downstream if backwater effects are absent. The flow pattern also depends on

the roughness of the riprap, the slope and the discharge. Similar to stepped spillways, it can be characterised by self-aeration and may resemble a skimming flow pattern (Pagliara et al. 2010).

The definition of water depth  $h$  (and implicitly of the velocity  $v$ ) for such conditions is difficult because, on the one hand, aeration hampers the definition of the water surface level (e.g. Bung 2013) and, on the other hand, the associated rough bed conditions require the definition of an arbitrary reference level for the determination of the water depth (e.g. DVWK 1990). Using the discharge per unit width  $q = vh$ , however, it becomes possible to avoid arbitrary definitions given that the cross-sectional width does not change. Using  $q$ , a stone-related Froude number  $F_s = q/(gd^3)^{0.5}$  can be formulated through the combination of the Froude number with the relative submergence  $h/d$ . At critical conditions (i.e. riprap failure)  $F_s$  becomes

$$F_{s,c} = \frac{q_c}{\sqrt{gd^3}} \quad (2)$$

where  $q_c$  denotes the discharge per unit width at riprap failure. The geometric boundary conditions of riprap are characterised by the slope  $S$ , the length  $L_s$  covered by the riprap and the width  $B$  of the channel or dam. These parameters are of importance for the failure mechanisms as discussed in the following.

### ***Failure mechanisms***

Riprap stability, or failure, needs to be considered in the light of different failure mechanisms for dumped and placed riprap. For dumped riprap, failure is usually considered when the underlying filter layer is exposed to the flow due to the erosion of the riprap (e.g. Linford and Saunders 1967; Abt and Johnson 1991; Robinson et al. 1998; Peirson et al. 2008). If the same definition is applied for a single-layer placed riprap, this would mean that erosion of a single stone would correspond to riprap failure

because the filter will be exposed at this particular location. However, if a stone is eroded out of a placed riprap, the remaining stones can absorb the loss because the interlocking pattern allows for the formation of a bearing structure. Therefore, progressive erosion of the riprap layer should be considered as the critical condition (Larsen et al. 1986; Sommer 1997; Dornack 2001; Hiller et al. 2017). Note that dumped and placed riprap may also fail via sliding if the friction forces between the filter and the riprap layer exceed a critical threshold. However, this failure mechanism is not in the scope of the present paper. Similarly, the global stability of the embankment such as safety against overturning or sliding circles, as e.g. summarised in Larsen et al. (1986) or Morán and Toledo (2011), is not discussed in this paper.

The interlocking between the stones in placed riprap allows for, besides the aforementioned bearing structure, the transfer of longitudinal forces. If these forces exceed a critical threshold, the riprap layer can be disrupted (Dornack 2001; Siebel 2007), or displacements of riprap stones can be triggered. The latter can cause failure of placed riprap, as displacements can gradually accumulate and create a gap within the riprap. If a larger gap develops, adjacent riprap stones may lose their interlocking placement and be eroded by the overtopping flow (Larsen et al. 1986; Sommer 1997; Hiller et al. 2017). In general, the largest gap can develop at the transition between the horizontal dam crest and the dam slope. It is worth mentioning that this transitional area has also been identified as a vulnerable area with regard to flow attack in investigations on the breach formation of dams, which were not additionally secured with riprap (e.g. Løvoll 2006; Morris et al. 2007; Schmocker et al. 2013).

### ***Riprap stability approaches***

There exist numerous approaches to estimate the stability of both dumped and placed riprap. A recent summary of design relationships for dumped riprap exposed to

overtopping, including data of corresponding stability studies, has been presented by Abt et al. (2013). These data are plotted in Figure 2a along with data from Godtland (1989), Larsen et al. (1986), Peirson et al. (2008), and Hiller et al. (2017) showing the critical stone-related Froude number  $F_{s,c}$  as a function of the slope  $S$ . The figure also contains the results of the model tests reported by Lia et al. (2013), but the data from their field tests are not included due to the reasons discussed below. In order to visualise the variability of the stone size  $d$  used in the corresponding studies, the marker size is proportional to this parameter in Figures 2a and 2b. Figure 2a illustrates that stability data for dumped riprap with large stone sizes or at steep slopes are rare. In fact, 75% of the data points presented by Abt et al. (2013) were obtained for  $S \leq 0.2$ , and less than 24% of the data points were obtained in studies with stone diameters  $d > 0.1$  m. Moreover, only four of their presented 96 data points were obtained in studies with  $d > 0.2$  m (extracted from Mishra 1998 and Robinson et al. 1998) even though stones used for riprap in prototype conditions are usually larger than 0.2 m.

The critical stone-related Froude number  $F_{s,c}$  for placed riprap is plotted as a function of slope in Figure 2b using data reported by Larsen et al. (1986), Dornack (2001), Peirson et al. (2008), Lia et al. (2013) and Hiller et al. (2017). The direct comparison of Figures 2a and 2b reveals that  $F_{s,c}$  scatters more for placed riprap than for dumped and that placed riprap is more stable, especially at steep slopes. Moreover, some studies found that the discharge capacity of the experimental facility was not large enough to induce failure of placed riprap (e.g. Sommer, 1997; Lia et al. 2013; Hiller et al. 2017). For these studies the lower limit for  $F_{s,c}$  corresponded to  $F_{s,c} > 3.3$  (Sommer 1997, with  $0.25 \leq S \leq 0.5$  and  $q_{\max} = 0.5 \text{ m}^2\text{s}^{-1}$ ),  $F_{s,c} > 3.1$  (Lia et al. 2013, with  $S = 0.67$  and  $q_{\max} = 0.19 \text{ m}^2\text{s}^{-1}$ ) and  $F_{s,c} > 11.5$  (Hiller et al. 2017, with  $S = 0.67$  and  $q_{\max} = 0.49 \text{ m}^2\text{s}^{-1}$ ). Few design relationships have been developed specifically for placed riprap, as

for example by Knauss (1979), Sommer (1997) and Dornack (2001). These approaches were evaluated in Hiller et al. (2017) and are not discussed here.

[Figure 2a and 2b somewhere here]

A possible explanation for the variability of  $F_{s,c}$  in Figure 2b is the difference in packing factors, which varied from  $P_c = 0.53$  (Hiller et al. 2017) to  $P_c = 0.65$  (Larsen et al. 1986),  $P_c = 0.80$  (Dornack 2001), and  $P_c = 0.94$  (Peirson et al. 2008). The different  $P_c$  values may be related to the shape of the stones used, in addition to the quality of the packing. The ratio between the longest and intermediate axes of the stones used in Hiller et al. (2017) was  $a/b_s = 2.0$ , and the stones were more oblong than in Dornack (2001),  $1.4 < a/b_s < 1.8$ , or Larsen et al. (1986),  $a/d_s = 1.6$  ( $d_s$  was used instead of  $b_s$  due to missing information for  $b$  and  $c$ ). No specific information about the stone shape was found for Peirson et al. (2008). Oblong stones placed with their  $a$ -axis towards the slope can be denser packed than stones having the same volume and a more cubical form, resulting in lower  $P_c$  values (Lindford and Saunders 1967). Moreover, Lia et al. (2013) found that denser arrangement of the riprap stones resulted in higher stability when varying the inclination angle  $\beta$  between the slope and the longest axes of the riprap stones (see Figure 1). They reported the highest stability for  $\beta = 90^\circ$ , i.e. stones placed with their longest axes perpendicular to the slope. However, there was not sufficient information available in their study to determine  $P_c$  for a quantitative comparison with the aforementioned studies.

Studies with prototype-scale riprap are rare, but results from two previous field tests have recently been reported by Lia et al. (2013) and Hiller and Lia (2015). Lia et al. (2013) investigated the stability of placed riprap at a field site with prototype stones of  $d_{50} = 0.65$  m ( $d_{50}$  is the stone size where 50% of the grains are finer by mass). Based on three tests they concluded that the riprap stability increased with increasing

inclination angle  $\beta$ . The test with  $\beta = 71^\circ$  (the target was  $\beta = 90^\circ$ , but could not be achieved during construction) withstood the maximum available discharge per unit width of  $q = 8.3 \text{ m}^2\text{s}^{-1}$ , indicating  $F_{s,c} > 5.1$ . A comparative test with dumped riprap failed at  $q_c = 2.1 \text{ m}^2\text{s}^{-1}$  ( $F_{s,c} = 1.3$ ). Hiller and Lia (2015) used the same facility but a reduced stone size ( $d_{50} = 0.54 \text{ m}$ ) to achieve riprap failure with the available discharge. The placed riprap consequently failed at  $q_c = 6.2 \text{ m}^2\text{s}^{-1}$  ( $F_{s,c} = 5.1$ ) and  $q_c = 2.0 \text{ m}^2\text{s}^{-1}$  ( $F_{s,c} = 1.6$ ). It is worth mentioning that the latter riprap failed due to an instability in the riprap foundation. The corresponding result should therefore not be used for further analyses in regard to failure through overtopping, but it shows how construction-related boundary conditions can affect riprap-stability.

The construction-related properties of riprap might depend on the size of the riprap stones. However, reported results for prototype-scale riprap and corresponding model tests to analyse their comparability were not found. The present study provides such a comparison and presents a novel set of both prototype and laboratory data for riprap on steep slopes.

## **Experiments**

The stability of both dumped and placed riprap was tested at a temporary field site in Sirdal in Southwestern Norway and in the hydraulic laboratory at the Norwegian University of Science and Technology (NTNU) in Trondheim. The field tests were carried out with riprap stones of a mean diameter  $d_{50} = 0.37 \text{ m}$  (herein defined as prototype tests) and the model tests with stones characterised by  $d_{50} = 0.057 \text{ m}$ . The ratio of the prototype to model diameter results in a geometrical scale of 1:6.5 and the flow in the laboratory tests was subsequently scaled by applying Froude's model law. For both the laboratory and field experiments, the critical discharge  $q_c$  per unit width

was defined as the discharge where progressive erosion of the riprap stones occurred. Moreover, the discharge for which erosion of the first riprap stone was observed, but did not necessarily result in a complete failure of the riprap, was denoted  $q_s$ . The corresponding critical stone-related Froude numbers are denoted  $F_{s,c}$  and  $F_{s,s}$ , respectively.

### **Field tests**

Only a limited number of field tests could be carried out due to the pre-defined time frame provided by the dam owner, the logistics and available resources. As a consequence, two tests were carried out with placed riprap (F15P1 and F15P2) and one with dumped riprap (F15D1) within a period of three weeks. The test dams of approximately 3 m height and 12 m top width (9.5 m bottom width) were built in the outlet channel of a tunnel spillway, as shown in Figure 3.

[Figure 3 somewhere here]

The trapezoidal dam profile had an adverse slope of  $S = 0.5$  upstream of the horizontal crest and a downstream slope of  $S = 0.67$ . The length of the downstream riprap cover in flow direction was  $L_s \approx 4.5$  m. Ideally, this length should be longer to allow for flow development, but the achievable length was limited due to local peculiarities. Table 1 summarises the boundary conditions for the test dams.

[Table 1 somewhere here]

Angular stones with  $d_{50} = 0.37$  m were used for the riprap. The  $d_{50}$  was derived from the grain size distribution (by mass) of the nominal diameter  $d = (abc)^{1/3}$  (Bunte & Abt, 2001) of the riprap stones located in the central area of the riprap. The  $d_{50}$  is based on the analysis of a sample of 153 stones for which  $a$ ,  $b$  and  $c$  were measured manually using a folding rule (approximately 240 stones were used for construction of the placed riprap). The riprap stones were slightly oblong ( $a/b = 1.5$  in average) and the mass of



the stones was estimated using  $m = C_f \cdot \rho_s \cdot d^3$  (NVE 2012) with a shape factor  $C_f = 0.48$ . The grain size distribution of the stones can be characterised as uniform as the coefficient of uniformity  $C_u = d_{60}/d_{10} = 1.24$  with  $d_{\min} = 0.19$  m and  $d_{\max} = 0.50$  m (see row F15 in Table 2).

The test dams were constructed with an excavator and the riprap covered the central part on the downstream slope and about 1 m of the crest (see Figure 3). The remaining part of the crest was secured with large stones (approximately 1.5 to 2 times the diameter of the stones used for the riprap) because the excavator was unable to reach this part to place the stones in an interlocking pattern. Furthermore, such large stones were used to lock the downstream end of the riprap, to prevent riprap failure along the abutments, and to support the adverse upstream slope.

The construction of the test dams started with placing a row of large stones across the channel on the clean bedrock as dam toe. Afterwards, a permeable support fill consisting of angular stones with  $d_{50} = 0.22$  m ( $C_u = 2.3$ ) was constructed upstream of the initial stone row. Finally, the test dams were covered from down- to upstream with either placed or dumped riprap. The test dams were permeable and allowed a small percentage of the flow to pass through the dams as described and quantified later. Placed riprap for F15P1 and F15P2 was constructed by placing the stones one by one in an interlocking pattern and assuring that the longest axis of the stone ( $a$ -axis) was inclined towards the dam with a target angle  $\beta = 60^\circ$ . The target angle differed intentionally from the most stable arrangement at  $\beta = 90^\circ$  to simulate a realistic inclination angle as typically observed in placed riprap on the downstream slopes of rockfill dams (Hiller 2016). The subsequent survey with an inclination meter (Leica DISTO™ X310;  $\pm 0.2^\circ$ ) revealed angles of  $53^\circ$  and  $55^\circ$  for the two test dams, respectively, which were even lower than the target value. The packing factors

corresponded to 0.75 and 0.64 (Table 1). The dumped riprap for test F15D1 was constructed by putting the stones on the slope with random orientation and without interlocking pattern. Due to the steep slope, the stones could not be dumped and spread, but had to be put one by one by the excavator.

[Table 2 somewhere here]

During overtopping, the water surface elevation at the tunnel outlet was monitored by two ultrasonic sensors (Microsonic™ mic+340;  $\pm 1\%$ ; referred to as ‘mic1’ and ‘mic2’) with a sampling frequency of 10 Hz. A pressure cell (Global Water™ WL16;  $\pm 0.1\%$ ) installed at the side of the outlet in a zone of back flow measured the water depth with a sampling frequency of 0.1 Hz (Figure 3). Additional pressure sensors (Schlumberger Water Services™, Mini-Diver, DI501;  $\pm 0.5$  cm H<sub>2</sub>O), usually used in groundwater wells, were installed along the dam to monitor the stage. Two additional pressure sensors were placed in riprap stones in drilled holes and secured with a bolted steal band. Sensor ‘D1’ was installed in a stone at the transition between the dam crest and the slope and ‘D2’ in a stone close to the dam toe (see Figure 3) to monitor the water level over the downstream slope. These two stones equipped with sensors were coloured to ease their recovery after riprap failure. Additional three pressure sensors were mounted in the rock under the test dams, and one sensor was installed approximately 2 m downstream of the dam (labelled with ‘U1’ to ‘U4’ from up- to downstream, not visible in Figure 3 because they are under the dam). The positions of the ultrasonic sensors, the pressure cell and sensors were measured with a handheld Leica™ GPS1200 (see Table 5 in the Appendix for the coordinates). The readings of the aforementioned sensors were used to determine the elevation of the water surface and averaged over 60 s. For each individual sensor, the reference level for the water depth corresponded to the measured water surface elevation at  $F_s = 0.6$  ( $q =$

0.4 m<sup>2</sup>s<sup>-1</sup>) to compensate for some minor irregularities in dam construction (see dam height and width in Table 1) and the uneven surface of the dam due to the riprap stones. For this discharge, the riprap stones were just submerged (i.e. the water depth extracted from data corresponded approximately to the difference of the water surface elevation to the top of the riprap stones), and this definition enabled the calculation of the relative submergence  $\Delta h_i/d_{50}$  for each sensor (the index  $i$  denotes the sensor; the reference level is sensor specific). All tests were monitored with three video cameras. A raster was sprayed on the test dams to facilitate visual monitoring and to determine the packing factor  $P_c$ .

Water was discharged from the reservoir by operating an outlet gate within the tunnel (2 m wide and 3 m high; not visible in Figure 3). The discharge was determined using the calibration curve of the gate, which was known from previous scale model tests (Vassdrags- og havnelaboratoriet 1973). The water level in the reservoir varied between the tests (see Table 1) which affected the discharge in the experiments for identical gate positions (differences of < 1% between corresponding gate openings for F15P1 and F15P2).

The placed riprap in F15P1 and F15P2 were loaded in a first step by opening the gate 0.4 m and releasing a discharge per unit width of  $q = 1.6 \text{ m}^2\text{s}^{-1}$  for 60 minutes. Following this initial loading period, the discharge was stopped to inspect the riprap for potential displacements or damage. Thereafter,  $q = 0.4 \text{ m}^2\text{s}^{-1}$  was released until the stage upstream of the dam stabilised, to estimate the percentage of flow passing through the permeable test dam, followed by 15 minutes of  $q = 1.6 \text{ m}^2\text{s}^{-1}$ . Afterwards, the discharge was stepwise increased in 5 minute intervals until the riprap failed. The increase in discharge was achieved by opening the gate additional 0.1 m resulting in increments of  $\Delta q \approx 0.4 \text{ m}^2\text{s}^{-1}$ . The time interval was kept as short as possible to minimise the loss of

water from the reservoir. Almost one million  $\text{m}^3$  of water was used for the three field tests and the water could consequently not be utilised for power production. The dumped riprap in test F15D1 was expected to fail at a significantly lower discharge than the placed riprap in the previous tests and loading started with  $q = 0.2 \text{ m}^2\text{s}^{-1}$ . This discharge was applied until the stage remained stable to check the percentage of flow conveyed through the test dam. In the next step, the dam was overtopped for 30 minutes with  $q = 0.4 \text{ m}^2\text{s}^{-1}$ . The riprap failed while increasing the discharge to  $0.8 \text{ m}^2\text{s}^{-1}$ .

### ***Physical model tests***

Model tests were carried out with scaled discharges from the field tests to investigate the comparability of scale model tests with the prototype situation. A total of five model tests were carried out, four with placed riprap (P05 – P08) and one with dumped, D02. In these tests, the discharge per unit width was scaled with  $1:6.5^{1.5}$  and the time with  $1:6.5^{0.5}$  according to Froude's model law using the geometrical scale defined above. The experimental setup, described in detail in Hiller et al. (2017), was built in a 1.00 m wide flume and consisted of an inclined chute with a horizontal crest (Figure 4), which were covered with a 0.1 m thick filter layer of angular stones with  $d_{50} = 0.025 \text{ m}$  and  $C_u = 1.50$ . The chute and the adjacent 0.15 m of the crest were covered with riprap stones. The remaining part of the crest was secured with larger stones, similar to the field setup. Angular stones with  $d_{50} = 0.057 \text{ m}$  and  $C_u = 1.17$  were used for the riprap. These values were derived by weighing 500 stones and measuring their  $a$ ,  $b$  and  $c$ -axis with a calliper (Table 2). Placed riprap was constructed by manually setting the stones one by one in an interlocking pattern with  $\beta = 60^\circ$ . For the test with dumped riprap the riprap stones were put one by one with random orientation and without interlocking pattern.

[Figure 4 somewhere here]

The packing factors and  $L_s$  are summarised in Table 3 together with the critical discharges for erosion of the first stone  $q_s$  and riprap failure  $q_c$ . The placed riprap in tests P05, P06 and P07 did not fail when  $q$  was increased to the maximum possible discharge in the flume ( $q_{\max} = 0.49 \text{ m}^2\text{s}^{-1}$  corresponding to  $8.1 \text{ m}^2\text{s}^{-1}$  in prototype scale). For these three tests, riprap failure was finally initiated by manually removing stones during overtopping. The test P08 was specifically designed to achieve riprap failure by extending the riprap length to  $L_s = 1.8 \text{ m}$  as, for this riprap length, failure could be achieved with  $q_c < 0.49 \text{ m}^2\text{s}^{-1}$  in previous tests (Hiller et al. 2017).

[Table 3 somewhere here]

As mentioned in the background section, stone displacements can be crucial for the stability of placed riprap on steep slopes. In order to investigate the displacements in flow direction,  $\Delta x$ , in the laboratory tests, the positions of four riprap stones were determined in P05 – P07 with a laser displacement meter attached to traverse system. The stones were located in the middle of the flume at  $x \approx 0.0 \text{ m}$ ,  $0.2 \text{ m}$ ,  $0.6 \text{ m}$ ,  $0.8 \text{ m}$  ( $x$  indicates the distance in flow direction from the edge between the horizontal crest and the slope, see Figure 4). Two additional stones were monitored in the test P08 due to the increased chute length. In this test, the stones were located at  $x \approx 0.0 \text{ m}$ ,  $0.2 \text{ m}$ ,  $0.6 \text{ m}$ ,  $1.0 \text{ m}$ ,  $1.4 \text{ m}$ ,  $1.8 \text{ m}$ . The measured maximum displacements, reported in Table 3, were always detected at the transition from the crest to the chute ( $x \approx 0.0 \text{ m}$ ). Note that in Table 3  $\Delta x_{init}$  denotes the displacement after the initial loading and  $\Delta x_{load}$  after reaching  $q_{\max}$ , but before manual interference.

The upstream water level was monitored  $1.6 \text{ m}$  upstream of the crest with an ultrasonic sensor of the same type as in the field. In order to monitor the water elevation over the riprap, pressure sensors (Schlumberger Water Services, Mini-Diver<sup>TM</sup>, DI501;  $\pm 0.5 \text{ cm H}_2\text{O}$ ) were mounted along the centreline under the filter at  $x \approx 0.00 \text{ m}$ ,  $0.40 \text{ m}$ ,

0.75 m for tests P06, P07 and D02, and  $x \approx -0.2$  m, 0.2 m, 0.6 m, 1.0 m, 1.4 m for test P08 (see Figure 4; the sensor at  $x \approx 0.2$  m turned out to be punctured and its data could not be used). No pressure sensors were installed for test P05, which was therefore excluded from the subsequent data analysis. The sampling frequency was 0.1 Hz for P06, 0.2 Hz for P07 and 1 Hz for P08 and D02. The sampling frequencies were adjusted according to the available memory of the pressure sensors and the assumed duration of the experiment. For the analysis below, the sensor data were averaged over 24 s corresponding to averaging over 60 s in the prototype. As for the prototype tests, the relative submergence  $\Delta h_i/d_{50}$  was calculated using the stage at  $F_s = 0.6$  as reference for each sensor. The discharge to the flume was controlled by valves and delivered by two pipes equipped with discharge meters (Siemens Sitrans<sup>TM</sup> Mag5000;  $\pm 0.5\%$ ). All tests were monitored with two video cameras, one mounted in the flume facing the chute covered with riprap and the other facing the profile through the flume window.

## **Results and discussion**

Table 4 summarises the packing factors and stone-related Froude numbers  $F_{s,s}$  and  $F_{s,c}$ . The corresponding results will be presented and discussed below in regard to the riprap types.

[Table 4 somewhere here]

### ***Dumped riprap***

The dumped riprap in the field test F15D1 failed during the increase of the discharge from  $0.4 \text{ m}^2\text{s}^{-1}$  to  $0.8 \text{ m}^2\text{s}^{-1}$  (i.e.  $0.6 < F_{s,c} < 1.2$ ) and the corresponding model test D02 failed at  $F_{s,c} = 1.2$  ( $q_c = 0.05 \text{ m}^2\text{s}^{-1}$ ). The packing factors in the field and model tests agreed well with  $P_c = 0.84$  and  $P_c = 0.83$ , respectively, and  $F_{s,c}$  was in the same range as the majority of the data points in Figure 2a.

The flow in the prototype test during the lowest discharge step of  $q = 0.2 \text{ m}^2\text{s}^{-1}$  ( $F_s = 0.3$ ) is visualised in Figure 5a. For this discharge, the main flow was conveyed through the permeable dam and the riprap was partly overtopped in the lower half of the test dam. This flow pattern can be associated with the dam-setup as the flow through the permeable dam body resulted in an increasing water level along the riprap. In the lower part, the flow pattern can be characterised as cascading over the riprap stones similar to nappe flow on stepped spillways. Despite this pattern, it can be reasonably assumed that the flow through the test dam was  $q \leq 0.2 \text{ m}^2\text{s}^{-1}$ . The cascading flow pattern prevailed also during the increased discharge of  $q = 0.4 \text{ m}^2\text{s}^{-1}$  ( $F_s = 0.6$ ; see Figure 5b). There were no visible differences in the flow pattern compared to the corresponding discharge over placed riprap (Figure 6a). The dumped riprap failed during a further increase in discharge as the central part of the riprap became unstable and slid down the supporting fill. Thereafter, the supporting fill was eroded as the protecting layer was missing. The flow pattern in the model tests corresponded to cascading flow as observed in the field. Moreover, the model crest was partly overtopped for  $F_s = 0.3$  ( $q = 0.01 \text{ m}^2\text{s}^{-1}$ ). Hence, it is reasonable to assume the portion of discharge corresponding to  $F_s = 0.3$  flowed through the test dams in the field and through the filter layer in the model tests, respectively.

[Figure 5a and 5b somewhere here]

### ***Placed riprap***

#### *Stability and packing density*

The placed riprap in the tests F15P1 and F15P2 failed at discharges corresponding to  $F_{s,c} = 8.6$  ( $q_c = 6.1 \text{ m}^2\text{s}^{-1}$ ) and  $10.7 \leq F_{s,c} \leq 11.3$  ( $7.5 \text{ m}^2\text{s}^{-1} \leq q_c \leq 8.0 \text{ m}^2\text{s}^{-1}$ ; failed while increasing the discharge), respectively. In test F15P1, erosion of the first stone was

observed at  $F_{s,s} = 6.4$  while in F15P2 four stones were eroded from the downstream edge of the crest at  $F_s = F_{s,s} = 8.9$ , among them the marked stone containing the sensor D1. Note that the flow through the permeable dam was included in the total discharge, but that it contributed less than 5% to  $F_{s,s}$  or  $F_{s,c}$ .

The model tests P05, P06 and P07 withstood the maximum possible discharge  $q_{\max} = 0.49 \text{ m}^2\text{s}^{-1}$ , corresponding to  $F_s = 11.5$ . The discharge could not be further increased as otherwise the inflow tank would have been overtopped. Therefore, discharges close to  $q_{\max}$  were applied for a longer time period of up to 12 hours. As this extended exposure of the riprap to overtopping did not result in failure, riprap failure was finally initiated by manually removing stones during overtopping. Compared to the tests with shorter riprap length (P05 – P07), the placed riprap in P08 with  $L_s = 1.8 \text{ m}$  failed at  $F_{s,c} = 5.6$  ( $q_c = 0.24 \text{ m}^2\text{s}^{-1}$ ) which may be attributed to the influence of displacements (see Hiller et al. 2017).

The reason for the observed differences in  $F_{s,c}$  for the field and laboratory tests may partly be associated with the packing of the riprap. In fact, the placed riprap in the field tests were looser packed and were characterised by significantly higher  $P_c$  values than the model tests (see Table 4). Constructing the riprap, it was challenging to keep the variation in  $P_c$  small as this parameter cannot be determined before finishing the riprap structure. As indicated by the numbering of the experiments, the placed riprap in the tests P05 and P06 were not the first riprap that were built in the laboratory (see Hiller et al. 2017 for a detailed overview on the laboratory experiments) and the low  $P_c$  values for these tests reflect that the experimentalists became more experienced in constructing the placed riprap. To counteract this tendency, the riprap stones in the subsequent tests P07 and P08 were randomly picked and placed in an interlocking pattern without further optimisation (keeping in mind the required inclination angle),



resulting in increased  $P_c$  values for the respective tests. The different  $P_c$  values between the model ( $P_c = 0.52$  on average) and the field tests ( $P_c = 0.70$  on average) indicate laboratory effects in the placement, because the human dexterity allows denser packing compared to machine placement (Pardo et al. 2014). Moreover, differences in  $P_c$  can also result from the stone shape as the field-stones were slightly more cubical than the model-stones, apparent by the ratios  $a/b_s = 1.8$  and  $a/b_s = 2.0$ , respectively.

### *Flow pattern*

The visually observed flow patterns in the field and the model are first described and then compared with each other using exemplarily F15P2 in Figure 6 and P08 in Figure 7. A video of F15P2 is available in the supplementary material.

[Figure 6abcd somewhere here]

The flow pattern for the lowest field discharge resembled a nappe flow over the entire downstream slope (Figure 6a). When the discharge was increased, the flow became aerated and was, for  $F_s > 2.3$  ( $q > 1.6 \text{ m}^2\text{s}^{-1}$ ), similar to a non-aerated skimming flow (Figure 6b). The flow along the abutments was affected by the uneven surface of the channel and the larger stones, resulting in boundary effects visible as white water (Figure 6b, 6c, 6d). Despite these boundary effects, the flow pattern in the center of the test dams was still comparable to the corresponding pattern in the model tests shown in Figure 7. The marked stones were visible without difficulties up to  $F_s = 5.5$  ( $q = 3.9 \text{ m}^2\text{s}^{-1}$ , Figure 6c) and the water surface upstream of the dam was nearly flat and not much disturbed by the pillar in the tunnel opening. Upon a further increase of the discharge, the flow became more and more affected by the pillar causing a standing wave and an uneven water surface upstream of the test dams (Figure 6d). The hydraulic jump downstream of the test dams was not observed to affect the riprap stability.

In the model tests, the flow pattern in the upstream part in test P08 (Figure 7) corresponded the observed flow pattern in P05, P06 and P07, which were carried out with shorter  $L_s$  (indicated in the figure by the drawn horizontal line). Nappe flow occurred for  $F_s = 0.7$  ( $q = 0.03 \text{ m}^2\text{s}^{-1}$ , Figure 7a) which changed to skimming flow when increasing the discharge. Self-aeration started around  $x = 0.8 \text{ m}$  (corresponding to the dam toe in the field tests or the lower end of the riprap in the laboratory tests P05 – P07) for  $F_s = 2.4$  ( $q = 0.10 \text{ m}^2\text{s}^{-1}$ , Figure 7b). The point of aeration moved further downstream with increasing discharge, as was observed in the field where aeration could no longer be observed for  $F_s > 2.3$  ( $q > 1.6 \text{ m}^2\text{s}^{-1}$ , Figure 6b). Accordingly, the aeration started downstream of the drawn line in Figure 7c, indicating the scaled  $L_s$  of the prototype tests. The figure shows P08 just before riprap failure at  $F_s = 5.6$  ( $q = 0.24 \text{ m}^2\text{s}^{-1}$ ).

[Figure 7 abc somewhere here]

#### *Pressure measurements and water levels*

The relative submergence  $\Delta h_i/d_{50}$  upstream of the riprap corresponds to the relative overtopping depth over the test dams in the field and model and is presented in Figure 8 as a function of  $F_s$ . The figure shows two data series for each field test representing the two different sensor types ‘mic’ (average of ‘mic1’ and ‘mic2’) and ‘WL16’. The deviation between the two sensor readings can be attributed to the different locations of the sensors (see Figures 3 and 6). The comparison of the field values  $\Delta h_{mic}/d_{50}$  with the data from the model tests shows good agreement for  $F_s < 6$ , before the two series deviate for higher  $F_s$ . The deviation can be attributed to the undulating water surface in the field for  $F_s > 6$  (see Figures 6c and 6d). Furthermore, changes in the dam crest due to stone displacements might had an effect on the overtopping characteristics in the field and hence the relation between the unit discharge and the overtopping depth. This

assumption is supported for F15P1 by the observation of stone erosion from the crest at  $F_{s,s} = 6.4$ . The shape of the curves for the model tests P06, P07 and P08 in Figure 8 is regular and no deviation is visible around  $F_s = 6$  indicating that the discharge coefficient of the crest did not change. This is supported by the observation that only small stone displacements ( $\Delta x_{load} < 0.020$  m, Table 3) developed close to the transition between the crest and the slope in the model tests P05 – P07. Note that this does not contradict the statement above that displacements can be crucial for the stability of placed riprap on steep slopes. The displacements did not exceed the critical size of one stone length (Hiller et al. 2017), implying that the placed riprap was still stable, and reflected by the fact that the riprap in P05 – P07 did not fail.

[Figure 8 somewhere here]

The relative submergence  $\Delta h_i/d_{50}$  measured by the pressure sensors are plotted as a function of  $F_s$  in Figures 9 and 10 for the field and model tests, respectively. The data for the field sensors D1 and D2 in Figure 9a agree well with the observation of the flow pattern and the relative overtopping depth for  $\Delta h_{mic}/d_{50}$  as described above. The gradient for  $\Delta h_{D1}/d_{50}$  for F15P1 and F15P2 changes at  $F_s = 5.8$ , when the undulating water level due to the pillar became more important, and when a change in the discharge coefficient of the crest due to the erosion of several stones from the crest might have occurred at  $F_s = F_{s,s} = 6.4$ . It is worth mentioning that the sensors mounted inside riprap stones could not be placed exactly at the same location in F15P1 and F15P2. The different sensor locations provide an explanation for the offset between  $\Delta h_i/d_{50}$  for F15P1 and F15P2. The series  $\Delta h_{D1}/d_{50}$  for F15P2 is limited to  $F_s \leq 8.3$  as the stone containing D1 was eroded at  $F_s = 8.3$ .

Figure 9b shows the data of the pressure sensors which were located under the tests dams and which were not moved between the field tests. The increasing flow

irregularities due to the high discharge and the consequent destabilisation of the riprap is reflected by the increasing scatter for  $F_s > 6.4$  in the F15P1 data series. The difference in the gradient of the data series  $\Delta h_{U2}/d_{50}$  and  $\Delta h_{U3}/d_{50}$  for both field tests indicates that the flow was still under acceleration over the riprap. The sensor U4 was mounted 2 m downstream of the test dam in F15P1 and hence  $\Delta h_{U4}/d_{50}$  deviates from the other data series. During riprap failure in F15P1, the sensor was damaged and not replaced for the subsequent tests.

[Figure 9a and 9b somewhere here]

Figure 10 presents the data of the pressure sensors recorded during the model tests. The pressure sensors were placed at different locations compared to the field tests and a direct comparison with the field data is therefore hampered. The data series in Figure 10a for the model tests P06 and P07, which were carried out with a chute length corresponding to the scaled test dams in the field, have different gradients affirming non-uniform flow over the riprap. The larger deviations for  $\Delta h_{D0}/d_{50}$  between P06 and P07 can be attributed to the close position of the sensor to transition from sub- to supercritical flow and the corresponding rapid change in  $h$ , meaning that small differences in the riprap constructions can affect the recordings at this particular location. A significant decrease in  $\Delta h_{D750}/d_{50}$  for  $5.6 < F_s < 6.1$  coincides with the observation that the point of aeration passed the downstream end of the riprap. The data of P08 are presented separately in Figure 10b because P08 was run with increased chute length of 1.8 m and the pressure cells were mounted at different locations than in P06 and P07. The data series for  $\Delta h_{D600}/d_{50}$ ,  $\Delta h_{D1000}/d_{50}$  and  $\Delta h_{D1400}/d_{50}$  in P08 have a similar gradient.

[Figure 10a and 10b somewhere here]

### ***Comparison between dumped and placed riprap***

The critical stone-related Froude numbers in the present study were  $F_{s,c} \leq 1.2$  for dumped riprap and  $F_{s,c} \geq 5.6$  for placed riprap (Table 4). The values for dumped riprap are in the same range as reported in the literature (see Figure 2a) whereas  $F_{s,c}$  for placed riprap are generally larger than the values reported by Larsen et al. (1986), Dornack (2001) and Peirson et al. (2008) (see Figure 2b). However, these studies were carried out on gentler slopes, except for the three experiments of Dornack (2001) with  $S = 0.67$ . The field tests with placed riprap and a comparable stone inclination  $\beta$  reported by Lia et al. 2013 and Hiller and Lia 2015 had similar  $F_{s,c}$  than in the present study. The stability of placed riprap in terms of  $F_{s,c}$  is on average nine times higher than for dumped riprap (based on the data in Table 4, using  $F_{s,c} = 11.5$  for P05 - P07) and is hence larger than the stability gain between dumped and placed riprap in the study by Larsen et al. (1986) or Peirson et al. (2008). The stability gain is also higher than the gain reported in Hiller et al. (2017). However, Hiller et al. (2017) focused solely on results from the laboratory study and did not include the results of the field tests, excluding also the results of P05 – P07. Possible reasons for the different stability gain compared to Larsen et al. (1986) and Peirson et al. (2008) are the different packing factors and boundary conditions in terms of the chute length.

The packing factors for dumped riprap were nearly identical in the prototype and the model scale. On the other hand, the placed riprap in the field tests were looser packed (i.e. higher  $P_c$  values) than in the model tests. This observation indicates laboratory effects, which are present for placed, but not for dumped riprap.

The scope of this paper is the comparability of large-scale and model-scale riprap tests and a generalisation of the results in terms of a riprap sizing formula was abandoned due to the limited number of data points with similar packing factors.

However, the packing factor can be used as an indicator for the quality of placed riprap. A detailed description of placed riprap in terms of used stone size and shape, placement pattern and packing density is crucial to allow comparison with different studies.

## **Conclusions**

Unique field tests were carried out with large-scale riprap and compared with corresponding model tests in the scale of 1:6.5. The comparability between the model and laboratory tests was investigated in terms of stability, packing density, flow pattern and overtopping depth. Measurements of the upstream water level and along the riprap helped to detect flow changes, which were a consequence of changes in the riprap. The study showed good agreement for the dumped riprap tests between the field and the model tests in terms of the critical stone-related Froude number, packing factors and flow pattern. Placed riprap showed good comparability in the visual observed flow pattern and the relative overtopping depth, but the stability in terms of the stone-related Froude number was higher in the model tests. The packing factor was lower in the model, indicating denser packing than in the field, and gives a possible explanation for the deviation in stability between the model and the field tests. The packing factor seems to be an adequate measure to describe the quality of placed riprap. However, it is challenging to control this construction-related parameter and laboratory effects in the packing factor should be considered and further evaluated.

## **Acknowledgements**

We thank the Master students Fredrikke Kjosavik and Bastian Dost for their help in carrying out the physical model tests and field tests and the staff in the NTNU hydraulic laboratory for technical assistance. The collaboration and support by Sira-Kvina Power Company for access to the field site at dam Svartevatn and water supply are kindly

acknowledged. The permissions to use the reports of Larsen et al. (1986) and Sommer (1997) by the Regierungspräsidium Karlsruhe and the Karlsruhe Institute of Technology are acknowledged. We thank also the editor and reviewers for their comments, which helped to improve this paper.

## References

- Abt SR, Johnson TL. 1991. Riprap design for overtopping flow. *J Hydraul Eng.* 117:959-972.
- Abt SR, Thornton CI, Scholl BA, Bender TR. 2013. Evaluation of overtopping riprap design relationships. *J Am Water Resour Ass.* 49:923-937.
- Bung DB. 2013. Non-intrusive detection of air–water surface roughness in self-aerated chute flows. *J Hydraul Res.* 51:322-329.
- Bunte K, Abt SR. 2001. Sampling surface and subsurface particle-size distributions in wadable gravel- and cobble-bed streams for analyses in sediment transport, hydraulics, and streambed monitoring. Fort Collins, CO (USA): USDA, Rocky Mountain Research Station. (General Technical Report; RMRS-GTR-74).
- Chanson H. 2015. Embankment overtopping protection systems. *Acta Geotech.* 10:305-318.
- CIRIA, CUR, CETMEF. 2007. *The rock manual: The use of rock in hydraulic engineering.* 2nd ed. London: CIRIA.
- [DVWK] Deutscher Verband für Wasserwirtschaft und Kulturbau. 1990. *Hydraulische Methoden zur Erfassung von Rauheiten [Hydraulic methods to determine roughnesses].* Hamburg, Berlin: Parey.
- Dornack S. 2001. *Überströmbare Dämme - Beitrag zur Bemessung von Deckwerken aus Bruchsteinen [Overtoppable dams – a contribution to the design of riprap] [dissertation].* Dresden (Germany): Technische Universität Dresden. German.
- Godtland K. 1989. *Steinfyllingsdammer: dimensjonering av nedstrøms plastringsstein unntatt damfoten [Rockfill dams: design of riprap stones on the downstream slope except the dam toe].* Trondheim (Norway): Norsk hydroteknisk laboratorium. (ISBN: 82-595-5892-0). Norwegian.
- Harris MJ. 2015. Failure of dams due to overtopping — a historical prospective. In: Toledo MA, Morán R, Oñate E. *Proceedings of the Dam Protections against*

- Overtopping and Accidental Leakage - Proceedings of the 1st International Seminar on Dam Protections Against Overtopping and Accidental Leakage; 2014 Nov 24-26; Madrid. CRC Press/Balkema.
- Hiller PH. 2016. Kartlegging av plastring på nedstrøms skråning av fyllingsdammer. Trondheim [Survey of placed riprap on the downstream slope of rockfill dams]. Trondheim (Norway): Norwegian University of Science and Technology. (ISBN-10: 978-827598-095-1). Norwegian.
- Hiller PH, Aberle J, Lia L. Forthcoming 2017. Accumulating stone displacements as failure origin in placed riprap on steep slopes. *J Hydraul Res.*
- Hiller PH, Lia L. 2015. Practical challenges and experience from large-scale overtopping tests with placed riprap. In: In: Toledo MA, Morán R, Oñate E. Proceedings of the Dam Protections against Overtopping and Accidental Leakage - Proceedings of the 1st International Seminar on Dam Protections Against Overtopping and Accidental Leakage; 2014 Nov 24-26; Madrid. CRC Press/Balkema.
- [ICOLD] International Commission on Large Dams. 1995. Dam failures statistical analysis. Paris: ICOLD.
- Jafarnejad M, Franca MJ, Pfister M, Schleiss AJ. 2016. Time-based failure analysis of compressed riverbank riprap. *J Hydraul Res.* [Internet]. [published online 2016 Aug 23; cited 2016 Nov 30];12. Available from: <http://dx.doi.org/10.1080/00221686.2016.1212940>
- Knauss J. 1979. Computation of maximum discharge at overflow rockfill dams (a comparison of different model test results). In: International Commission on Large Dams. 13th Congress on Large Dams; 1979; New Delhi.
- Larsen P, Bernhart HH, Schenk E, Blinde A, Brauns J, Degen FP. 1986. Überströmbare Dämme, Hochwasserentlastung über Dammscharten [Overtoppable dams, spillways over dam notches] (unpublished report prepared for Regierungspräsidium Karlsruhe). Karlsruhe (Germany): Universität Karlsruhe. German.
- Lia L, Vartdal EA, Skoglund M, Campos HE. 2013. Rip rap protection of downstream slopes of rock fill dams - a measure to increase safety in an unpredictable future climate. Paper presented at: 9th ICOLD European Club Symposium; Venice.



- Linford A, Saunders DH. 1967. A hydraulic investigation of through and overflow rockfill dams. British Hydromechanics Research Association.
- Løvoll A. 2006. Breach formation in rockfill dams - results from Norwegian field tests. In: International Commission on Large Dams. 22nd Congress on Large Dams; 2006 Jun; Barcelona.
- [OED] Ministry of Petroleum and Energy. 2009. Forskrift om sikkerhet ved vassdragsanlegg (Damsikkerhetsforskriften) [Dam safety regulation]. OED. (FOR 2009-12-18-1600). Norwegian.
- Mishra SK. 1998. Riprap design of overtopped embankments [dissertation]. Fort Collins (CO): Colorado State University.
- Morán R, Toledo MA. 2011. Research into protection of rockfill dams from overtopping using rockfill downstream toes. *Can J Civ Eng.* 38:1314-1326.
- Morris MW, Hassan MAAM, Vaskinn KA. 2007. Breach formation: Field test and laboratory experiments. *J Hydraul Res.* 45:9-17.
- [NVE] Norwegian Water Resources and Energy Directorate. 2012. Veileder for fyllingsdammer [Guidelines for embankment dams]. Oslo (Norway): NVE. (guideline 4/2012). Norwegian.
- Olivier H. 1967. Through and overflow rockfill dams - new design techniques: Institution of Civil Engineers. (Paper no. 7012).
- Pagliara S, Carnacina I, Roshni T. 2010. Self-Aeration and friction over rock chutes in uniform flow conditions. *J Hydraul Eng.* 136:959-964.
- Pardo V, Herrera M, Molines J, Medina J. 2014. Placement test, porosity, and randomness of cube and cubipod armor layers. *J Waterway Port Coast Ocean Eng.* 140:04014017.
- Peirson WL, Cameron S. 2006. Design of rock protection to prevent erosion by water flows down steep slopes. *J Hydraul Eng.* 132:1110-1114.
- Peirson WL, Figlus J, Pells SE, Cox RJ. 2008. Placed rock as protection against erosion by flow down steep slopes. *J Hydraul Eng.* 134:1370-1375.
- Robinson KM, Rice CE, Kadavy KC. 1998. Design of rock chutes. *Transactions of the American Society of Agricultural Engineers.* 41:621-626.
- Schmocker L, Höck E, Mayor P, Weitbrecht V. 2013. Hydraulic model study of the fuse plug spillway at Hagneck canal, Switzerland. *J Hydraul Eng.* 139:894-904.

- Siebel R. 2007. Experimental investigations on the stability of riprap layers on overtoppable earthdams. *Environ Fluid Mech.* 7:455-467.
- Sommer P. 1997. Überströmbare Deckwerke [Overtoppable erosion protections] (unpublished report). Karlsruhe (Germany): Institut für Wasserbau und Kulturtechnik, Versuchsanstalt für Wasserbau, Universität Karlsruhe. German.
- Toledo MÁ, Morán R, Oñate E editors. 2015. Dam protections against overtopping and accidental leakage. London: CRC Press/ Balkema.
- Vassdrags- og havnelaboratoriet. 1973. Dam Svartevann, flomløp: Øvre tappeluke, kalibreringskurver [Dam Svartevann, spillway: upper releasing gate, calibration curves]. Trondheim (Norway): Vassdrags- og havnelaboratoriet ved Norges tekniske høgskole. Norwegian.

## **Appendices**

Table over coordinates of the measuring equipment in 2015.

[insert Table 5 here]

Table 1 Boundary conditions for the field tests in 2015 including the dam height  $h_d$ , the dam width  $B$ , the reservoir level  $H_r$ , the inclination angle  $\beta$  and the packing factor  $P_c$ . The size of the riprap stones was  $d_{50} = 0.37$  m, the extension of the slope covered with riprap  $L_s \approx 4.5$  m and the target inclination angle  $\beta_{target} = 60^\circ$ .

Test	$h_d$ (m)	$B$ (m)	$H_r$ (m a.s.l.)	$\beta$ ( $^\circ$ )	$P_c$ (-)
F15P1	3.2	12.2	896.03	53	0.75
F15P2	3.0	11.9	896.67	55	0.64
F15D1	3.1	12.5	897.03	-	0.84

Table 2 Stone properties in terms of the average axes  $\bar{a}$ ,  $\bar{b}$ ,  $\bar{c}$ , the average stone diameter  $\bar{d}$  and the  $d_{50}$ , coefficient of uniformity  $C_u$ , and density for the riprap stones  $\rho_s$  used in the field and for the model tests.

	$\bar{a}$ (m)	$\bar{b}$ (m)	$\bar{c}$ (m)	$\bar{d}$ (m)	$d_{50}$ (m)	$C_u$	$\rho_s$ (kg m <sup>-3</sup> )
F15	0.53	0.35	0.23	0.35	0.37	1.24	2750
Model	0.091	0.053	0.038	0.056	0.057	1.17	2710

Table 3 Experimental boundary conditions for the model tests including chute length covered with riprap  $L_s$ , packing factor  $P_c$  and the discharges per unit width  $q_s$  and  $q_c$  corresponding to erosion of the first stone and bulk erosion of the riprap, respectively.  $\Delta x_{init}$  and  $\Delta x_{load}$  denote the displacement in flow direction after the initial loading and up to  $q_{max}$ , respectively. All model tests were carried out with a stone size  $d_{50} = 0.057$  m and a target stone inclination  $\beta_{target} = 60^\circ$ .

Test	$L_s$ (m)	$P_c$ (-)	$q_s$ (m <sup>2</sup> s <sup>-1</sup> )	$q_c$ (m <sup>2</sup> s <sup>-1</sup> )	$\Delta x_{init}$ (m)	$\Delta x_{load}$ (m)
P05	1.0	0.48	< 0.49	> 0.49	0.000	0.006
P06	0.8	0.50	0.36	> 0.49	0.002	0.010
P07	0.8	0.56	> 0.49	> 0.49	0.002	0.019
P08	1.8	0.55	0.19	0.24	0.038	-
D02	0.8	0.83	0.05	0.05	-	-

Table 4 Results of the field and model test in terms of the packing factor  $P_c$  and the stone-related Froude number for the erosion of the first stones  $F_{s,s}$  as well as for riprap failure  $F_{s,c}$ .

Test	$P_c$ (-)	$F_{s,s}$ (-)	$F_{s,c}$ (-)
F15P1	0.75	6.4	8.7
F15P2	0.64	8.9	10.6-11.3
F15D1	0.84	0.6-1.2	0.6-1.2
P05	0.48	< 11.5 <sup>a</sup>	> 11.5
P06	0.50	8.4	> 11.5
P07	0.56	< 11.5 <sup>a</sup>	> 11.5
P08	0.55	4.5	5.6
D02	0.83	1.2	1.2

<sup>a</sup> The erosion of the first stone was not observed and the given value corresponds to the  $F_s$  when the first missing stone was detected.

Table 5 Coordinates for the pressure cell WL16, microsonic sensors mic1 and mic2 and the pressure sensors ('U' indicating placement under the dam and 'D' on the dam, numbering from upstream to downstream). Coordinates given in Euref89 UTM32, height in NN1954.

	Item	X (m)	Y (m)	Z (m)
All tests	WL16	n/a	n/a	772.27
	mic1	6556225.31	379769.55	777.94
	mic2	6556224.28	379766.01	777.91
	U1	6556213.90	379770.65	770.74
	U2	6556212.51	379770.22	770.88
	U3	6556210.94	379771.89	770.85
F15P1	Bottom left	6556211.23	379776.05	771.38
	Bottom right	6556209.17	379766.81	771.42
	Top right	6556211.94	379764.89	773.88
	Top left	6556215.76	379776.48	774.05
	D1	6556214.60	379770.58	773.95
	D2	6556211.23	379771.29	772.11
	U4	6556208.27	379771.90	771.04
F15P2	Bottom left	6556211.80	379776.04	771.24
	Bottom right	6556210.11	379766.82	771.26
	Top right	6556212.76	379764.62	773.85
	Top left	6556215.42	379776.25	773.59
	D1	6556214.50	379770.69	773.70
	D2	6556211.70	379770.18	772.11
F15D	Bottom left	6556211.77	379776.15	771.33
	Bottom right	6556210.09	379766.83	771.24
	Top right	6556212.60	379764.56	773.80
	Top left	6556215.52	379776.70	773.84
	D1	6556213.85	379770.51	773.57
	D2	6556211.46	379771.84	771.68



Figure 1 Rehabilitation work on the 129 m high dam Svartevatn in Norway. The riprap stones on the downstream slope are placed one by one in an interlocking pattern with their longest axes inclined towards the dam. The inclination angle  $\beta$  is the angle between the longest axis of a stone and the slope as indicated in the picture. (Photo NTNU)



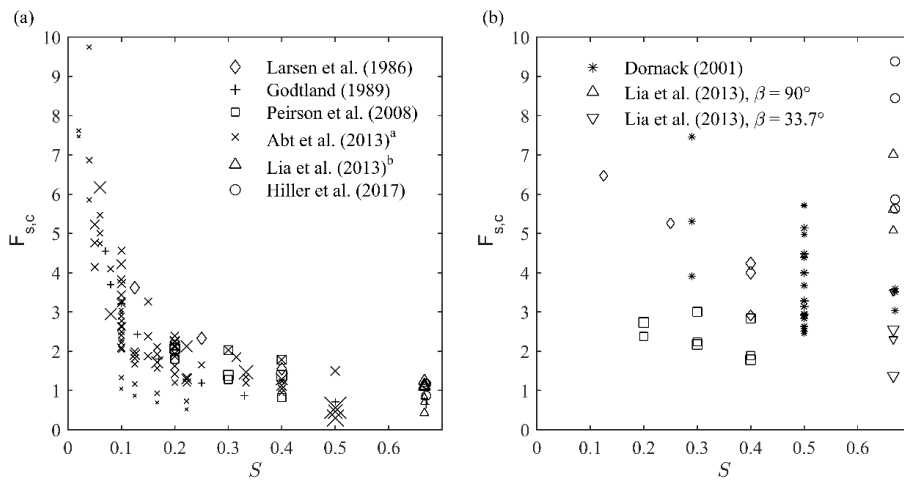


Figure 2 Existing data for the stability of dumped (a) and placed (b) riprap. The marker size is proportional to the used stone size (the marker size in the legend corresponds to  $d = 0.1$  m). The legend for (a) applies also for (b). <sup>a</sup> The data from Abt et al. (2013) include data points of eight different studies. <sup>b</sup> Only data are presented from experiments with a locked dam toe.

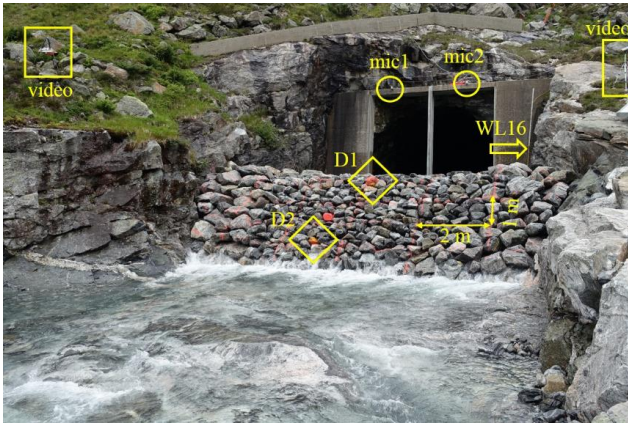


Figure 3 Test dam F15P2 between two loadings. The highlighted measurement equipment indicates the positions of the video cameras, ultrasonic sensors mic1 and mic2, the pressure cell WL16 (the measuring point is behind the dam), and the equipped stones D1 and D2. (Photo: NTNU)

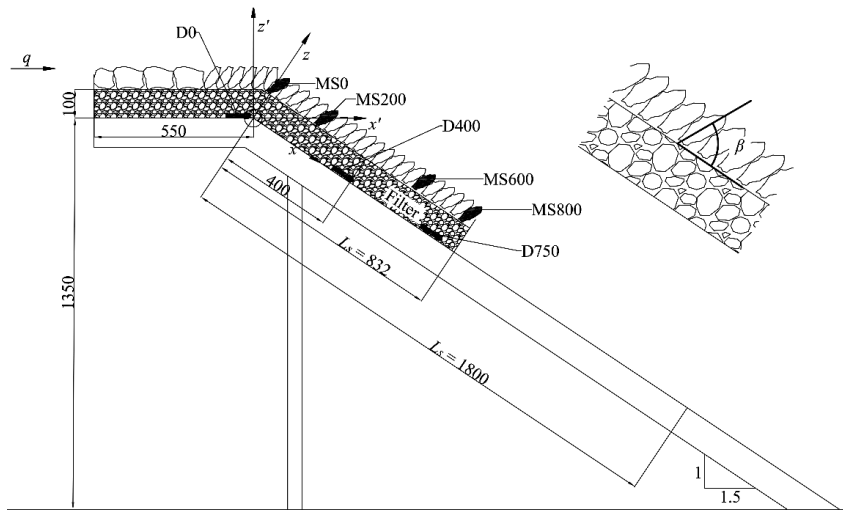


Figure 4 Setup for the scaled model tests with placed riprap P06 and P07. The chute was impervious and was overtopped with discharge from the left to the right. The marked stones ‘MSxx’ as well as the position of the pressure cells Diver ‘Dxx’ are marked. In the upper right corner, there is an enlarged part of the filter and the placed riprap stones to define the inclination angle  $\beta$ . All measures in (mm).



Figure 5 Picture frames of the test F15D1 with dumped riprap: (a) partly overtopped test dam with most of discharge as through flow  $q = 0.2 \text{ m}^2\text{s}^{-1}$  ( $F_s = 0.3$ ); (b) cascading flow at  $q = 0.4 \text{ m}^2\text{s}^{-1}$  ( $F_s = 0.6$ ). (Video: S. R. Skilnand)

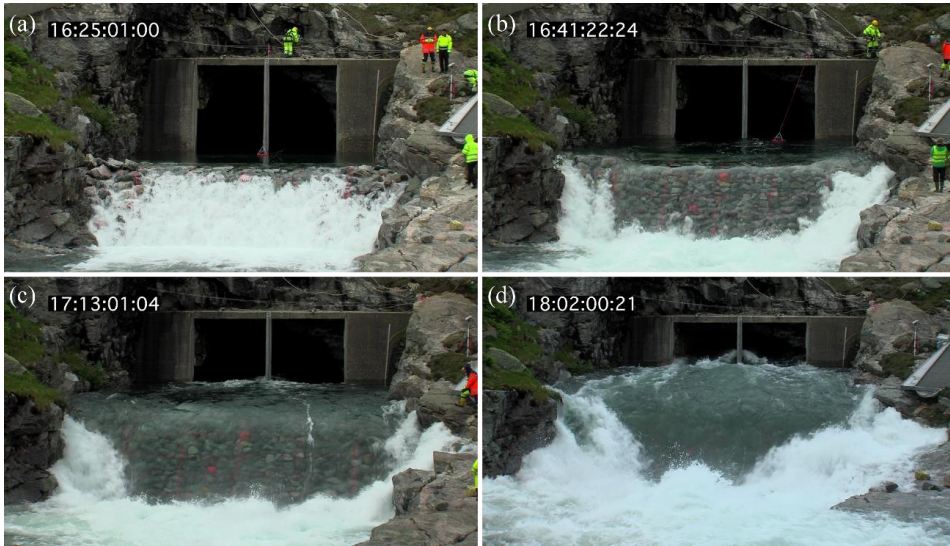


Figure 6 Picture series of F15P2: (a) nappe flow with  $q = 0.5 \text{ m}^2\text{s}^{-1}$  ( $F_s = 0.6$ ); (b) skimming flow with  $q = 1.6 \text{ m}^2\text{s}^{-1}$  ( $F_s = 2.3$ ); (c) skimming flow with still sound flow conditions upstream of the test dam at  $q = 3.9 \text{ m}^2\text{s}^{-1}$  ( $F_s = 5.5$ ); and (d) skimming flow in the centre part of the tests dam at  $q = 7.5 \text{ m}^2\text{s}^{-1}$  ( $F_s = 10.7$ ). The flow upstream of the test dam is uneven due to the inflow conditions and the high discharge of  $Q = 90 \text{ m}^3\text{s}^{-1}$ . The coloured stone in the top containing D1 is missing because it was eroded at  $q_s = 6.3 \text{ m}^2\text{s}^{-1}$  ( $F_{s,s} = 8.9$ ). (Video: S. R. Skilnand)

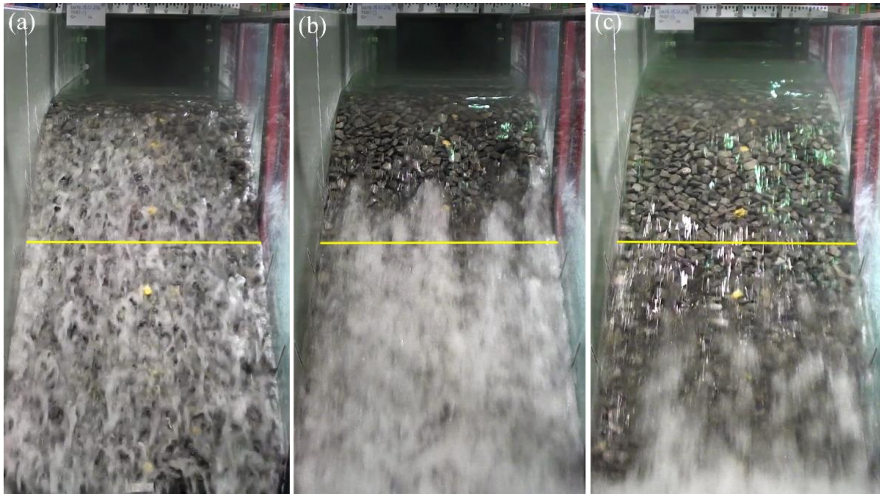


Figure 7 Video frames of P08. The yellow line at  $x = 0.8$  m indicates the downstream end of the riprap in P06 and P07 and the corresponding field tests. (a) nappe flow over the whole slope at  $q = 0.03 \text{ m}^2\text{s}^{-1}$  ( $F_s = 0.7$ ); (b) skimming flow without aeration in the upper third of the slope and aerated further downstream with  $q = 0.10 \text{ m}^2\text{s}^{-1}$  ( $F_s = 2.4$ ); (c) skimming flow with partial aeration in the downstream third of the slope just before riprap failure at  $q = q_c = 0.24 \text{ m}^2\text{s}^{-1}$  ( $F_s = F_{s,c} = 5.6$ ). (Video NTNU)

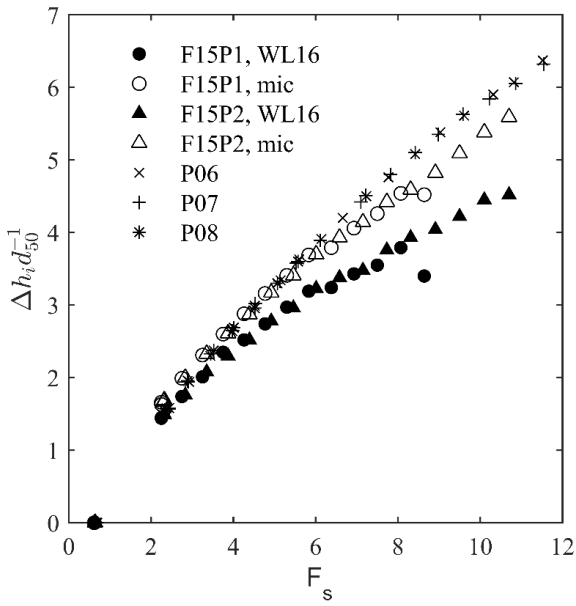


Figure 8 Relative submergence  $\Delta h_i/d_{50}$  as a function of the stone-related Froude number for the field and model tests.

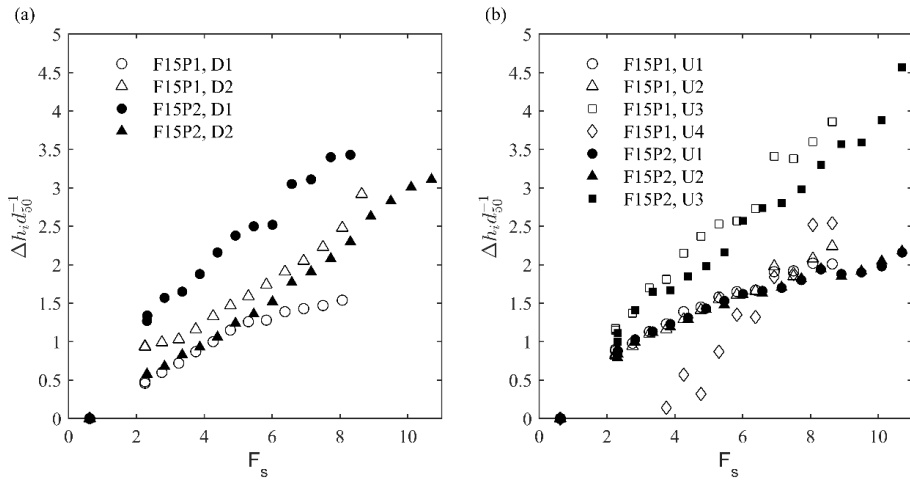


Figure 9 Relative submergence as a function of  $F_s$  for the data of the pressure cells during the field tests: (a) Data of the sensors D1 and D2 placed in riprap stones. (b) Data of the sensors placed in the bottom of the channel, U1 to U3 under the test dams and U4 approximately 2 m downstream (damaged under F15P1 and not replaced for the remaining tests).



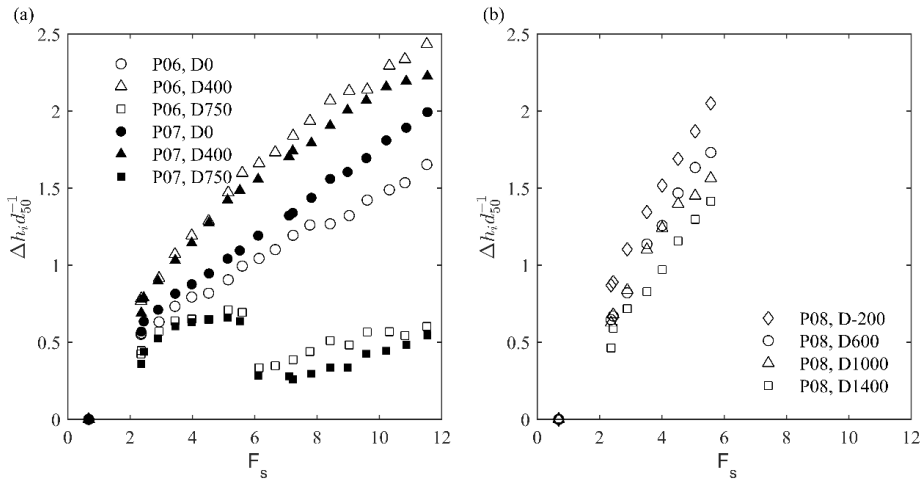


Figure 10 Relative submergence as a function of  $F_s$  for the data recorded by the pressure cells in the model tests. The number in the label indicates the distance in [mm] to the edge between the crest and the slope in flow direction. Data of P06 and P07 in (a) and of P08 in (b).

## Paper III

---

### **Smartstones: A small 9-axis sensor implanted in stones to track their movements**

Oliver Gronz, Priska H. Hiller, Stefan Wirtz, Kerstin Becker, Thomas Iserloh, Manuel Seeger, Christine Brings, Jochen Aberle, Markus C. Casper, Johannes B. Ries (2016)

CATENA, 142, 245-251, doi: <http://dx.doi.org/10.1016/j.catena.2016.03.030>  
(Open Access).

---





## Smartstones: A small 9-axis sensor implanted in stones to track their movements



Oliver Gronz <sup>a,\*</sup>, Priska H. Hiller <sup>b</sup>, Stefan Wirtz <sup>a</sup>, Kerstin Becker <sup>a</sup>, Thomas Iserloh <sup>a</sup>, Manuel Seeger <sup>a</sup>, Christine Brings <sup>a</sup>, Jochen Aberle <sup>b</sup>, Markus C. Casper <sup>a</sup>, Johannes B. Ries <sup>a</sup>

<sup>a</sup> Department of Physical Geography, Trier University, 54286 Trier, Germany

<sup>b</sup> Department of Hydraulic and Environmental Engineering, Norwegian University of Science and Technology NTNU, S. P. Andersens veg 5, 7491 Trondheim, Norway

### ARTICLE INFO

#### Article history:

Received 29 April 2015

Received in revised form 8 January 2016

Accepted 24 March 2016

Available online 6 April 2016

#### Keywords:

Active tracer

Geomorphology

Hydraulic engineering

Stone movement

Active RFID (radio frequency identification)

### ABSTRACT

The movement of stones is important in a variety of disciplines such as geomorphology or hydraulic engineering. Plenty of different sensors, visual, active or passive tracers exist to capture movements in various ways. However, none of them is sufficiently small to be implanted in pebbles with a longest axis of approx. 60 mm.

In this article, a sufficiently small probe is introduced: the Smartstone probe. It consists of a metal cylinder (diameter 8 mm, length 55 mm) with a flexible antenna and contains a Bosch BMX055 sensor composed of a triaxial accelerometer, magnetometer and gyroscope, respectively. Additional components inside the probe are memory to store data, active RFID (Radio-frequency identification) technique to transmit data and two button cells as power supply.

Mounted into a pebble, the applicability of this probe was tested in laboratory flume experiments by determining the pebble movement using the Smartstone measurements and comparing them to the movement pattern captured by a high-speed camera. The derived orientations and positions in these test experiments resulted in deviations of 32.4% compared to the visual footage. The different reasons for deviations are noise, quantization error, integration error, orientation error and clipping. The error sources were divided with supplementary experiments resulting in mean absolute deviation (MAE) of 3.3% due to noise, quantization, and integration errors; orientation errors result in an increased MAE of 13.7% in natural environment and 21.7% in laboratory. The MAE of all experiments containing clipping was 63.2%.

These deviations will be reduced in future by application of methods like Kalman filtering or Markov models, which are established in other disciplines like computer science, robotics or (pedestrian) navigation.

© 2016 The Authors. Published by Elsevier B.V. This is an open access article under the CC BY-NC-ND license (<http://creativecommons.org/licenses/by-nc-nd/4.0/>).

### 1. Introduction

Movements of stones are an important part of several geomorphological and hydrological processes as well as engineering applications. This includes fast movements like rockfalls or other mass movements in high mountain regions, slower movements in fluvial and glacial environments, and erosion protection measures.

To identify stone movements, different methods have been developed and applied in earlier research. This includes visual tracers such as coloured rocks (De Jong, 1991; Foster, 2000) or fluorescent dye (Cameron, 2012), passive or active tracers (Cameron, 2012;

Ergenzinger and De Jong, 2003; Gray et al., 2010; Ryan et al., 2005), sediment traps (Ergenzinger et al., 1994; Habersack, 1997; Reid et al., 1980; Schaffernak, 1916), video observation (Krause, 1997), acoustic sensors (Bedeus and Ivicsics, 1963; Johnson and Muir, 1969; Krein et al., 2008), as well as recent applications like Passive Integrated Transponder (PIT) tags (Ergenzinger et al., 1989; Lamarre and Roy, 2008; Liébault et al., 2012; Oikawa, 2011; Schneider et al., 2010).

All these methods have limitations impeding a thorough observation of the transportation path, movement types and forces affecting the ground. Recently developed PIT tags have made significant progress towards a thorough observation, but have mainly been developed for the monitoring of bigger stones and boulders. For the observation of smaller stones, a system is still missing. Moreover, the measurement of the acceleration that a stone experiences at incipient motion conditions would allow for calculating the resulting force acting on the stone. This would deepen our understanding of the erosion process itself. A more specific application is the design of slope protections with riprap,

\* Corresponding author.

E-mail addresses: [gronz@uni-trier.de](mailto:gronz@uni-trier.de) (O. Gronz), [priska.hiller@ntnu.no](mailto:priska.hiller@ntnu.no) (P.H. Hiller), [wirtz@uni-trier.de](mailto:wirtz@uni-trier.de) (S. Wirtz), [k.becker0712@gmx.de](mailto:k.becker0712@gmx.de) (K. Becker), [iserloh@uni-trier.de](mailto:iserloh@uni-trier.de) (T. Iserloh), [seeger@uni-trier.de](mailto:seeger@uni-trier.de) (M. Seeger), [brings@uni-trier.de](mailto:brings@uni-trier.de) (C. Brings), [jochen.aberle@ntnu.no](mailto:jochen.aberle@ntnu.no) (J. Aberle), [casper@uni-trier.de](mailto:casper@uni-trier.de) (M.C. Casper), [riesj@uni-trier.de](mailto:riesj@uni-trier.de) (J.B. Ries).

where such information may be helpful for the development of improved design approaches.

To avoid the limitations, a sensor carrier was developed for stones including an active radio-frequency identification (RFID) chip, an accelerometer, a magnetometer and a gyroscope. Developer was the company SST (smart sensor technologies) in Rheinberg, Germany for the Department of Physical Geography at Trier University in cooperation with the Department of Hydraulic and Environmental Engineering at the Norwegian University of Science and Technology, NTNU Trondheim. The probe uses a protocol protected by patent US20140240088. However, the data analysis described in the sample application of this technical note is open for further developments.

The relatively compact dimensions of the Smartstone probe (described in Section 2) allow its insertion into larger pebbles. This subsequently called “Smartstone” can be used as an advanced RFID-based tracer stone. Such tracer stones have a wide application range from laboratory use to fluvial environments. For example, within the laboratory, such tracer stones may be used to acquire directly data on the movement of individual particles with a high temporal resolution, i.e. to study sediment transport mechanics without the need of visual access to the particles (e.g. photogrammetry). Within field applications, much more detailed information can be extracted from RFID-based tracer stones than by “conventional” tracer stones given the stones can be adequately contacted via gateways along the transport path and that the battery lifetime is adequate. Last but not least, the RFID technology is helpful for the localisation of tracer stones as the probe can still receive radio signals even if it is in sleeping mode.

The main objectives of this article are to:

- describe the Smartstone probe, its specification and usage,
- describe an exemplary laboratory flume experiment demonstrating the probe’s capabilities and present limitations,
- discuss the measuring principle by means of an application.

## 2. Description of the Smartstone system

### 2.1. Probe specifications

The Smartstone prototype kit consists of the Smartstone probe, a gateway, an optional wireless router, and a computer for data communication. The Smartstone probe is a 55 mm long and 8 mm wide cylinder with a 70 mm long flexible antenna (Fig. 1a). It weighs 0.0075 kg including battery. The self-calibrating probe is powered by two silver-oxide button cells (1.55 V, 20 mAh) and contains the core unit of the Smartstone-kit: a BMX055 sensor module. This module comprises a tri-axial 12 bit acceleration sensor, a tri-axial 16 bit gyroscope, and a geomagnetic sensor (sometimes also referred to as e-compass or geomagnetic sensor), together with an active RFID tag, 261.92 kB memory, a chronometer, and a thermometer. The sensor module data provides orientation, tilt, motion, acceleration, rotation, shock, vibration and heading of the probe (Bosch Sensortec, 2014). The chronometer

and thermometer provide auxiliary data on time (resolution 1/32,768 s) and temperature. For the presented prototype, the ranges of the sensor module are  $\pm 4$  g for the accelerometer (where  $g$  denotes the acceleration due to gravity),  $\pm 2500$   $\mu$ T for the magnetometer (where T denotes the unit Tesla), and  $\pm 2000$   $^{\circ}$  s $^{-1}$  for the gyroscope. One sensor axis is aligned with the long axis of the cylinder, the other two axes orientations are indicated by the battery screw (Fig. 1b).

### 2.2. Data transmission

The sensed data are transferred to a Linux-based gateway via an 868 MHz radio antenna. The gateway uses a SSH (Secure Shell) server to enable controlling the probes. Additionally, it stores the data (of several probes) in a database. The sensed data are either forwarded to a wireless router at a frequency of 2.4 GHz or directly to a computer connected with an Ethernet cable. The data transfer from the gateway is based on the Hypertext Transfer Protocol (HTTP), so that the data can be directly assessed and post-processed using mathematical software or spreadsheet applications. If several Smartstone probes are used simultaneously, the data are assigned to the specific probes via the RFID tag. The data transfer is managed via a specific software developed by SST.

The radio frequency (RF) transmitted data from the probe to the gateway includes information on date and time, temperature, battery voltage, memory fill level, probe ID (RFID-tag), and measurement mode.

### 2.3. Probe setup options

The probe has different modes indicating recording, standby, and configuration. In recording mode, impacts are recorded with very short response times. After a period with impacts below a user-defined threshold, the probe switches to standby mode with reduced power consumption. From standby mode, the probe switches either to recording mode through new impacts or to configuration mode after longer periods without further impacts. The time intervals for automatically switching between the modes and the impact thresholds are software-defined and can be adapted with regard to individual applications.

The configuration mode can be used for active communication with the probe to synchronize the time with the gateway, to activate/deactivate individual sensors (i.e. accelerometer, magnetometer or gyroscope), to read out or clear the memory, and to define the selection of the aforementioned thresholds. Moreover, the configuration mode allows also selecting between different settings varying in power consumption and accuracy. In total, four different power settings can be chosen. The setting with lowest power consumption results in a noise of 10 mg for the accelerometer, 2  $\mu$ T for the magnetometer, 2 $^{\circ}$  s $^{-1}$  for the gyroscope. On the other side of the spectrum, the setting with lowest noise and highest power consumption results in a noise of 1.2 mg for the accelerometer, 0.5  $\mu$ T for the magnetometer and 0.24 $^{\circ}$  s $^{-1}$  for the gyroscope. More detailed information is given in the data sheet (Bosch Sensortec, 2014). The description also contains information about the

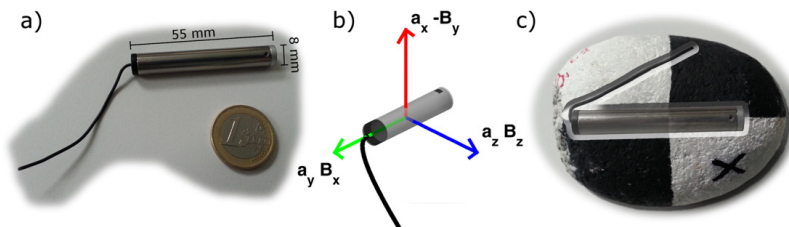


Fig. 1. a) The Smartstone probe and its dimensions, b) three dimensional coordinate systems of the acceleration sensor ( $a_x, a_y, a_z$ ) and the geomagnetic sensor ( $B_x, B_y, B_z$ ), black point indicates battery screw, c) artist-illustration of the probe inserted into a tracer pebble.

applied filters and the discretization resulting from different accelerometer ranges.

The prototype probe presented in this paper allows for sampling intervals ranging from 12 ms to 100 ms. Using sampling intervals shorter than 100 ms precludes acquisition of gyroscope data due to the relatively large response time of the gyroscope. Therefore, operation of the gyroscope depends on the expected stone (rotation) velocity: If rotation velocity exceeds five rotations per second, sub-Nyquist sampling does not allow for derivation of velocities.

### 3. Preliminary tests

#### 3.1. Data transmission range

The distance in which a Smartstone probe remains in regular contact with the gateway is considered as functional range. If this distance is exceeded, the probe has irregular contact with the gateway until the signal transfer finally stops, i.e. the maximum range is reached. The functional and maximum signal ranges of the Smartstone probe through air were evaluated by moving the probe stepwise away from the gateway. The functional range with intervisibility was 220 m (max. range 280 m). However, any disturbance, like plants, buildings, walls, will decrease those ranges.

To examine the effect of bodies in which the probe is embedded, the range experiments were repeated with the probe being inserted into stones of different sizes and materials:

1. Pebble (which is later used in the experiments in Section 3.3): longest axis 76 mm, short axis 46 mm, and 57 mm along the middle axis; density 2680 kg m<sup>-3</sup>; granite; two holes like described in Section 3.3.2; functional range with pebble-gateway intervisibility 48 m.
2. Cobble: 155 mm × 90 mm × 110 mm; density 2640 kg m<sup>-3</sup>; granite; one borehole with depth 105 mm (centred sensor) with the antenna routed like a spiral spring in the same hole, rest of hole filled with drilling dust resulting from the specific stone and modelling mass cap; functional range with intervisibility 52 m.
3. Cubic paving stone: all axes approx. 90 mm; density 2810 kg m<sup>-3</sup>; basalt (iron-rich); one borehole (depth 72.5 mm) with antenna routed like a spiral spring in the same hole, drilling dust, modelling mass; functional range with intervisibility 50 m.

The results of these tests show that the routing of the antenna has a stronger influence than the body-diameter and that the antenna elongating the probe cylinder is better than a side-by-side position.

The data transmission under water was tested in a small natural lake with the gateway being placed at the lakefront and using the aforementioned pebble. In this test, the transmission was still working at the lake's maximum depth of 1.15 m. Additional tests at different environments showed a stronger influence of surrounding: in a sufficiently deep lock chamber with armoured concrete walls, data transmission stopped working at 0.4 to 0.5 m. In an underground water storage in a building (armoured concrete walls, metal doors), the signal transmission did not work at all.

These tests thus showed that the influence of the environment is stronger than the water depth and that especially metal and armoured concrete decrease the range. Therefore, before using the probe in a specific environment, preliminary range tests should be carried out.

It is worth mentioning that exceeding the maximum transmission range does not result in data loss: the probe works autonomously without gateway. Communication with the gateway is only necessary to adjust settings or to transfer data stored in the probe's own memory.

#### 3.2. Battery lifetime

The battery lifetime of the probe during continuous motion was evaluated by mounting the probe to a drill (sampling at an interval of

100 ms). After approximately 15 min of continuous drilling, the internal memory was filled. Once the memory was filled, the data were transferred via the gateway and the memory subsequently cleared. The procedure was repeated until the battery voltage dropped below the critical threshold for probe operation.

Five data acquisition and download cycles could be completed during two tests with activated accelerometer and magnetometer (i.e. without gyroscope). After the fifth cycle, the memory could be filled to approximately 50% before the battery was empty. When the gyroscope was additionally activated, only two to three complete cycles were possible. Repeating the tests with different power settings resulted in four cycles and 20% filled memory for the lowest power setting (highest noise – lowest power), four cycles and 25% filled memory for the default setting (noisy – low power) and almost four cycles (the battery died during data download) for the highest power setting (lowest noise – highest power). 1.5 additional cycles were possible when using high quality batteries from a different producer. To summarize: Three to four cycles are feasible with high quality batteries and all the three sensors activated, almost independent of the power setting.

Consequently, the battery lifetime and though the operation time of the probe depends mainly on the battery quality and on which sensors are turned on. The power settings have a minor influence. Other conditions such as temperature will also influence the battery lifetime but have not been tested specifically.

#### 3.3. Sample application: Smartstone embedded in a pebble

##### 3.3.1. Flume and camera setup

The performance of a Smartstone probe embedded in a pebble (Fig. 1c) was tested in a series of preliminary experiments, which were carried out in a 2.7 m long and 0.265 m wide flume at the Trier University, Germany. In these tests, the flume's slope was adjusted to an angle of 11° to enable large pebble velocities resulting from flow forces supported by gravity forces. The flume was formerly used to analyse pebble movement patterns in the context of soil erosion (Becker et al., 2015). In the corresponding experiments, the mouldable soil surface in natural rills was imitated by covering the flume bottom with floral foam. The same foam was used in the present experiments. The water was recirculated in the flume by an electrical effluent pump with a maximum discharge of 4.6 l s<sup>-1</sup>. In the tests, the pump was run slightly below maximum capacity resulting in a flow velocity of ≈ 1 m s<sup>-1</sup> at a water depth of ≈ 1.2 cm.

##### 3.3.2. Probe installation

In the following, we present and discuss data obtained in a specific experiment with the tracer pebble shown in Fig. 1c, which was selected from a range of differently shaped tracer stones (Becker et al., 2015). The pebble, which was specified in Section 3.1, was painted with black and white patterns, which were aligned with the pebble's main axes (Fig. 1c) to facilitate image analysis.

In order to equip the pebble with the Smartstone probe, a hole with a diameter of 8 mm was drilled into the pebble. The hole is located at the point, where the lines of the pebble's painting intersect at the end of the pebble's long axis. The 60 mm deep hole was precisely aligned with the longest axis. Next to this hole, a second hole with a 3 mm diameter was drilled for the antenna. For optimal signal transmission, the angle between both holes should be approx. 30°. Afterwards, 2–3 mm of the partition wall between the two holes was removed to route the flexible antenna. The probe was inserted completely into the bigger hole and the antenna was routed to the other hole. The bend part at the holes' ends was covered with a piece of paper to prevent it from gluing to the waterproof modelling mass, with which the holes were sealed at the end. The modelling mass was moulded to recover the original shape of the pebble.

As mentioned above, special care was taken to align the probe coordinate system with the pebble axes, i.e. the pebble a-axis with the long

axis of the cylinder (green axis in Fig. 1b), the b-axis with the red cylinder axis in Fig. 1b (which was defined to be vertical when the battery screw was located on top of the probe), and the c-axis with the blue-sensor axis (which is orthogonal to the red cylinder axis in Fig. 1b).

The alignment of the Smartstone probe and the colour code with the pebble's main axes has two main advantages: Centring avoids additional centrifugal forces, which superimpose the accelerations captured by the accelerometer (gravity and relevant changes in velocity); and the comparison of Smartstone data with image data is much more straightforward.

Including the probe, the pebble weighed 0.2867 kg. For this specific pebble, the sensor installation changed the total weight only by 0.0005 kg. For different stone densities, the aforementioned centred installation is even more important to influence the kinetic behaviour of the stone as little as possible.

In order to gain independent data with regard to pebble movement, the pebble's motion was additionally recorded using an Optronix CR4000x2 high-speed camera (see also Becker et al., 2015). The camera was placed perpendicularly to the middle of the working range of the flume at a distance of 3 m and captured hence a large portion of the working section. The camera was inclined by 11° to align the flume's longitudinal axis with the camera frame. The frame rate of the camera was 250 frames per second and the image resolution 2304 × 1720 pixels (one pixel ≈ 0.8 mm of the flume).

At the beginning of an experimental run, the pebble was manually placed at the top of the flume in the flume centreline, with its a-axis perpendicular to the flow direction. The pebble was inserted into a small recess area in the floral foam to prevent its movement without external forcing. Before data acquisition, the Smartstone memory was cleared, the database emptied and the probe was directly set to recording mode with a sampling interval of 12 ms. The data acquisition by the Smartstone was initiated by switching on the pump, which caused the movement of the pebble. The high-speed camera measurements were manually started at approximately the same time. After the pebble reached the flume's end, the Smartstone data were transmitted, labelled and stored together with the high-speed images. The lateral movement of the pebble, which was not observable from the high-speed camera's point of view, was recorded by a conventional camera (25 fps), which was located at the flume's downstream end.

### 3.3.3. Merging high-speed images and Smartstone data

In order to facilitate the accurate comparison of the Smartstone data with the results from the image analysis, a synchronization of both data sets in time was required. The absolute point in time of each sample or image was not known, i.e. the start of the sampling of both data acquisition systems could not be triggered simultaneously. However, the aforementioned experimental procedure (initiation of pebble movement by switching on the pump and starting image acquisition manually at approximately the same time) allowed for the development of a software-based synchronization of both signals by shifting the Smartstone time series in time.

For this purpose, a new set of images was generated by a MATLAB script, containing the high-speed image information and Smartstone data (Fig. 2).

An instantaneous high-speed image, cropped to the section containing the relevant information, is shown in Fig. 2d. Fig. 2e presents the data acquired by the Smartstone probe (left: magnetometer; right: accelerometer; markers indicate the actual sample points in time). The black lines indicate the point in time corresponding to the shown high-speed image. The Smartstone data were shifted in time by adding an offset. The optimal offset was determined by shifting forward and backward in small increments until the magnetometer peaks coincide with the same pebble orientation within the whole image series. This offset is unique, as the rotation velocity changes over time. Therefore, only one specific offset will result in a match for the whole series. To facilitate the identification of the orientation, two aspects are useful: The

axes orientation of the probe inside the pebble is known, as described in Section 3.3.2 and in Fig. 1b, and the direction and inclination of the earth's magnetic field relative to the flume has been determined. For the evaluation of the offset, also the accelerometer peaks (Fig. 2e, right chart) were used to check if the peaks coincide with the saltations of the pebble in the images. Note that in this specific case, the Smartstone data did not cover the experiment's beginning.

In Fig. 2a, bar charts visualize the Smartstone data tuple corresponding to the sensors reading at the point in time as indicated by the black lines in Fig. 2e. The scale was adjusted to the maximum values of each run (different measurement environments will result in different values of magnetometer due to the spatial variability of the earth's magnetic field).

The whole set of images was used to produce a video showing the complete run in slow motion (factor 40), see Video 1 in the online publication.

### 3.3.4. Deriving pebble orientation

The Smartstone probe measures data that can be used to reconstruct its orientation and movement as a function of time. As the Smartstone-kit presented in this Technical Note represents a prototype system, a methodology had to be developed to derive successive orientations from the sensor data. Therefore, a preliminary approach was developed by applying algorithms that are used for tilt-compensated compasses (e.g. Ozyagcilar, 2012). Such algorithms have been developed for devices that do not move during measurement. Applying these algorithms to the Smartstone pebble, the accelerometer readings could theoretically be used to estimate two angles of the orientation and the remaining angle using the magnetometer.

However, the Smartstone probe is moving so that the accelerometer does not only show gravity-induced accelerations but also motion related accelerations due to the forcing by water and the interaction of the pebble with the flume boundaries (walls and bed). To overcome this shortcoming, the more stable magnetometer values were used to estimate firstly the pitch (rotation around green axis in Fig. 1b,  $\tan(\text{pitch}) = B_y/B_z$ ). This value was then used to rotate the sensor axes and estimate roll (rotation around the blue axis in Fig. 1b,  $\tan(\text{roll}) = B_x/B_z$ ). If the sensor is rotated around the line of magnetic flux, the magnetometer readings will deliver constant values, as the angles do not change. Thus, the transformation from magnetometer readings to three angles – pitch, roll and yaw (rotation around red axis) – is not unique. The last value, yaw can only be derived by sensor fusion, i.e. the additional use of the accelerometer data. However, as pointed out before, these values are superimposed by accelerations caused by other parameters than gravity introducing deviations if they would not be filtered. Corresponding filters were not readily available and the obtained results for yaw were not satisfactory with this simple approach. Therefore, we decided to focus on pitch and roll, as the pebble did not change its rotation axis during the run. A rotated CAD-model of the pebble is shown in Fig. 2b showing the derived orientation of the pebble corresponding to the time indicated by the black lines in Fig. 2e. The supplementary online video shows the whole sequence.

### 3.3.5. Comparison of derived positions

Knowing the orientation of the pebble for each point in time, the corresponding accelerometer tuple can be rotated to be aligned with the flume's axes. One axis represents longitudinal acceleration (in flow direction), the next axis lateral acceleration and the third axis vertical acceleration. The pebble's velocity along each axis and its position can then be estimated based on kinematic principles. As the beginning of the run was not contained in the Smartstone data, the initial velocity for the first available data tuple was taken from image analysis. For the analysis of the high-speed images, the positions were derived by marking the left and right pebble boundary in each image, calculating the mean, and correcting the deviation resulting from the projection.

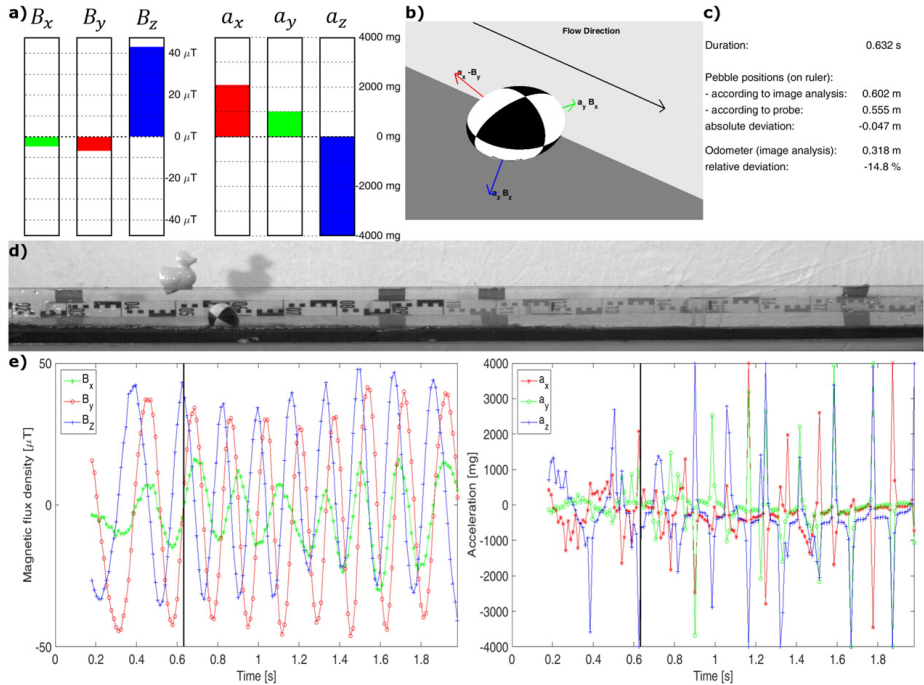


**Fig. 2.** Composition of (a) bar chart showing the sensor readings of the current point in time, (b) computer model illustrating the probe-derived pebble orientation of the current point in time, (c) summary of relevant data for the current point in time, (d) cropped high speed image of the current point in time and (e) Smartstone data charts showing the complete time series of magnetometer (left) and accelerometer (right); the black vertical lines indicate the current point in time of the complete frame.

Fig. 2c presents the derived longitudinal position of the pebble from both the Smartstone data and image analysis at the indicated point in time (i.e. black lines in Fig. 2e); the reference for the derived values is the ruler shown in Fig. 2d. We focused solely on the determination of the longitudinal movement, as the transverse and vertical movement were negligible compared to the longitudinal movement due to the narrow flume width and transport as bed load. Moreover, the corresponding values are rather uncertain due to several reasons that will be discussed later. Besides the positions as seen on the ruler, the odometer shows the total distance from the starting position to the current position. The last value in Fig. 2c shows the relative deviation of the probe-derived position, which is the percentage of absolute deviation as a fraction of the odometer.

### 3.3.6. Results and discussion

In the following, several interesting issues contained in the dataset will be highlighted and discussed. They are visible in Video 1 and their identification can be facilitated by using the repeat and pause functions of the video player.

Firstly, the magnetometer readings  $B_y$  and  $B_z$  (red and blue lines in Fig. 2e, left chart) show a sinusoidal development. For example the readings  $B_z$  (blue line) show their first minimum at 0.220 s. The second minimum is at 0.516 s; the first rotation takes 0.296 s. The third minimum is at 0.728 s; the second rotation takes 0.212 s. The fourth minimum is at 0.904 s; the third rotation takes 0.176 s. This decrease in period is caused by the acceleration of the pebble. Thus, analysing the periods in more detail allows for the determination of the rotation speed and

the number of rotations. The offset between the  $B_y$  and  $B_z$  time series is  $\pi/2$ , as these two axes are perpendicular to each other.

For the accelerometer time series (Fig. 2e, right chart), only the first rotation is visible: values change from  $a_z \approx 1000$  mg to  $a_z \approx -1000$  mg within half a rotation. Afterwards, the acceleration values are influenced by additional forces apart from gravity. Finally, when the pebble reaches its terminal velocity after approx. 1.5 s, it touches ground only twice during each rotation and saltates in between: all accelerometer values are close to zero, interrupted by peaks with alternating signs.

For the whole duration, the readings of the Smartstone can be comprehended by image analysis: peaks of magnetometer readings occur always for the same rotation angle; impacts shown in accelerometer data coincide with bounces visible in image data.

However, there are several deviations visible in the orientation visualization, e.g. after 0.532 s, 0.716 s or 0.936 s etc. in Video 1. One of the main reasons might be the unstable magnetic field in the laboratory. It was found that the resultants of the magnetometer values fluctuated between 26 and 51  $\mu\text{T}$  during the run. Additional tests with a conventional compass, which was positioned at several places in the flume, confirmed this result as the indicated direction to magnetic north deviated up to  $20^\circ$  for single positions. This may be caused by the metal frame of the flume or additional sources (such as light, electric equipment), which can influence the magnetic field.

A second aspect worth discussing is the deviation of the derived positions (Video 1). The position derived from image analysis is biased up to  $\pm 0.03$  m, as the correction of the projection is only valid as long as the pebble remains in the centre of the flume (which it did not). Nevertheless, these deviations and the respective correction are limited as



mentioned above to approx. 0.03 m at the left and right end of the image. This indicates that the observed deviation is mainly due to the Smartstone data. There are mainly five different reasons for these deviations, ordered by magnitude:

1. The quantisation error is an intrinsic reason: the precision of the values is limited. For the chosen range of 4 g, the resolution is 2 mg. Assuming that the true values are rounded during quantization, the upper boundary for the difference between the true value and the displayed value is 1 mg. For the duration of our experiment ( $\approx 2$  s), the maximum deviation resulting from quantisation error is  $0.0196$  m ( $s = 0.5 a t^2$ , where  $s$  denotes the distance,  $a$  the acceleration in  $m s^{-2}$  and  $t$  the time). If the range of the accelerometer is increased to the maximum of  $\pm 16$  g, the maximum error after 2 s increases to  $0.0785$  m. The fraction of deviation resulting from this source will differ with the duration of the experiment and the magnitude of acceleration.
2. Noise: The noise depends on the setting: For the lowest power consumption and 12 ms sampling intervals, the noise is 10 mg. For highest power consumption and intervals greater than 24 ms, the noise drops to 1.2 mg. The given values are root mean square errors. Without further assumptions concerning their distribution, the resulting deviation cannot be estimated, but will later be evaluated empirically.
3. Integration error: the estimation of the position from kinematic principles is based on double integration, thus errors are integrated twice. It is a numerical integration of values with finite time steps and data that is sampled with a finite sampling rate. This error is intrinsic to the method and consequently, the derived position will always increasingly differ over distance and time (the derived position of a pebble not moving will tend to move).
4. Orientation error: the derived orientation was used to align the accelerometer readings to the flume. These orientations are imprecise, and thus, the derived velocity and position are defective, too. If the orientation is off by only  $1^\circ$ , the gravity residuals for the axis perpendicular to the gravity vector will be  $17.45$  mg ( $\sin(1^\circ) 1000$  mg). This results in a deviation of  $0.3424$  m after 2 s.
5. Clipping error: this important reason becomes apparent from Fig. 2e (and/or the online video): Several values of the accelerometer were outside the measurement range of  $\pm 4000$  mg. There is even more evidence for this conclusion: The pebble bounces several times in an angle stressing two axes  $a_y$  and  $a_z$  (e.g. at 1.164 s) and sometimes even all three axes (e.g. at 1.872 s). In the latter case, all axes show the maximum value (resultant 6.928 g). If an impact of the same magnitude occurs in a different orientation of the pebble stressing only one axis (force aligned with one axis), this impact would have been clipped. The effect is also visible in the video: The deviation increases monotonically until the first big impact occurs after 0.624 s. Then the deviation remains almost stable until the next big impact after 1.164 s. After this point in time, the deviation starts to increase faster. The influence of this clipping is very strong: If the pebble is accelerated with 4000 mg for 12 ms, the resulting velocity is  $0.47$  m  $s^{-1}$ . If the true acceleration was 6928 mg, the resulting velocity is  $0.8146$  m  $s^{-1}$ . The deviation in the position

estimation due to this difference between true velocity and estimated velocity will increase with time: it will increase by  $0.3446$  m every second for only one clipped peak.

To support this theoretical argumentation, additional experiments were conducted to disentangle the different reasons for deviations. Their results are shown in Table 1.

The second column shows the results of the first experiment in which the sensor was mounted to a cart thereby being precisely aligned with the cart trajectory to stress only one axis. The cart was then moved 5 times for 1.5 m, which corresponds to the same travel distance as in the laboratory flume. The duration of each move was approx. 2 s. Afterwards, the distance was derived from the sensor data resulting in a mean absolute deviation of 3.32% and a standard deviation of 4.03%. These deviations are due to quantisation error, noise, integration error and the true deviation of the travelled distance to 1.5 m.

The third column of Table 1 shows the results of the second experiment. In this test, the sensor setting was changed to lowest power consumption and 12 ms sampling intervals, which resulted in increased noise. The deviations were smaller compared to the 24 ms intervals, which does not perfectly agree with theory.

In a further experiment, the sensor was mounted in a cylinder rolling down a ramp outside of a building, avoiding acceleration peaks above 4000 mg. The distance was again 1.5 m, the inclination was the same as in the laboratory flume, the movement's duration was approx. 2 s. In this type of experiment, the orientation error is added, but the error is smaller compared to the laboratory flume where the earth's magnetic field is disturbed by the flume's metal frame. Analysing the measurements, the mean absolute deviation increased to 13.74%.

Following the rolling-test, the same cylinder was moved without water in the laboratory flume, introducing the deviations resulting from the disturbed magnetic field. Consequently, the mean absolute deviation increased to 21.65%.

Finally, several runs of the actual laboratory flume experiment were evaluated (first run is the run shown in the video), which includes strong clipping. Considering these experiments, the mean absolute deviation increased to 63.18%. In the runs showing the largest deviation, the pebble hit the flume's sidewalls, which resulted in maximum accelerometer readings.

We conclude that the orientation and clipping errors are the main reasons for the observed deviations. However, both of them can be reduced in future applications as the presented preliminary analysis is based on a simple approach to derive the orientation in order to test the general applicability of the Smartstone. In fact, there exist many more sophisticated methods such as Kalman filtering or hidden Markov models, which are well established in other disciplines like computer science, robotics or (pedestrian) navigation. Both methods can be used to calculate probabilities of certain orientations taking into account respective uncertainties and the temporal development of the movement. As we also generate three-dimensional models of the experimental environment (Brings et al., 2015), it might even be possible to apply a probabilistic map based localization like Markov localization (e.g. DeSouza and Kak, 2002; Fox et al., 1998).

**Table 1**

Summary of five runs of five different experimental settings, which incorporate increasing numbers of deviation reasons from left to right.

	One axis, 24 ms sampling (low noise)	One axis, 12 ms sampling (high noise)	Smooth rolling, undistorted magnetic field	Smooth rolling, laboratory flume	Pebble with acceleration peaks in laboratory flume
1st run	-3.0%	-5.3%	7.9%	-28.1%	32.4%
2nd run	-4.3%	-4.0%	-1.9%	-15.1%	30.7%
3rd run	1.9%	-0.9%	32.3%	10.8%	-58.5%
4th run	5.3%	4.5%	-1.8%	35.0%	131.3%
5th run	-2.6%	-1.0%	-21.8%	24.8%	-75.2%
Mean absolute deviation	3.3%	2.6%	13.7%	21.7%	63.2%
Standard deviation	4.0%	3.8%	19.7%	26.6%	83.0%

The clipping issue with regard to the accelerometer might be easier to tackle as it has an adjustable range up to  $\pm 16$  g (Bosch Sensortec, 2014) and the extended range will therefore be implemented in the probe's next generation. However, changing the measuring range, the discretization gets coarser (8 mg) and thus, the quantisation and integration errors may become more significant. The user has to consider the suitable range according to the expected magnitude of impacts, which will vary strongly for different applications, e.g. a soft mouldable wet soil surface, as imitated by the floral foam in the here described experiments, or stony surfaces without any dampening characteristics.

#### 4. Summary and outlook

The described Smartstone probe fits into stones with a longest axis exceeding 60 mm and allows for tracking of their movement in water using wireless signal transfer, identification by an active RFID tag and a 9-axis sensor module. The qualitative results from a first application with a pebble rolling down a flume clearly show a rotation of the pebble indicated by both the accelerometer and the magnetometer values. A sampling interval of 12 ms was sufficient to track the movements avoiding sub-Nyquist sampling. The gyroscope data were omitted because the gyroscope is linked to a maximum sampling frequency of 10 Hz. Increased measuring frequency reduces the possible measuring time due to limited memory and increases the duration of data transmission. The pictures of the high-speed camera are suitable as reference of the real movement. In addition, they support the understanding of Smartstone data and their interpretation in a sense of three-dimensional movement. Even with simple approaches, it is possible to estimate a rough orientation and derive probe positions. These quantitative results can still be optimized by more sophisticated post-processing of the acquired data.

For the next probe generation, an additional mode will be introduced, which adjusts the accelerometer's range to  $\pm 16$  g.

In the geomorphological context, the probe will be applied in rill erosion experiments like described in Wirtz et al. (2012). The sample application showed the principal applicability of the probe for these experiments, where a high-speed camera cannot be used for several reasons like turbid water etc. Here, one long-term objective is to derive complete movement patterns like published in Becker et al. (2015) directly from Smartstone data.

Furthermore, the Smartstone probe will be used in physical model testing of riprap in hydraulic engineering. Experiments will include small-scale laboratory model testing as well as large-scale tests in the field (Hiller and Lia, 2015).

The applicability of the probe in different conditions – e.g. increased water depth or the probe being buried in sediment – is still to be tested as these obstacles will dampen the signals used for data transfer. However, the magnitude of this effect is difficult to predict.

Besides these applications, it has to be checked if the accuracy of the Bosch 9-axis sensor is preserved in the composite of the Smartstone probe.

Supplementary data to this article can be found online at <http://dx.doi.org/10.1016/j.catena.2016.03.030>.

#### Acknowledgements

We thank SST (smart sensor technologies) Rheinberg (contact: [info@smart-sensor-technologies.de](mailto:info@smart-sensor-technologies.de)) for the collaboration with the development of the Smartstone measuring equipment. We also thank Bosch Sensortec for letting us use their pictograms in the Graphical Abstract. Furthermore, we appreciate the help of the students Jens Jakobsen and Johannes Kobel for the evaluation of battery lifetime and

range. The financial support from Energy Norway and the Research Council of Norway within the project 235730 is acknowledged.

#### References

- Becker, K., Gronz, O., Wirtz, S., Seeger, M., Brings, C., Iserloh, T., Casper, M.C., Ries, J.B., 2015. Characterization of complex pebble movement patterns in channel flow – a laboratory study. *Cuadernos de Investigación Geográfica* 41 (1).
- Bedeus, K., Ivicsics, L., 1963. Observation of the noise of bed load. In: *Land Erosion Precipitations, Hydrometry, Soil, Moisture* (Proc. Berkeley Assembly, August 1963). Publ. Int. Assoc. Sci. Hydrol. 384–390.
- Brings, C., Gronz, O., Becker, K., Wirtz, S., Seeger, M., Ries, J.B., 2015. 3D surface reconstruction and volume calculation of rills. *Geophysical Research Abstracts*. Presented at the EGU General Assembly, European Geosciences Union.
- Cameron, C., 2012. A wireless sensor node for monitoring the effects of fluid flow on riverbed sediment. *Univ. Glasg. Sch. Comput. Sci. Level 4 Project*, p. 70.
- De Jong, C., 1991. A re-appraisal of the significance of obstacle clasts in cluster bedform dispersal. *Earth Surf. Process. Landf.* 16 (8), 737–744.
- DeSouza, G.N., Kak, A.C., 2002. Vision for mobile robot navigation: a survey. *IEEE Trans. Pattern Anal. Mach. Intell.* 24, 237–267.
- Ergenzinger, P., De Jong, C., 2003. Perspectives on bed load measurement. *IAHS Publ.* 113–125.
- Ergenzinger, P., Schmidt, K.-H., Busskamp, R., 1989. The pebble transmitter system (PETS): a technique for studying coarse material erosion, transport and deposition. *Z. Für Geomorphol.* 33, 503–508.
- Ergenzinger, P., de Jong, C., Laronne, J., Reid, I., 1994. Short term temporal variations in bed load transport rates: Squaw Creek, Montana, USA and Nahal Yatir and Nahal Eshetmoa, Israel. In: *Dynamics and Geomorphology of Mountain Rivers* (ed. by P. Ergenzinger & K.-H. Schmidt). Springer, Berlin, pp. 251–264.
- Foster, D.I., 2000. *Tracers in Geomorphology*. John Wiley & Sons, Chichester, UK.
- Fox, D., Burgard, W., Thrun, S., 1998. Active Markov localization for mobile robots. *Robot. Auton. Syst.* 25, 195–207. doi:[http://dx.doi.org/http://dx.doi.org/10.1016/S0921-8890\(98\)0049-9](http://dx.doi.org/http://dx.doi.org/10.1016/S0921-8890(98)0049-9)
- Gray, J.R., Gartner, J.W., Barton, J.S., Gaskin, J., Pittman, S.A., Rennie, C.D., 2010. Surrogate technologies for monitoring bed-load transport in rivers. *Sedimentol. Aqueous Syst.* 46–79.
- Habersack, H., 1997. *Raum-Zeitliche Variabilitäten im Geschiebehaushalt am Beispiel der Draa*. Universität für Bodenkultur, Wien.
- Hiller, P.H., Lia, L., 2015. Practical challenges and experience from large-scale overtopping tests with placed riprap. In: *Toledo, M.A., Morán, R., Oñate, E.* (Eds.), *Dam Protections against Overtopping and Accidental Leakage*. CRC Press/Balkema, London, pp. 151–157.
- Johnson, P., Muir, T.C., 1969. Acoustic detection of sediment movement. *J. Hydraul. Res.* 7, 519–540.
- Krause, L., 1997. *Neue Wege zur Entwicklung von zeitlich hochaufgelösten Meßtechniken des Grobgeschiebetransportes*. Institut f. Geographische Wissenschaften, Freie Universität Berlin, Berlin (Diploma Thesis).
- Krein, A., Klinck, H., Eiden, M., Synamder, W., Bieri, R., Hoffmann, L., Pfister, L., 2008. Investigating the transport dynamics and the properties of bedload material with a hydro-acoustic measuring system. *Earth Surf. Process. Landf.* 33, 152–163. <http://dx.doi.org/10.1002/esp.1576>.
- Lamarre, H., Roy, A.G., 2008. The role of morphology on the displacement of particles in a step-pool river system. *Geomorphology* 99, 270–279. <http://dx.doi.org/10.1016/j.geomorph.2007.11.005>.
- Liébault, F., Bellot, H., Chapuis, M., Klotz, S., Deschâtres, M., 2012. Bedload tracing in a high-sediment-load mountain stream. *Earth Surf. Process. Landforms* 37, 385–399. <http://dx.doi.org/10.1002/esp.2245>.
- Oikawa, Y., 2011. Tag movement direction estimation methods in an RFID gate system. In: C. Turcu (Ed.), *Current Trends and Challenges in RFID*, pp. 441–455.
- Ozyagcilar, T., 2012. *Implementing a Tilt-Compensated eCompass Using Accelerometer and Magnetometer Sensors* (Application Note No. AN4248). Freescale Semiconductor.
- Reid, I., Layman, J., Frostick, L.E., 1980. The continuous measurement of bed load discharge. *J. Hydraul. Res.* 18, 243–249.
- Ryan, S.E., Bunte, K., Potyondy, J.P., 2005. Breakout session II, Bedload-transport measurement: data needs, uncertainty, and new technologies. *Proceedings of the Federal Interagency Sediment Monitoring Instrument and Analysis Workshop*. Circular.
- Schaffernak, F., 1916. *Die Theorie des Geschiebetriebes und ihre Anwendung*. Z. Oesterreichischen Ing.-Archit.-Ver. 11.
- Schneider, J.M., Hegglin, R., Meier, S., Turowski, J.M., Nitsche, M., Rickenmann, D., 2010. Studying Sediment Transport in Mountain Rivers by Mobile and Stationary RFID Antennas. In: *Dittrich, A., Koll, K., Aberle, J., Geisenhainer, P.* (Eds.), *Proceedings of the International Conference on Fluvial Hydraulics: River Flow 2010*. Bundesanstalt für Wasserbau, Braunschweig, pp. 1723–1730.
- Sensortec, Bosch, 2014. *BMX055 Small, Versatile 9-Axis Sensor Module*, Data Sheet.
- Wirtz, S., Seeger, M., Ries, J.B., 2012. Field experiments for understanding and quantification of rill erosion processes. *Catena* 91, 21–34.



## Paper IV

---

**Placed riprap as erosion protection on the downstream slope of  
rockfill dams exposed to overtopping**

Priska H. Hiller, Leif Lia

25th Congress on Large Dams: Question 97, Response 20  
Stavanger, Norway, 2015

---



COMMISSION INTERNATIONALE  
DES GRANDS BARRAGES

-----  
VINGT-CINQUIÈME CONGRÈS  
DES GRANDS BARRAGES  
*Stavanger, Juin 2015*  
-----

**PLACED RIPRAP AS EROSION PROTECTION ON THE DOWNSTREAM  
SLOPE OF ROCKFILL DAMS EXPOSED TO OVERTOPPING (\*)**

Priska Helene HILLER

*PhD student, Norwegian University of Science and Technology, NTNU*

Leif LIA

*Professor, Norwegian University of Science and Technology, NTNU*

NORWAY

1. INTRODUCTION

Riprap is widely used as erosion protection to increase slope stability. In relation to rockfill dams, riprap can be used as protection on the upstream slope against action from altering water level, waves and ice. In some countries riprap is even used for the spillway over the downstream slope of low dams with gentle slopes. In Norway, the downstream slopes of high rockfill dams are armed with a layer of riprap stones placed in an interlocking pattern hereby referred to as "placed riprap". The reason for using placed riprap on the downstream slopes is to protect the dams against accidental loads such as: considerable leakage through the dam; overtopping of the dam because of a clogged spillway or a land slide generated wave; partial damage of the dam crest for any reason. Without protection of the downstream slope would these accidental loads lead to the immediate initiation of erosion.

Most of the Norwegian rockfill dams were built before 1990 (Kjærnsli *et al.*, 1992). The great era of rockfill dams in Norway was in the sixties and seventies, triggered by the availability of heavy equipment for efficient construction work at remote sites. Hence, many of the dams are currently being reassessed or will be

---

(\*) *Enrochements pour la protection contre l'érosion sur le versant aval des barrages exposés au déversement*

so in the near future. Several dams have to be upgraded for one or several reasons such as:

- Increased design flood
- Reclassification into a higher consequence class
- Weathering processes
- Larger settlements than expected
- Discrepancies according to the dam safety regulation (OED, 2009) which became valid in 2010 after a review process and which has fully retroactive effect. Details about the Norwegian dam safety regulation are described by Midttømme *et al.* (2010).

The upgrading of a rockfill dam often includes costly reconstruction of the placed riprap on the downstream slope. The upgrading of the 129 m high dam Svartevatn is an example described in Hiller *et al.* (2014) and shown in Fig. 1.

There is scarce data about placed riprap on steep slopes, i. e. slopes steeper than 1: 2 (vertical: horizontal) corresponding to  $S = 0.5$ ; Norwegian rockfill dams usually have a downstream slope of 1: 1.5 equal to  $S = 0.67$ . The recommendation for the design of placed riprap is based on data from riprap without any special pattern; i. e. randomly placed or dumped riprap. Hence, the actual factor of safety is not yet quantified. The objectives of this article are to summarize available data about placed riprap on steep slopes and to present preliminary results from a current research project on placed riprap discharge capacity. The presented data refers to the uppermost layer of a downstream dam slope and will not replace any geotechnical stability analyses of the whole slope, which have to be carried out in addition.



Fig. 1  
 Reconstruction of the riprap on the downstream slope of Svartevatn dam in south-western Norway.  
*Reconstruction de l'enrochement sur la pente aval du barrage de Svartevatn dans le sud-ouest de la Norvège*

## 2. METHODOLOGY FOR DATA COMPARISON AND RIPRAP TESTS

Literature about placed riprap in connection with embankment dams is scarce and consists mainly of results from physical model tests. The results are mainly published in German and Norwegian, hence a summary is presented in English. Generally accepted principles to evaluate and model the flow through and over a riprap on steep slopes are not yet formulated. Due to high turbulence and a free water surface Froude's model law can be used. To compare the different studies a stone related Froude number  $Fr_s$  in equation (1) is used, with the unit discharge  $q$ , the gravity acceleration  $g = 9.81 \text{ m/s}^2$  and the stone diameter  $d_s$ .

$$Fr_s = \frac{q}{\sqrt{g \cdot d_s^3}} \quad (1)$$

A current research project in Norway is investigating the quality and stability of placed riprap on the downstream slopes of rockfill dams. Both through flow and overtopping are included in the study. Physical model tests were conducted in the



hydraulic laboratory at the Norwegian University of Science and Technology and in the laboratory at the Technical University of Madrid, and are described in Lia *et al.* (2013). Placed riprap was tested on the downstream slope of homogeneous gravel test dams with an inclination of  $S = 0.67$  and with a fixed dam toe. The influence of the orientation of the riprap stones was investigated. The orientation is described by the angle between the longest stone axis which points towards the dam and the dam surface. Tests were run with horizontally oriented stones corresponding to an orientation angle of 34 degrees on a slope with  $S = 0.67$  and perpendicularly oriented stones. Tests with randomly placed riprap served as reference. In 2012 and 2013 some preliminary large scale field tests were run with approximately 3.5 m high test dams. The test set-up and results are described by Lia *et al.* (2013) and Hiller *et al.* (2014). Røer (2014) investigated during his Master thesis the influence of different flow patterns on placed riprap. He conducted physical model tests in a 0.15 m wide flume using stones with  $d_s = 25$  mm. The tests were run with either overtopping, through flow or a combination of both.

### 3. EXISTING RECOMMENDATIONS FOR RIPRAP EXPOSED TO OVERTOPPING

Studies with focus on steep slopes and placed riprap are summarized below. The data points are plotted in Fig. 2 for comparison. Abt *et al.* (2013) collected and compared several overtopping design relationships for riprap. Altogether 96 data points from 21 different studies are presented. The data covers a range of slopes from  $S = 0.2$  to 0.5 and stone diameters from 15 to 655 mm. A limited number of data is from steep slopes. Khan and Ahmad (2011) present a similar study, which includes a multiple regression analysis resulting in an empirical formula including layer thickness, slope, coefficient of uniformity and unit discharge to determine the stable stone diameter. Thornton *et al.* (2014) present a similar regression analysis based on the data summarized by Abt *et al.* (2013), and include the stone specific gravity as an additional parameter.

Few studies are available on placed riprap. Peirson *et al.* (2008) compare the results of model tests with riprap which was either placed or dumped. They conclude with a stability gain of approximately 30% in unit discharge for placed riprap compared to randomly dumped material. However, they mention an increased consumption of stones, approximately 35% increased mass per unit area, and higher construction costs as disadvantages.

Results from physical model tests as well as theoretical analyses have been produced in Germany since the 1990s in relation to the development of decentralised flood protection measures. A possible measure is to retard the flood discharge in retention basins by building small embankment dams, usually lower than 10 m in height. Also these dams need spillways due to dam safety

considerations. To reduce costs and to fit well into the landscape riprap or placed riprap is a favourable solution. Specific research resulted in a design guideline for dams or parts of dams which can be overtopped. The guideline is limited to dams < 10 m height, slopes flatter than  $S = 0.25$ , and a maximum unit discharge of 1 m<sup>3</sup>/s/m. The PhD theses of Rathgeb (2001), Dornack (2001) and Siebel (2013) contributed considerably to the development of the guideline and the research about dams or parts of dams exposed to overtopping. These studies apply a stone related Froude number to describe the stability of the riprap. Rathgeb and Siebel include in addition a density term. They distinguish between self-supporting and not self-supporting riprap and describe three different failure scenarios: erosion of single stones, sliding of the protection layer and disruption of the protecting layer. For randomly dumped riprap only the two first failure scenarios are decisive (Siebel, 2013).

Dornack (2001) presents the most interesting results in matters of Norwegian rockfill dams. He investigated placed riprap on slopes with an inclination of  $S = 0.3, 0.5$  and  $0.67$ . The stone size was 30, 40 and 50 mm. His results show a stability gain due to placing the riprap stones which is considerably larger compared to the one described by Peirson *et al.* (2008). The stability of loose riprap decreases by increasing the slope. For placed riprap however increased stability is observed, caused by the longitudinal force which occurs inside the placed riprap layers on steep slopes. This force increases the forces on the stone sides and further the friction which is stabilizing against the hydraulic forces. Dornack developed from theoretical analysis and physical model tests a design equation (2), shown as line in Fig. 2, which gives a critical stone related Froude number  $Fr_{s,cr}$  with the slope  $\tan \alpha = S$ , the density of the stone  $\rho_s$  and water  $\rho_w$ :

$$Fr_{s,cr} = (0.649 \cdot \tan \alpha^{-0.6} + 1.082 \cdot \tan \alpha^{0.4})^{5/4} \cdot \sqrt{\left(\frac{\rho_s}{\rho_w} - 1\right) \cdot \cos \alpha} \quad (2)$$

The term  $1.082 \cdot \tan \alpha^{0.4}$  incorporates the stabilising friction forces between the stones due to the steep slope. The range of application is for slopes between  $S = 0.1$  and  $0.67$ . The equation is applicable for overtopping of dams and dam parts with a constant width. Dornack points out that it has to be kept in mind that spillways with placed riprap do not have a hydraulic overload capacity. In the case of failure of the riprap, there is the danger of dam break and the riprap will fail usually without any evidence. The quality of the riprap is highly dependent on the quality of construction. For a secure design a reasonable safety factor should be included. He recommends a factor of 1.6 for the stone size which is approximately the same as a factor of 2.0 for the discharge when the stone related Froude number in equation (1) is used.

All dams in Norway are classified into five consequence classes according to the dam safety regulation (OED, 2009). Class 4 is the most severe class. The regulation requires a placed riprap on the downstream slopes of rockfill dams for

all classes. The stones have to be placed in an interlocking pattern with their longest axis pointing into the dam. It is further recommended to use stones with a volume of minimum 0.15 m<sup>3</sup> for dams in consequence class 4. To determine the stone size for dams in class 3 and 2, equation (3) can be used assuming a minimum unit discharge  $q$  of at least 0.5 or 0.3 m<sup>3</sup>/s/m respectively (NVE, 2012).

$$D_{min} = 1.0 \cdot S^{0.43} \cdot q^{0.78} \quad (3)$$

The factor 1.0 includes a safety factor of 2.3 compared to the fitting curve based on laboratory and field tests with dumped riprap described by EBL Kompetanse AS (2005). A stone diameter of 0.63 m, which approximately corresponds to a stone volume of 0.15 m<sup>3</sup>, is assumed to calculate the lines in Fig. 2.

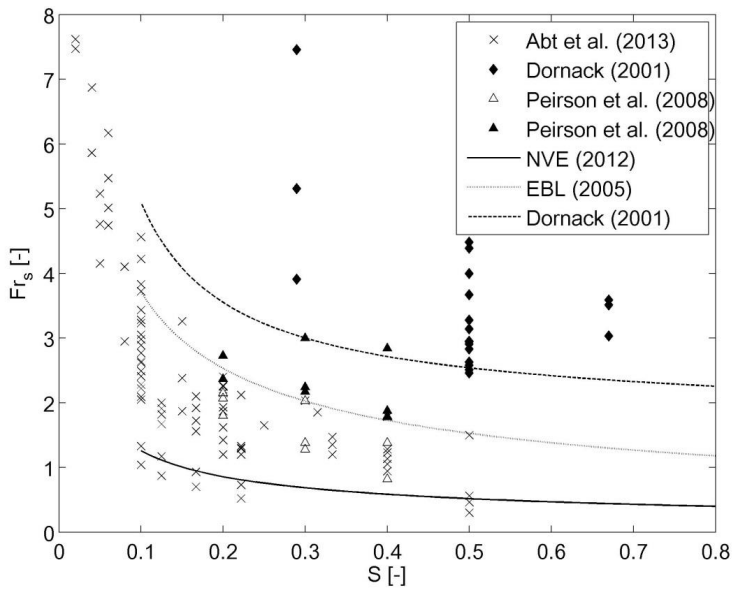


Fig. 2

Comparison of the data from the different studies. Filled markers are used to indicate placed riprap. For the lines NVE (2012) and EBL (2005) a stone diameter of 0.63 m is assumed.

*Comparaison des données des différentes études. Les carrés pleins sont utilisés pour indiquer les enrochements placés. Les courbes NVE (2012) et EBL (2005) sont associées à des rochers de diamètre 0,63 m.*

4. RECENT RESULTS FROM MODEL AND FIELD TESTS IN NORWAY

The requirements and recommendations from the Norwegian dam safety authorities are based on test results with dumped riprap. Hence, the aim of this research project is to develop results with placed riprap with a test set-up designed on the base of usual Norwegian rockfill dams, i. e. slopes of  $S = 0.67$ . Preliminary and qualitative results are shown in Fig. 3 and Fig. 4.

The stone related Froude numbers for dumped riprap are close to 1.0 and thus correspond well with the values presented in Fig. 2. An increased angle between the dam slope and the longest axis of the riprap stones increases the stability of the placed riprap as the results from Lia *et al.* (2013) show. The qualitative results from Røer (2014) show how flow through the dam reduces the stability of placed riprap. Both datasets are in a comparable magnitude as the ones from Dornack (2001).

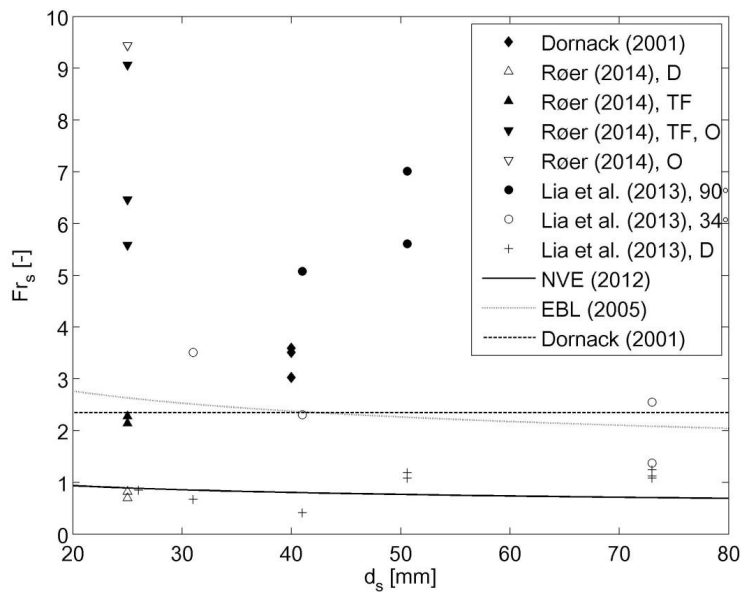


Fig. 3

Comparison of data for  $S = 1/1.5 = 0.67$ . “D” for dumped riprap, “TF” for through flow, “O” for overtopping.

*Comparaison des données pour  $S = 1/1.5 = 0.67$ . “D” pour les enrochements jetés, “TF” pour le débit, “O” pour déversement.*

The results from the large scale field tests in 2012 and 2013 are plotted separately in Fig. 4, because the uncertainties and conditions in the field do not allow a clear defined stone related Froude number. As the riprap stones are in a certain range,  $F_{r_s}$  is calculated for the minimum and maximum stone diameter. For test 3 in 2012 the unit failure discharge was between 6.3 and 8.3 m<sup>3</sup>/s/m, the plot in Fig. 4 takes this range into account. Test dam 4 in 2012 did not fail under a unit discharge of approximately 10 m<sup>3</sup>/s/m. Hence, the plot indicates this with an open upper border. Test dam 2 in 2013 failed due to instabilities in the dam foot resulting in sliding of the placed riprap. Hence, test 2 in 2013 should not be directly compared with the other results. It shows that a proper foundation of the riprap is essential for the global stability of a placed riprap.

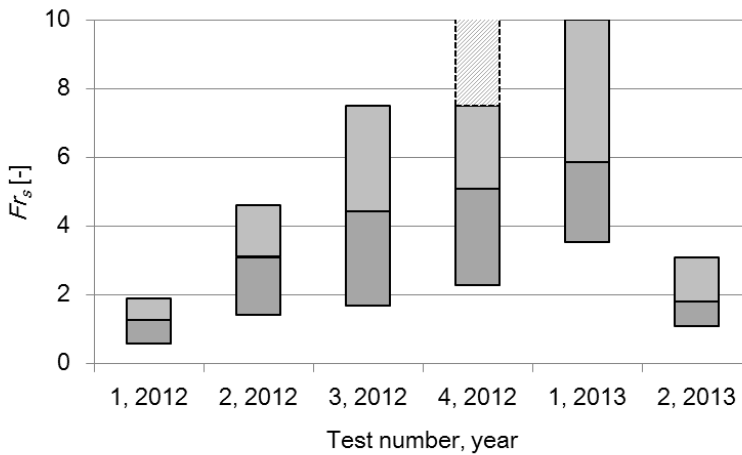


Fig. 4  
 Stone related Froude number for the field experiments.  
*Nombre de Froude lié au rocher pour les expériences de terrain*

## 5. DISCUSSION

The stone related Froude number  $F_{r_s}$  is adequate to compare results from different studies as it is dimensionless and considers the unit discharge as well as the stone size. However, it must be kept in mind that this relationship depends on the unit discharge. Hence, it depends on the failure criteria for the riprap. In some studies, the first movement of a single stone is considered as failure, in other studies it is the discharge at the collapse of the whole structure. In addition, the ratio of discharge flowing through and over the riprap may vary between different studies. A density term can be added to the Froude number, to consider

different densities of the stones. The most crucial challenge when comparing data from placed riprap is that there is no consistent way of describing the placement pattern. The quality of the pattern highly affects the stability of the protection layer and is a key parameter.

The stone related Froude numbers for placed riprap are principally higher than the numbers for dumped riprap. However, the results from Dornack (2001) and the preliminary results from Norway show higher stability gain than the results from Peirson *et al.* (2008). Using Dornack's equation (2) with a slope of  $S = 0.67$  gives  $Fr_s = 2.3$ . The results from the field tests, except test 1 in 2012 and test 2 in 2013, give larger  $Fr_s$  calculated with  $d_s$  than 2.3. To use the  $Fr_s$  corresponding to  $d_s$  is appropriate, as the lowest border in Fig. 4 is related to the maximum stone diameter used for the riprap and if the riprap is properly placed the large stones will not fail first.

For comparison, an example for the stone size for placed riprap on a rockfill dam in class 4 is calculated: The recommended stone size in the guideline for rockfill dams (NVE, 2012) is  $0.15 \text{ m}^3$  corresponding to a  $d_s = 0.63 \text{ m}$ . According to equation (3) it should withstand a unit discharge of  $q = 0.7 \text{ m}^3/\text{s}/\text{m}$ . Using Dornack's recommendation  $Fr_s = 2.3$  results in a stone size of  $d_s = 0.21 \text{ m}$  for  $q = 0.7 \text{ m}^3/\text{s}/\text{m}$ . Adding a safety factor of 1.6 gives the stone size for the design of  $0.34 \text{ m}$  which is only half of the size recommended by the Norwegian authorities. Consequently, this indicates a large safety factor or even oversized riprap stones. Hence, more test results are needed for slopes with  $S = 0.67$  and placed riprap to check if it is possible to optimize the current recommendation and potentially reduce the stone size. Regarding the results presented above placed riprap with  $d_s = 0.63 \text{ m}$  on a rockfill dam would probably withstand overtopping with a unit discharge of  $q = 2$  to  $3.5 \text{ m}^3/\text{s}/\text{m}$ . Scaling the field test to  $d_s = 0.63 \text{ m}$  shows that a properly constructed placed riprap might endure up to  $10 \text{ m}^3/\text{s}/\text{m}$  in an emergency situation. Anyway, potential overtopping has to be related to the dam height and the consequence of a dam break. Thus, it is included in an integrated risk consideration.

## 6. CONCLUSIONS

Recommendations for the design of placed riprap are rare, especially for steep slopes. Data for dumped riprap and flat slopes can be used as a conservative border line when dealing with placed riprap. The interaction of stones within a placed riprap results in significantly increased stability against hydraulic forces. In field tests with full scale riprap stones, the riprap withstood a unit discharge of up to  $8 \text{ m}^3/\text{s}/\text{m}$  which is over 10 times more than the recommendation of the dam safety authority. Interesting results were found in German literature which is limited to small dams. However, based on preliminary results from a current research project, it seems more reasonable to use a

formula based on data with placed riprap for design. For this matter, more tests are needed to check if Dornack's suggestions are also suitable for high rockfill dams and in regard to leakages. Furthermore, a consistent way to describe the pattern of placed riprap would make it easier to compare results from different studies and should lead to a user friendly recommendation for riprap construction on site.

#### ACKNOWLEDGEMENTS

The financial support from Energy Norway and the Norwegian research council is gratefully acknowledged. The field tests would not have been possible without the kind collaboration with Sira-Kvina Power Company in providing access and water supply from dam Svartevatn.

#### REFERENCES

- [1] ABT, S. R., THORNTON, C. I., SCHOLL, B. A. & BENDER, T. R. 2013. Evaluation of overtopping riprap design relationships. *Journal of the American Water Resources Association*, 49, 923-937.
- [2] DORNACK, S. 2001. *Überströmbare Dämme - Beitrag zur Bemessung von Deckwerken aus Bruchsteinen*. PhD thesis, Technische Universität Dresden, (in German).
- [3] EBL KOMPETANSE AS 2005. *Stability and breaching of embankment dams, Report on Sub-project 2, Stability of downstream shell and dam toe during large through-flow*, Oslo, EBL kompetanse AS.
- [4] HILLER, P. H., LIA, L., JOHANSEN, P. M. & GUDDAL, R. 2014. Dam Svartevatn - An example of challenging upgrading of a large rockfill dam. *ICOLD Annual Meeting and Symposium*. Bali.
- [5] KHAN, D. & AHMAD, Z. 2011. Stabilization of Angular-Shaped Riprap under Overtopping Flows. *International Journal of*, 5, 774-779.
- [6] KJÆRNSLI, B., VALSTAD, T. & HØEG, K. 1992. *Rockfill dams: design and construction*, Trondheim, Norwegian Institute of Technology. Department of Hydraulic Engineering.
- [7] LIA, L., VARTDAL, E. A., SKOGLUND, M. & CAMPOS, H. E. 2013. Rip rap protection of downstream slopes of rock fill dams - a measure to increase safety in an unpredictable future climate. *9th ICOLD European Club Symposium*. Venice: ITCOLD.
- [8] MIDTTØMMER, G. H., GRØTTÅ, L. & HYLLESTAD, E. 2010. New Norwegian Dam Safety Regulations. *In: AUSTRIAN NATIONAL COMMITTEE ON LARGE DAMS, A. (ed.) 8th ICOLD European Club Symposium*. Innsbruck: TU Graz.

- [9] NVE 2012. Veileder for fyllingsdammer. In: ENERGIDIREKTORAT, N. V.-O. (ed.) 4/2012. Oslo: NVE (in Norwegian).
- [10] OED 2009. Regulation on dam safety (Forskrift om sikkerhet ved vassdragsanlegg), FOR-2009-12-18-1600, Ministry of Petroleum and Energy (OED), available at [www.lovdatab.no](http://www.lovdatab.no) [accessed 24. Jan. 2011], (in Norwegian).
- [11] PEIRSON, W. L., FIGLUS, J., PELLER, S. E. & COX, R. J. 2008. Placed rock as protection against erosion by flow down steep slopes. *Journal of Hydraulic Engineering*, 134, 1370-1375.
- [12] RATHGEB, A. 2001. *Hydrodynamische Bemessungsgrundlagen für Lockerdeckerke an überströmbaren Erddämmen*. PhD Thesis, Universität Stuttgart, (in German).
- [13] RØER, H. E. 2014. Nedstrøms skråning av steinfyllingsdammer - modellforsøk av plastring under ulike strømningsforhold. Master thesis, Norwegian University of Science and Technology, NTNU Trondheim, (in Norwegian).
- [14] SIEBEL, R. 2013. *Experimentelle Untersuchungen zur hydrodynamischen Belastung und Standsicherheit von Deckwerken an überströmten Erddämmen*. PhD Thesis, Universität Stuttgart, (in German).
- [15] THORNTON, C., ABT, S., SCHOLL, B. & BENDER, T. 2014. Enhanced Stone Sizing for Overtopping Flow. *Journal of Hydraulic Engineering*, 140, 06014005.

#### SUMMARY

Data from literature as well as from preliminary model and field tests show a considerable stability gain when using placed instead of dumped riprap. Results from different studies are compared with the help of a stone related Froude number. Preliminary results show that the stability depends on the orientation of the riprap stones and that the hydraulic load due to through flow is more unfavourable than due to overtopping. There is a need for more data about placed riprap on steep slopes to quantify the real safety factor of placed riprap constructed according to Norwegian dam safety regulation. Literature as well as test results indicate that placed riprap with a diameter of 0.6 m withstands overtopping of 2 – 3.5 m<sup>3</sup>/s/m in an emergency situation. A test dam with full scale riprap stones even endured overtopping of 8 m<sup>3</sup>/s/m. Increased knowledge with specific data may lead to a more reasonable design.



## RÉSUMÉ

Les données de la littérature et celles issues d'un modèle préliminaire et des essais de terrain montrent un gain considérable de stabilité en utilisant des enrochements placés plutôt que jetés. Les résultats des différentes études sont comparés à l'aide d'un nombre de Froude lié au rocher. Les premiers résultats montrent que la stabilité dépend de l'orientation des rochers et que la charge hydraulique liée à l'écoulement traversant est plus défavorable que celle due au déversement. Il serait nécessaire d'obtenir plus de données sur les enrochements placés sur des pentes raides pour quantifier le facteur de sécurité réel des enrochements placés conformément à la réglementation norvégienne de sécurité des barrages. La littérature et les résultats de tests indiquent qu'un enrochement placé d'un diamètre de 0,6 m résiste à des déversements de 2 à 3,5 m<sup>3</sup>/s/m en cas d'urgence. Un barrage test avec des rochers à échelle réelle a même supporté un déversement de 8 m<sup>3</sup>/s/m. Des connaissances accrues grâce à des données spécifiques pourraient permettre une conception plus raisonnable.

# B

## Secondary papers

## **Dam Svartevatn - An example of challenging upgrading of a large rockfill dams**

Priska H. Hiller, Leif Lia, Per Magnus Johansen, Rolv Guddal

*ICOLD Annual Meeting and Symposium*

*Bali, Indonesia, 2014*

**Abstract:** Dam Svartevatn, built in 1973-1976, is the second highest rockfill dam in Norway ( $H = 129$  m). After a mandatory reassessment, the dam needed a major upgrading to meet the current dam safety requirements. The main reason was that the dam crest dimensions, freeboard and width did not satisfy the requirements for a dam in the highest consequence class.

The upgrading works included raising of the dam crest by 1.5 m, reestablishing the downstream slope from 1:1.35 (vertical: horizontal) to 1:1.5 and hence rebuilding the downstream slope by adding in total about 430 000 m<sup>3</sup> of rockfill and a new riprap cover. Creative solutions were needed, to access the downstream slope of the dam, to meet dam safety and environmental requirements as well as to guarantee safe working conditions. The landscape in the dam area had to remain unaffected, because dam Svartevatn is located in an environmental protected area. The chosen solution was to construct a temporary access road with an inclination of 1:4 on the existing dam and to place 85 000 m<sup>3</sup> of riprap on the downstream slope, by reversing the dumpers up and down the very steep access. The upgrading of the dam started in 2011 and is will be finished in 2014. The total cost for the works is estimated to 150 million NOK (25 million USD).

Furthermore, the Norwegian University of Science and Technology takes the opportunity to use the facilities at the construction site for research. Full scale tests of riprap protection under overtopping conditions were run, using the bottom outlet of the dam for discharge.

This paper gives a brief introduction to rockfill dams in Norway, describes the challenges and solutions of the upgrading works at dam Svartevatn and specifies the research site.

## **Riprap design on the downstream slope of rockfill dams**

Priska H. Hiller, Leif Lia, Jochen Aberle, Stefan Wirtz, Markus C. Casper  
*Mitteilungen - Leichtweiss-Institut für Wasserbau der Technischen Universität  
Braunschweig Vol. 161, 39-44, 2014*

**Abstract:** Riprap considerably increases the stability of a slope and its resistance against erosion. Therefore, the downstream slopes of rockfill dams in Norway are armed with a riprap by placing oblong stones in an interlocking pattern. Such riprap is designed as erosion protection measure to guarantee dam safety in case of substantial leakages through or overtopping of the dam. As a consequence of the renewed Norwegian dam safety regulation from 2010, several rockfill dams, most of them built before 1990, have to be upgraded nowadays because they do not longer comply with the renewed regulation which has fully retroactive effect. Thus, to ensure a technical and economical optimal design, the key parameters of placed riprap on the downstream slopes of rockfill dams with an inclination of 1:1.5 (vertical: horizontal) have to be reassessed. Despite the significance of riprap stability on such steep slopes, there are relatively few studies available and further investigations are required to develop improved design guidelines for riprap formed by interlocked stones on steep slopes. This paper focuses on the concept of an experimental investigation of riprap stability on steep slopes. The test rig designed for detailed studies of riprap stability under through flow and overtopping conditions is described. The concept of a novel sensor type based on Radio Frequency Identification technology will be presented. By installing sensors in some selected stones, the position and movement of these stones can be live monitored.

## **Large-scale overtopping tests - Practical challenges and experience**

Priska H. Hiller, Leif Lia

*1st International Seminar on Dam Protections against Overtopping and Accidental Leakage*

*Madrid, Spain, 2014*

Slightly modified for being published as:

## **Practical challenges and experience from large-scale overtopping tests with placed riprap**

Priska H. Hiller, Leif Lia (2015)

*In M. Á. Toledo, R. Morán, E. Oñate (Eds.), Dam Protections against Overtopping and Accidental Leakage, 151-157. London: CRC Press/ Balkema.*

**Abstract:** Downstream slopes of rockfill dams in Norway are protected with riprap against considerable leakages through the dam or overtopping. For this purpose, oblong stones are placed one by one in an interlocking pattern. Six large-scale field tests were run to increase the knowledge about placed riprap on steep slopes. The 3.5 m high and 10 m wide test dams withstood unit discharges of over 8 m<sup>3</sup>/s/m. There is a presentation of the facilities, test set-up and measuring equipment with focus on practical issues and challenges connected with large-scale tests in order to share useful experience about such uncommon experiments.

## Field tests of placed riprap as erosion protection against overtopping and leakage

Priska H. Hiller, Fredrikke Kjosavik, Leif Lia, Jochen Aberle

*United States Society on Dams - Annual Meeting and Conference*

*Denver CO, USA, 2016*

**Abstract:** Accidental overtopping or leakage can have fatal consequences for the stability of embankment dams. The downstream slopes of rockfill dams in Norway have to be protected with placed riprap as prescribed by regulations, to increase their resistance to erosion. Placed riprap consists of stones which are placed one by one in an interlocking pattern. This paper presents preliminary results from field tests carried out to investigate the resistance of placed riprap on steep slopes. Tests were also made using dumped riprap for comparison. The temporary test site was situated at the outlet channel of a spillway tunnel and water was discharged from the reservoir. For the tests, three 12-m wide and 3-m high permeable dams were specifically built and secured by riprap with a stone size of 0.4 m. The tests showed that the constructed placed r ripraps could, dependent on the boundary conditions, withstand unit discharges of  $8 \text{ m}^3/\text{s}/\text{m}$ . A reference test with dumped riprap withstood approximately  $1 \text{ m}^3/\text{s}/\text{m}$ , i. e. 1/8 of the unit discharge for placed riprap. The results show that placing riprap in an interlocking pattern increases its stability considerably compared to random placement.

## **Kartlegging av plastring på nedstrøms skråning av fyllingsdammer**

[Survey of placed riprap on the downstream slopes of rockfill dams]

Priska H. Hiller

*NTNU Report B1-2016-1, ISBN-10: 978-827598-095-1*

*Trondheim, Norway, 2016*

**Abstract** [translated, original in Norwegian]: The downstream slopes of rockfill dams in Norway are secured with placed riprap against erosion in connection with accidental loads from leaking water or overtopping. Placed riprap is formed of stones which are placed in an interlocking pattern and with their longest axes inclined towards the dam. A survey of placed riprap on 33 dams was carried out during summer 2015 and the results of the different dams were compared with each other and with current requirements and recommendations in the dams safety regulation and the guideline for embankment dams. Stone size, shape, placement and packing density were registered for riprap stones within selected areas.

The results show that 64% of the dams meet the recommendation for the minimum stone size and none fulfils the criterion about the ratio between the largest and the smallest stone. All the dams would meet the recommendation about the stone size if the 5-percentile would be used as reference instead of the smallest stone. By adjusting the current recommendation from that the ratio between the largest and the smallest stone has to be smaller than 1.7, to the ratio between the 90-percentile and the 10-percentile instead, 70% would fulfil that criterion. In average, 38% of the measured riprap stones had the wanted stone shape and the other stones are rather more flat or cubic. The requirement about the placement of the stones does not specify if it is valid for all the stones or just for a certain amount. The survey shows that for about 70% of the dams 80% or more of the riprap stones are placed with their longest axes inclining towards the dam.

The survey of placed riprap on 33 rockfill dams provides knowledge about how placed riprap actually is implemented. The principles in the current requirements and recommendations are adequate and will still be met if the current criteria would be adjusted to percentiles instead of the maximum and minimum stone size. In that way, the natural variation in stones as building material would be better represented as usually applied in specifications for erosion protection made of stones. The recommended change would allow that placed riprap, as implemented in practice, can meet the criteria in the dam safety regulation and the guideline for embankment dams without

increased use of resources and measurable impact for dam safety. Potential changes should be discussed with experts from different stakeholders before implementation.





# C

Permissions from journals and  
statements from co-authors



NTNU

Encl. to application for assessment of PhD thesis

STATEMENT FROM CO-AUTHOR (cf. section 10.1 in the PhD regulations)

Priska Helene Hiller applies to have the following thesis assessed: Name of candidate

Riprap design on the downstream slopes of rockfill dams title

\*) The statement is to describe the work process and the sharing of work and approve that the article may be used in the thesis.

\*) Statement from co-author on article: Hiller, P. H., Aberle, J., Lia, L. Accumulating stone displacements as failure origin in placed riprap on steep slopes Journal of Hydraulic Research (in re-review) I hereby declare that I am aware that the article mentioned above, of which I am co-author, will form part of the PhD Thesis by the PhD Candidate Priska H. Hiller who made a major contribution to the work in the experiment, data analysis and writing phase. Trondheim, 2/2-2017 Place, date Signature co-author

\*) Statement from co-author on article: Hiller, P. H., Aberle, J., Lia, L. Accumulating stone displacements as failure origin in placed riprap on steep slopes Journal of Hydraulic Research (in re-review) I hereby declare that I am aware that the article mentioned above, of which I am co-author, will form part of the PhD Thesis by the PhD Candidate Priska H. Hiller who made a major contribution to the work in the experiment, data analysis and writing phase. Trondheim, 2.2.17 Place, date Signature co-author



NTNU

Encl. to application for assessment of PhD thesis

### STATEMENT FROM CO-AUTHOR

(cf. section 10.1 in the PhD regulations)

Priska Helene Hiller .....applies to have the following thesis assessed:  
Name of candidate

..... Riprap design on the downstream slopes of rockfill dams .....  
title

\*) The statement is to describe the work process and the sharing of work and approve that the article may be used in the thesis.

\*)  
Statement from co-author on article: Hiller, P. H., Lia, L., Aberle, J. ....  
.....

**Field and model tests of riprap on steep slopes exposed to overtopping**  
Journal of Applied Water Engineering and Research (submitted)

I hereby declare that I am aware that the article mentioned above, of which I am co-author, will form part of the PhD Thesis by the PhD Candidate Priska H. Hiller who made a major contribution to the work in the experiment, data analysis and writing phase.

26-2017, Trondheim .....  
Place, date

.....  
Signature co-author

\*)  
Statement from co-author on article: .. Hiller, P. H., Lia, L., Aberle, J. ....  
.....

**Field and model tests of riprap on steep slopes exposed to overtopping**  
Journal of Applied Water Engineering and Research (submitted)

I hereby declare that I am aware that the article mentioned above, of which I am co-author, will form part of the PhD Thesis by the PhD Candidate Priska H. Hiller who made a major contribution to the work in the experiment, data analysis and writing phase.

2.2.17, Trondheim .....  
Place, date

.....  
Signature co-author



Home

Create Account

Help



**Title:** Smartstones: A small 9-axis sensor implanted in stones to track their movements

**Author:** Oliver Gronz, Priska H. Hiller, Stefan Wirtz, Kerstin Becker, Thomas Iserloh, Manuel Seeger, Christine Brings, Jochen Aberle, Markus C. Casper, Johannes B. Ries

**Publication:** CATENA

**Publisher:** Elsevier

**Date:** July 2016

© 2016 The Authors. Published by Elsevier B.V.

**LOGIN**

If you're a **copyright.com user**, you can login to RightsLink using your copyright.com credentials. Already a **RightsLink user** or want to [learn more?](#)

### Creative Commons Attribution-NonCommercial-No Derivatives License (CC BY NC ND)

This article is published under the terms of the [Creative Commons Attribution-NonCommercial-No Derivatives License \(CC BY NC ND\)](#).

For non-commercial purposes you may copy and distribute the article, use portions or extracts from the article in other works, and text or data mine the article, provided you do not alter or modify the article without permission from Elsevier. You may also create adaptations of the article for your own personal use only, but not distribute these to others. You must give appropriate credit to the original work, together with a link to the formal publication through the relevant DOI, and a link to the Creative Commons user license above. If changes are permitted, you must indicate if any changes are made but not in any way that suggests the licensor endorses you or your use of the work.

Permission is not required for this non-commercial use. For commercial use please continue to request permission via Rightslink.

**BACK**

**CLOSE WINDOW**

Copyright © 2016 [Copyright Clearance Center, Inc.](#) All Rights Reserved. [Privacy statement](#). [Terms and Conditions](#). Comments? We would like to hear from you. E-mail us at [customercare@copyright.com](mailto:customercare@copyright.com)



NTNU

Encl. to application for assessment of PhD thesis

### STATEMENT FROM CO-AUTHOR

(cf. section 10.1 in the PhD regulations)

Priska Helene Hiller.....applies to have the following thesis assessed:  
Name of candidate

not decided yet.....  
title

\*) The statement is to describe the work process and the sharing of work and approve that the article may be used in the thesis.

\*)  
Statement from co-author on article: Gronz, O., Hiller, P. H., Wirtz, S., Becker, K., Iserloh, T., Seeger, M., Brings, C., Aberle, J., Casper, M. C., Ries, J. B......

**Smartstones: A small 9-axis sensor implanted in stones to track their movement**  
Catena 142 (2016) pp. 245-251, doi:10.1016/j.catena.2016.03.030

I hereby declare that I am aware that the article mentioned above, of which I am co-author, will form part of the PhD Thesis by the PhD Candidate Priska H. Hiller who made a major contribution to the work in the experiment, data analysis and writing phase.

Tries, 28.6.2016  
Place, date

[Signature]  
Signature co-author

\*)  
Statement from co-author on article: Gronz, O., Hiller, P. H., Wirtz, S., Becker, K., Iserloh, T., Seeger, M., Brings, C., Aberle, J., Casper, M. C., Ries, J. B......

**Smartstones: A small 9-axis sensor implanted in stones to track their movement**  
Catena 142 (2016) pp. 245-251, doi:10.1016/j.catena.2016.03.030

I hereby declare that I am aware that the article mentioned above, of which I am co-author, will form part of the PhD Thesis by the PhD Candidate Priska H. Hiller who made a major contribution to the work in the experiment, data analysis and writing phase.

Tries, 28.6.16  
Place, date

[Signature]  
Signature co-author

\*)

Statement from co-author on article: Gronz, O., Hiller, P. H., Wirtz, S., Becker, K., Iserloh, T.,  
Seeger, M., Brings, C., Aberle, J., Casper, M. C., Ries, J. B.

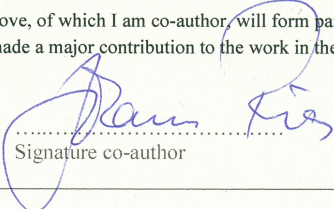
**Smartstones: A small 9-axis sensor implanted in stones to track their movement**

Catena 142 (2016) pp. 245-251, doi:10.1016/j.catena.2016.03.030

I hereby declare that I am aware that the article mentioned above, of which I am co-author, will form part of the PhD Thesis by the PhD Candidate Priska H. Hiller who made a major contribution to the work in the experiment, data analysis and writing phase.

28.06.16

Place, date

  
Signature co-author

\*)

Statement from co-author on article: Gronz, O., Hiller, P. H., Wirtz, S., Becker, K., Iserloh, T.,  
Seeger, M., Brings, C., Aberle, J., Casper, M. C., Ries, J. B.

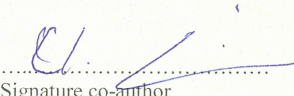
**Smartstones: A small 9-axis sensor implanted in stones to track their movement**

Catena 142 (2016) pp. 245-251, doi:10.1016/j.catena.2016.03.030

I hereby declare that I am aware that the article mentioned above, of which I am co-author, will form part of the PhD Thesis by the PhD Candidate Priska H. Hiller who made a major contribution to the work in the experiment, data analysis and writing phase.

Trier, 28.6.16

Place, date

  
Signature co-author

\*)

Statement from co-author on article: Gronz, O., Hiller, P. H., Wirtz, S., Becker, K., Iserloh, T.,  
Seeger, M., Brings, C., Aberle, J., Casper, M. C., Ries, J. B.

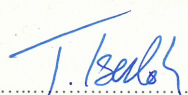
**Smartstones: A small 9-axis sensor implanted in stones to track their movement**

Catena 142 (2016) pp. 245-251, doi:10.1016/j.catena.2016.03.030

I hereby declare that I am aware that the article mentioned above, of which I am co-author, will form part of the PhD Thesis by the PhD Candidate Priska H. Hiller who made a major contribution to the work in the experiment, data analysis and writing phase.

Trier, 28.6.16

Place, date

  
Signature co-author

\*)

Statement from co-author on article: Gronz, O., Hiller, P. H., Wirtz, S., Becker, K., Iserloh, T.,  
Seeger, M., Brings, C., Aberle, J., Casper, M. C., Ries, J. B. ....

**Smartstones: A small 9-axis sensor implanted in stones to track their movement**

Catena 142 (2016) pp. 245-251, doi:10.1016/j.catena.2016.03.030

I hereby declare that I am aware that the article mentioned above, of which I am co-author, will form part of the PhD Thesis by the PhD Candidate Priska H. Hiller who made a major contribution to the work in the experiment, data analysis and writing phase.

Trier, 29.6.2016

Place, date

Signature co-author

\*)

Statement from co-author on article: Gronz, O., Hiller, P. H., Wirtz, S., Becker, K., Iserloh, T.,  
Seeger, M., Brings, C., Aberle, J., Casper, M. C., Ries, J. B. ....

**Smartstones: A small 9-axis sensor implanted in stones to track their movement**

Catena 142 (2016) pp. 245-251, doi:10.1016/j.catena.2016.03.030

I hereby declare that I am aware that the article mentioned above, of which I am co-author, will form part of the PhD Thesis by the PhD Candidate Priska H. Hiller who made a major contribution to the work in the experiment, data analysis and writing phase.

.....  
Place, date

.....  
Signature co-author

\*)

Statement from co-author on article: Gronz, O., Hiller, P. H., Wirtz, S., Becker, K., Iserloh, T.,  
Seeger, M., Brings, C., Aberle, J., Casper, M. C., Ries, J. B. ....

**Smartstones: A small 9-axis sensor implanted in stones to track their movement**

Catena 142 (2016) pp. 245-251, doi:10.1016/j.catena.2016.03.030

I hereby declare that I am aware that the article mentioned above, of which I am co-author, will form part of the PhD Thesis by the PhD Candidate Priska H. Hiller who made a major contribution to the work in the experiment, data analysis and writing phase.

.....  
Place, date

.....  
Signature co-author





### STATEMENT FROM CO-AUTHOR

(cf. section 10.1 in the PhD regulations)

Priska Helene Hiller

.....applies to have the following thesis assessed  
Name of candidate

not decided yet

.....  
title

\*) The statement is to describe the work process and the sharing of work and approve that the article may be used in the thesis.

\*)  
Statement from co-author on article: Gronz, O., Hiller, P. H., Wirtz, S., Becker, K., Iserloh, T., Seeger, M., Brings, C., Aberle, J., Casper, M. C., Ries, J. B. ....

**Smartstones: A small 9-axis sensor implanted in stones to track their movement**  
Catena 142 (2016) pp. 245-251, doi:10.1016/j.catena.2016.03.030

I hereby declare that I am aware that the article mentioned above, of which I am co-author, will form part of the PhD Thesis by the PhD Candidate Priska H. Hiller who made a major contribution to the work in the experiment, data analysis and writing phase.

*Finkenfeldt* 29.06.2016  
.....  
Place, date

*[Signature]*  
.....  
Signature co-author

\*)  
Statement from co-author on article: Gronz, O., Hiller, P. H., Wirtz, S., Becker, K., Iserloh, T., Seeger, M., Brings, C., Aberle, J., Casper, M. C., Ries, J. B. ....

**Smartstones: A small 9-axis sensor implanted in stones to track their movement**  
Catena 142 (2016) pp. 245-251, doi:10.1016/j.catena.2016.03.030

I hereby declare that I am aware that the article mentioned above, of which I am co-author, will form part of the PhD Thesis by the PhD Candidate Priska H. Hiller who made a major contribution to the work in the experiment, data analysis and writing phase.

.....  
Place, date

.....  
Signature co-author



NTNU

Encl. to application for assessment of PhD thesis

### STATEMENT FROM CO-AUTHOR

(cf. section 10.1 in the PhD regulations)

Priska Helene Hiller .....applies to have the following thesis assessed:  
Name of candidate

.....Riprap design on the downstream slopes of rockfill dams .....  
title

\*) The statement is to describe the work process and the sharing of work and approve that the article may be used in the thesis.

\*)  
Statement from co-author on article: Gronz, O., Hiller, P. H., Wirtz, S., Becker, K., Iserloh, T., Seeger, M., Brings, C., Aberle, J., Casper, M. C., Ries, J. B. ....

**Smartstones: A small 9-axis sensor implanted in stones to track their movement**  
Catena 142 (2016) pp. 245-251, doi:10.1016/j.catena.2016.03.030

I hereby declare that I am aware that the article mentioned above, of which I am co-author, will form part of the PhD Thesis by the PhD Candidate Priska H. Hiller who made a major contribution to the work in the experiment, data analysis and writing phase.

.....  
Place, date

.....  
Signature co-author

\*)  
Statement from co-author on article: Gronz, O., Hiller, P. H., Wirtz, S., Becker, K., Iserloh, T., Seeger, M., Brings, C., Aberle, J., Casper, M. C., Ries, J. B. ....

**Smartstones: A small 9-axis sensor implanted in stones to track their movement**  
Catena 142 (2016) pp. 245-251, doi:10.1016/j.catena.2016.03.030

I hereby declare that I am aware that the article mentioned above, of which I am co-author, will form part of the PhD Thesis by the PhD Candidate Priska H. Hiller who made a major contribution to the work in the experiment, data analysis and writing phase.

*Trondheim, 2.2.17*  
Place, date

*[Signature]*  
Signature co-author

**Priska Helene Hiller**

---

**From:** Michel de Vivo <secretaire.general@icold-cigb.org>  
**Sent:** 25. januar 2017 17:25  
**To:** Priska Helene Hiller  
**Subject:** Re: Copyright use of article in PhD-thesis

Dera Priska

We give you the permission for including this article in your PhD Thesis but indicating specifically the ICOLD sources.

Best regards

**Michel de VIVO**

Secretary General of the International Commission On Large Dams

**ICOLD** 61, Avenue KLEBER 75116 PARIS

**Tel: +33 1 47 04 17 80 Mob: +33 6 07 24 41 95**

**Website: [www.icold-cigb.org](http://www.icold-cigb.org)**

---

**De :** Priska Helene Hiller <priska.hiller@ntnu.no>

**Date :** lundi 23 janvier 2017 15:46

**À :** Michel De Vivo <secretaire.general@icold-cigb.org>

**Objet :** Copyright use of article in PhD-thesis

Dear Secretary General,

I am currently in the last phase of my PhD studies about the topic "Riprap design on the downstream slopes of rockfill dams". At the Norwegian University of Science and Technology where I conduct my PhD studies, it is usual to compile a set of articles when writing a PhD thesis. With respect to this, I kindly ask for permission to include the following article, presented at the 25<sup>th</sup> Congress on Large Dams in my thesis:

Hiller PH, Lia L. 2015. *Placed riprap as erosion protection on the downstream slope of rockfill dams exposed to overtopping*. 25th Congress on Large Dams, Q97, R20.

Thank you for your willingness to allow to include the given paper in my thesis and for your quick handling of this request.

Sincerely,  
Priska H. Hiller

-----  
Priska Helene Hiller  
PhD Candidate «Riprap design on rockfill dams»  
Department of Hydraulic and Environmental Engineering  
Norwegian University of Science and Technology, NTNU Trondheim  
+47 73 59 51 57/ +47 910 02 108



NTNU

Encl. to application for assessment of PhD thesis

STATEMENT FROM CO-AUTHOR (cf. section 10.1 in the PhD regulations)

Priska Helene Hiller applies to have the following thesis assessed: Name of candidate

Riprap design on the downstream slopes of rockfill dams title

\*) The statement is to describe the work process and the sharing of work and approve that the article may be used in the thesis.

\*) Statement from co-author on article: Hiller, P. H., Lia, L. Placed riprap as erosion protection on the downstream slope of rockfill dams exposed to overtopping 25th Congress on Large Dams, Q. 97 - R. 20 I hereby declare that I am aware that the article mentioned above, of which I am co-author, will form part of the PhD Thesis by the PhD Candidate Priska H. Hiller who made a major contribution to the work in the experiment, data analysis and writing phase. Trondheim, 2/2-2017 Place, date Helene Lia Signature co-author

\*) Statement from co-author on article: Place, date Signature co-author